PROBING *PSEUDOMONAS AERUGINOSA* PHYSIOLOGY DURING INFECTION USING -OMICS TECHNIQUES, PHENOTYPIC ASSAYS AND MOUSE MODELS

A Dissertation
Presented to
The Academic Faculty

by

Kelly Leorah Michie

In Partial Fulfillment
of the Requirements for the Degree
Doctorate of Philosophy in the
School of Biological Sciences

Georgia Institute of Technology

August 2020

PROBING *PSEUDOMONAS AERUGINOSA* PHYSIOLOGY DURING INFECTION USING -OMICS TECHNIQUES, PHENOTYPIC ASSAYS AND MOUSE MODELS

Approved by:

Dr. Marvin Whiteley, Advisor
School of Biological Sciences
Georgia Institute of Technology

Dr. Greg Gibson
School of Biological Sciences
Georgia Institute of Technology

Dr. Edward Botchwey
School of Biomedical Engineering
Georgia Institute of Technology

Dr. Joanna B. Goldberg
School of Biological and Biomedical Sciences
Emory University

Dr. Sam Brown
School of Biological Sciences
Georgia Institute of Technology

Date Approved: July 8th, 2020

ACKNOWLEDGEMENTS

To start, I would like to thank my Ph.D mentor, Dr. Marvin Whiteley, for welcoming me into his lab and for guiding my thesis research every step of the way. I would also like to thank my undergraduate mentor, Dr. Diane Ordway at Colorado State University for getting me started on my scientific journey and encouraging me to pursue a Ph.D. Thanks go out to all Whiteley lab members, past and present, for the help, advice, good times, and distractions. Thank you to our collaborators, Dr. Kendra Rumbaugh's lab at Texas Tech, Dr. Joanna Goldberg's lab at Emory, Dr. Sam Brown's lab and Dr. Steve Diggle's lab at Georgia Tech, as well as Dr. Stephen Dolan at the University of Cambridge, UK. This work would not be possible without funding from the National Institutes of Health, the Cystic Fibrosis Foundation, and the Burroughs Wellcome fund. I would like to acknowledge all of my friends and family for their unending love and support; you guys make it all worth it. Finally, a big thank you to sushi and Pokémon Go.

TABLE OF CONTENTS

LIST OF TABLES

LIST OF FIGURES

LIST OF SYMBOLS AND ABBREVIATIONS

Mbp	Mega base pairs
CDC	Centers for Disease Control and Prevention
ROS	Reactive oxygen species
RNS	Reactive nitrogen species
LPS	Lipopolysaccharide
HAP	Hospital-squired pneumonia
VAP	Ventilator-associated pneumonia
T3SS	Type III secretion system
MDR	Multi-drug resistant
NIH	National Institutes of Health
HGT	Horizontal gene transfer
EPS	Extracellular polymeric substances
AHL	Acyl homoserine lactone
SCFM	Synthetic cystic fibrosis sputum medium
WLM	Wound-like medium
TLR	Toll-like receptor
GSH	Glutathione
WT	Wild-type
MOPS	3-(N-morpholino)propanesulfonic acid
CDM	Chemically defined media
H_2O_2	Hydrogen peroxide
HOCl	Hypochlorous acid
AMPs	Antimicrobial peptides
Tn-seq	Transposon sequencing

BSO	Buthionine sulfoximine
DEM	Diethylmaletate
CFUs	Colony forming units
FISH	Fluorescence *in situ* hybridization
RNA-seq	RNA sequencing
PCA	Principal component analysis
L2FC	Log2 fold-change
IP	Intraperitoneal
IV	Intravenous
TEER	Transepithelial electrical resistance
HPLC	High-pressure liquid chromatography
BHI	Brain heart infusion
MAB	*Mycobacterium abscessus* complex
NTM	Nontuberculous mycobacteria
FBA	Flux balance analysis
LASSO	Least absolute shrinkage and selection operator

SUMMARY

The opportunistic pathogen *Pseudomonas aeruginosa* causes severe disease in people with compromised immune systems or co-morbidities such as diabetes or cystic fibrosis. Since even intense antibiotic regimens are often ineffective, there is a great need to better understand *P. aeruginosa* infection biology. Our first research goal was to elucidate the role of glutathione (GSH) biosynthesis for *P. aeruginosa* during infection. GSH is a major cellular antioxidant that is important for protection from oxidative stress. We found that GSH biosynthesis provides protection against some antimicrobials, such as bleach and ciprofloxacin. We also discovered that GSH biosynthesis provides a modest fitness benefit to *P. aeruginosa* in a mouse model of acute pneumonia, but not in chronic wound, abscess, and burn wound mouse models. Our second research goal was to characterize the transcriptomic and proteomic signatures of growth rate in *P. aeruginosa*. Growth rate has significant impacts on cellular physiology, from cell size to stress tolerance. We cultured *P. aeruginosa* at four different growth rates using a chemostat, and quantified mRNA and protein abundances using RNA-seq and proteomics mass spectrometry, respectively. We observed modest correlations between mRNA and protein expression. We also discovered that there was greater variation in mRNA expression compared to protein expression, and that mRNA expression was more strongly affected by changes in growth rate. We calculated protein-to-mRNA ratios, or conversion factors, which could be used to more accurately predict protein abundance from RNA-seq data. The information presented in this work may be useful for better understanding, and ultimately treating, *P. aeruginosa* infections.

.

INTRODUCTION[1]

1.1 Overview

Infections caused by the bacterium *Pseudomonas aeruginosa* are a major public health threat (1). This Gram-negative bacterium is most commonly isolated from areas associated with human activity, including contaminated soil, water, and hospital fomites (1-3). As an opportunistic pathogen, it primarily infects people with compromised immune systems and underlying comorbidities, particularly cystic fibrosis and diabetes (1). It can infect multiple body sites, including the skin and soft tissues, lungs, eyes, bloodstream, and urinary tract (1). A large number of *in vitro* and *in vivo* models are used to study *P. aeruginosa* virulence, and it is clear that the traits required for *P. aeruginosa* fitness in these models can vary (4-6). This may be due to differences in nutrient availability, innate immune defenses, or other environmental factors, such as oxygen tension or pH. *P. aeruginosa* is naturally tolerant to many conventional disinfectants and antibiotics, and there is increasing global incidence of *P. aeruginosa* strains with multi-drug resistance traits (7-9). There is currently no vaccine against *P. aeruginosa*, and therapeutic regimens used to treat this bacterium are often ineffective. For these reasons, there is an urgent need to better understand *P. aeruginosa* infection biology. This thesis is focused on

[1] Parts of this subsection were adapted from the following reference: Michie, K.L., *et al*., *The Role of Pseudomonas aeruginosa Glutathione Biosynthesis in Lung and Soft Tissue Infection*. Infection and Immunity, 2020. IAI.00116-20; DOI: 10.1128/IAI.00116-20. Copyright © American Society for Microbiology 2020. Reused with permission. I was the primary author of this work.

elucidating the mechanisms of *P. aeruginosa* pathophysiology in human infections. Chapter 1, the introduction, details the basic microbiology of *P. aeruginosa*. This includes: a discussion of the types of infections caused by *P. aeruginosa*; antimicrobial resistance; virulence factors; quorum sensing and social behaviors; and laboratory models used to study *P. aeruginosa* pathophysiology. Chapter 2 presents research on the role of glutathione biosynthesis in *P. aeruginosa* mammalian infection. In Chapter 3 the gene and protein expression signatures correlated with growth rate in *P. aeruginosa* are characterized. Finally, Chapter 4 summarizes the main conclusions of this body of work and explores potential future directions

1.2 *P. aeruginosa* microbiology

P. aeruginosa is a Gram-negative, flagellated, rod-shaped member of the Proteobacteria phylum (10). *P. aeruginosa* has a relatively large genome, on average about 6 Mbp, and the core genome is highly conserved between strains (11). This large genome equips *P. aeruginosa* with a broad, versatile repertoire of physiological functions and traits. For example, *P. aeruginosa* can thrive in a wide variety of habitats. It is an environmental organism that is ubiquitously found in soil, water, and on man-made surfaces, particularly environments associated with human contact (2, 3). This is especially problematic in hospital settings, where *P. aeruginosa* can readily colonize sinks, faucets, doorknobs, and surgical or respiratory equipment (12-15). *P. aeruginosa* is a facultative anaerobe, meaning that it grows most efficiently in the presence of oxygen, but it can survive without oxygen by switching to a fermentative metabolism using alternative electron acceptors such as nitrate (10). *P. aeruginosa* has extensive metabolic capabilities, and can catabolize a wide variety of organic compounds (16). These features allow *P. aeruginosa* to grow even in harsh, nutrient-poor environments.

1.3 Types of infections caused by *P. aeruginosa*

1.3.1 P. aeruginosa epidemiology

P. aeruginosa is a leading cause of morbidity and mortality worldwide. The Centers for Disease Control and Prevention (CDC) classify *P. aeruginosa* as a "threat level serious pathogen", their 2nd highest threat ranking (17). In 2019, the CDC reported 32,600 nosocomial (hospital-acquired) *P. aeruginosa* infections and 2,700 deaths (17). *P. aeruginosa* infections also place a tremendous burden on the healthcare system; in 2019 the CDC estimated that $767 million was spent on healthcare costs associated with these infections in the US (17). *P. aeruginosa* is an opportunistic pathogen, meaning that it rarely causes disease in healthy individuals, but can cause serious or lethal disease in individuals with compromised immune defenses. Common comorbidities associated with *P. aeruginosa* infection include type 2 diabetes, cystic fibrosis, cancer, HIV, burns, surgical wounds, catheterization, and ventilation (1, 10, 15). *P. aeruginosa* is a major cause of nosocomial infections because hospitalized patients are often susceptible to *P. aeruginosa*, it easily colonizes hospital surfaces (12-15), and it can transfer person-to-person. As described in further detail in section 1.4, *P. aeruginosa* infections are difficult to treat due to its high innate tolerance to disinfectants and antibiotics. Its ability to grow in diverse, harsh environments, coupled with its arsenal of virulence factors, allow *P. aeruginosa* to cause disease in many different infection sites throughout the body. These sites include the skin and soft tissues, lungs, eyes, ears, bloodstream, and urinary tract (1, 10, 15). This work focuses on *P. aeruginosa* infections of the lungs and soft tissues.

1.3.2 Chronic wound infections

Approximately 6.5 million Americans suffer from chronic wound infections annually (18). These painful infections are associated with steep declines in patient quality of life, and

severe cases can lead to permanent tissue damage, amputation, and death (18). Chronic wound infections are defined as soft-tissue injuries that fail to proceed through normal reparative stages and have not healed by 3 months (18, 19). Chronic wounds may stay open and infected for months, years, or may never heal (18, 19). They are characterized by prolonged, uncontrolled inflammatory responses, leading to tissue damage and weakened immune defenses (18, 19). Common causes of chronic wound infections include pressure ulcers, surgical incisions, and acute trauma (19). Chronic wounds are rare in normally healthy people, but are linked to comorbidities such as diabetes, obesity, and old age (18, 19). Type 2 diabetics are 3 times more likely to develop chronic wound infections and are 28 times more likely to undergo lower extremity amputation due to these infections than non-diabetics (18, 20) Caring for chronic wounds is also very expensive; the associated healthcare costs total $25 billion in the US annually (18). Unfortunately, the incidence of these infections is only projected to increase as the number of Americans with comorbidities such as diabetes and obesity continue to rise (18).

Chronic wounds are typically colonized by complex polymicrobial communities that are often comprised of more than 10 bacterial species (21-27). Although highly diverse, particular species often predominate, and several species have been correlated with prolonged wound healing and tolerance to antimicrobial treatment. Although the data varies based on the type of wound and the methodology, large-scale studies indicate that *P. aeruginosa* is present in 15% to 80% of human chronic wounds (21, 22, 24, 25). There is also evidence that its prevalence may be even higher, since *P. aeruginosa* occupies deeper sites within the wound, hampering identification (28). *P. aeruginosa* is believed to exacerbate the prolonged inflammatory response and contribute to tissue destruction. Compared to chronic wounds that do not contain *P. aeruginosa*, chronic wounds that contain *P. aeruginosa* are more severe, heal at a slower rate, and are more likely to result

in amputation or death. *P. aeruginosa* is also very difficult to eradicate from chronic wounds, owing to its ability to form multi-species biofilms in the wound (29-31). For these reasons, there is strong evidence that *P. aeruginosa* is a key mediator of chronic wound persistence (24, 32, 33).

1.3.3 Burn wound infections

Like chronic wounds, burn wounds also affect the skin and soft tissues. However, unlike chronic wounds, burns are acute pathologies. Burns are associated with rapid, uncontrolled inflammatory responses and oxidative damage. Following a thermal injury, there is a heightened inflammatory response that leads to production of reactive oxygen species (ROS) and reactive nitrogen species (RNS); activation of phagocytic cells; lipid peroxidation; tissue thrombosis, ischemia and reperfusion; and activation of tissue proteases (34-36). These effects cause both local and systemic acute tissue damage, and can lead to tissue necrosis, shock, multiple organ failure, and death (34, 35).

P. aeruginosa is a pathogen of major importance in burn wounds. *P. aeruginosa* spread is particularly threatening in hospital burn care centers, where it can be introduced into burn wounds through exposure from contaminated stool, water, and hospital surfaces (10, 15, 37). It is one of the most common organisms isolated from infected burned patients (10, 15, 37). Various burn wound centers have reported *P. aeruginosa* incidence in about 15%-30% of patients (38-40). Unlike chronic wound infections, *P. aeruginosa* can kill infected burn wound patients in days or weeks. As an opportunistic pathogen, *P. aeruginosa* proliferates rapidly in immunologically weakened burned tissue, and can contribute to tissue destruction, sepsis, and death. Burn wounds containing *P. aeruginosa* are associated with a sharply increased risk of tissue damage and mortality, with reported fatality rates of 50% to 60% (10, 15, 41).

1.3.4 Cystic fibrosis lung infections

An estimated 30,000 people in the US (70,000 globally) have cystic fibrosis (CF), a life-long genetic disease caused by mutations in the cystic fibrosis transmembrane conductance regulator (CFTR) gene (1, 42). The CFTR protein regulates chloride transport across epithelial cell membranes. Defective CFTR function results in the build-up of extremely thick, viscous mucus in the airways. Normally, the cilia lining the respiratory tract beat rhythmically to shuttle mucus out of the lungs, helping to trap and expel invading bacteria. However, in CF, the cilia are unable to clear the thick mucus, which significantly weakens the lung's innate immune defenses. The relatively static environment, impaired immune defences, and the rich nutritional density of the mucus (43) makes the CF lung highly susceptible to bacterial infection (42). Similarly to chronic wound infections, CF lungs are also chronically infected by complex, polymicrobial communities of bacteria and other microbes (42). CF patients suffer from chronic bacterial lung infections and from recurring flare-ups, despite intensive therapeutic regimens. Bacterial colonization in turn triggers sustained inflammation and immune cell infiltration into the lung, further contributing to lung tissue damage (42). While therapeutic advances over the past several decades have dramatically improved CF patient quality of life and lifespan, there is still no cure for CF (44).

In CF patients, *P. aeruginosa* is considered the major cause of morbidity and mortality (44). Early in life, people with CF tend to be initially colonized with other bacterial species, such as *Staphylococcus aureus*, but as they grow into adulthood, *P. aeruginosa* tends to predominate (45, 46). About 80% of all adult CF patients will become persistently infected with *P. aeruginosa* (44, 45, 47). Acquisition of *P. aeruginosa* is associated with an accelerated decline in lung function and worsened survival (47-49). Over the course of prolonged CF lung infection, *P. aeruginosa* undergoes several important adaptations that

enhance its ability to evade the immune system and resist antibiotics (50, 51). One of the most striking adaptations is the mucoidy phenotype, in which *P. aeruginosa* overproduces the extracellular exopolysaccharide alginate. Alginate overproduction makes colonies slick and sticky, which may impede phagocytosis or antibody binding (10, 52, 53). Other evolutionary adaptations include modulation of immunostimulatory components and virulence factors (as described in section 1.5), such as loss of O-antigen subunits from lipopolysaccharide (LPS) (54-56), downregulation of pili and flagella, upregulation of multi-drug efflux pumps (50, 51), hypermutator mutations in DNA repair machinery (57), and loss of quorum sensing (58, 59).

1.3.5 Acute pneumonia

Pneumonia is defined as infection and inflammation of the lungs, and can be accompanied by coughing, fever, chills, build-up of fluid and pus, difficulty breathing, and ultimately death (60). Hospital-acquired pneumonia (HAP) occurs when someone receiving hospital treatment for a different reason acquires pneumonia during their hospital stay (60-62). HAP places a tremendous burden on the healthcare system by contributing to lengthened hospital stays, poorer clinical outcomes, and increased healthcare costs. It is also the most life-threatening type of nosocomial infection (61, 62). HAP typically affects individuals that are already sick, and risk factors include age (over 65), cancer, and HIV. Patients on ventilators in intensive care units are at especially high risk of developing a specific type of HAP called ventilator-associated pneumonia (VAP) (60). 10%-20% of people on ventilators for 48 hours or longer develop VAP (62).

P. aeruginosa is one of the leading causes of HAP, particularly VAP, and is found in 16-30% of all HAP cases (61, 63, 64). HAP cases caused by *P. aeruginosa* typically require lengthier hospital stays and have a higher likelihood of death, with morality rates as high

as 70% (61, 63, 64). As described in section 1.3.1, *P. aeruginosa* is exceedingly difficult to control in a hospital setting because it can spread person-to-person and it readily colonizes hospital surfaces, including respiratory equipment. During acute lung infections, *P. aeruginosa* surface antigens such as LPS and flagella trigger a robust inflammatory response. This leads to recruitment of neutrophils and release of ROS, which also cause lung tissue damage (64). Furthermore, virulence factors, such as the T3SS (type III secretion system, described in section 1.5), allow *P. aeruginosa* to inject lung cells with toxins. These can disrupt the lung epithelial barrier and allow the bacteria to invade and become septic, which can lead to shock, multiple organ failure, and death (64).

1.4 Antimicrobial resistance in *P. aeruginosa*

Over the past few years, improvements in prevention strategies have helped reduce the yearly burden of antibiotic resistant infections. These strategies include improved hospital hygiene and sterilization practices, adoption of more careful antibiotic stewardship, and aggressive antibiotic resistant organism detection and response (17). However, the threat from antibiotic resistant infections remains very high. The CDC estimates that each year in the US there are over 2.8 million antibiotic-resistant infections and over 35,000 associated deaths (17). The National Institutes of Health (NIH) names *P. aeruginosa* a member of the six ESKAPE pathogens, which are clinically relevant for their high virulence, transmissibility in hospital settings, and antibiotic resistance. The six ESKAPE pathogens are ***E**nterococcus faecium, **S**taphylococcus aureus, **K**lebsiella pneumoniae, **A**cinetobacter baumannii, **P**. aeruginosa, and **E**nterobacter spp*. (65). A major problem in common with all 4 types of *P. aeruginosa* infections discussed in section 1.3 (chronic wound, burn wound, CF lung infection, and acute pneumonia) is the difficulty in preventing and treating *P. aeruginosa* infections due to its high resistance to disinfectants and antibiotics. *P. aeruginosa* is a veritable Swiss Army Knife of antimicrobial resistance,

thanks to its relatively large genome and ability to gain new antibiotic resistance mechanisms. These resistance mechanisms can be classified into two categories: intrinsic or acquired.

1.4.1 Intrinsic antibiotic resistance mechanisms

Intrinsic antimicrobial resistance mechanisms are part of an organism's innate ability to tolerate antimicrobials. These mechanisms are encoded in the organism's genome, and are usually fundamental structural or physiological properties that provide protection against harmful substances (1, 66). *P. aeruginosa* has multiple mechanisms of intrinsic antimicrobial resistance that make it naturally highly tolerant to many common disinfectants and antibiotics. Many of these defense mechanisms likely evolved to protect *P. aeruginosa* from naturally occurring toxic compounds present in the environment or produced by competing environmental organisms (66, 67).

One intrinsic resistance strategy is limiting the entry of antimicrobials. Hydrophilic antimicrobials can diffuse into the *P. aeruginosa* cell membrane through porins or non-specific membrane channels. Therefore, reducing expression of these non-specific channels or porins, such as the OprD porin, limits entry of antimicrobials (1, 66, 68). Another strategy is export of antimicrobials. Multi-drug efflux pumps are membrane-spanning protein complexes that pump harmful substances out of the cell (1, 66, 69). Multi-drug efflux pumps can have broad specificity and be active against a range of chemically unrelated compounds, including multiple classes of antibiotics (1, 66, 69). *P. aeruginosa* encodes several different multi-drug efflux pumps, including MexAB-OprM, MexXY/OprM(OprA), MexCD-OprJ, and MexEF-OprN (1, 66, 69). A third mechanism of innate resistance is inactivating harmful compounds. For example, *P. aeruginosa* encodes an inducible β-lactamase (AmpC) that degrades aminopenicillins and most

cephalosporins (1, 57, 66). *P. aeruginosa* also produces a variety of proteins and metabolites for detoxifying ROS and RNS, such as glutathione, catalases, and superoxide dismutases (70, 71).

1.4.2 Acquired antibiotic resistance mechanisms

Acquired mechanisms involve mutations in intrinsic antibiotic resistance genes or acquisition of new antibiotic resistance genes via horizontal gene transfer (HGT) (1, 57). Unlike intrinsic antibiotic resistance mechanisms, acquired mechanisms have evolved and spread due to intense selection pressure from human antibiotic usage (1). Acquired resistance mechanisms are genetically stable and are passed onto progeny, which allows strains with acquired resistance mechanisms to proliferate and spread rapidly (1). The spread of multi-drug resistant (MDR) *P. aeruginosa* strains is a particularly serious problem in hospital settings, where patients are typically at higher risk for infection and MDR strains can spread person-to-person (1, 38, 39). *P. aeruginosa* strains are classified as multi-drug resistant (MDR) if they are resistant to 1 or more drugs in at least 3 antibiotic classes (17). Some strains of MDR *P. aeruginosa* are resistant to nearly all antibiotics, including carbapenems (17).

One method of acquired resistance involves mutations in intrinsic antibiotic resistance regulatory mechanisms. Intrinsic resistance mechanisms are typically under the control of one or more regulatory systems; mutations in these systems can cause overexpression of resistance mechanisms, thereby increasing antibiotic resistance (1). For example, mutations in the negative regulators of AmpC or various multidrug efflux pumps results in enhanced antibiotic resistance in *P. aeruginosa* (1, 57, 69, 72). In the case of OprD, inactivating mutations reducing or eliminating the expression of OprD can enhance resistance (1, 68). Acquired antibiotic resistance mechanisms can also include mutation

in the drug target site. For instance, mutations in binding sites for the fluoroquinolone targets, DNA gyrase and topoisomerase IV, confers *P. aeruginosa* resistance to fluoroquinolones (57, 73).

The second method of acquired antibiotic resistance is acquisition of new genes from different strains or species through HGT (57, 74). HGT can be accomplished through conjugation, transduction, or transformation, and may involve mobile genetic elements such as plasmids, integrons, or transposons (57, 74). Mobile genetic elements are easily shared between bacterial species, which can lead to rapid rises in antibiotic resistance (17). Reservoirs of mobile antibiotic resistance genes emerge from environments with heavy antibiotic usage, such as hospitals (75), industrial feedlots (76), fisheries (77), and areas with pharmaceutical industrial pollution (78). More than one antibiotic resistance gene may be present on a plasmid, enabling bacteria to become MDR upon acquisition (74). Some examples of antibiotic resistance genes acquired through HGT in *P. aeruginosa* include acquired extended-spectrum β-lactamases (7, 79), carbapenemases (79), aminoglycoside modifying enzymes (80), and 16s rRNA modifying enzymes (57, 81).

1.5 *P. aeruginosa* virulence factors

Virulence factors are commonly defined as physiological traits that aid an organism's ability to cause disease (51, 82). Virulence factors may help a pathogen initially colonize the host, disseminate throughout the host, evade the immune response, replicate, or persist during infection (82). *P. aeruginosa* is equipped with a large, diverse set of both cell-associated and secreted virulence factors. Having an extensive selection of virulence factors allows *P. aeruginosa* to successfully colonize a wide variety of environmental habitats as well as infect multiple human body sites.

Extracellular proteases

P. aeruginosa secretes several extracellular proteases that digest complex proteins and peptides. These include elastase A (staphylolysin), elastase B, protease IV (lysyl endopeptidase), and alkaline protease (aeruginolysin). These proteases together can degrade important structural components of tissue, such as elastin, fibrin, collagen, and laminin, which causes tissue necrosis and hemorrhagic lesions (15, 83).

Hemolysins

Hemolysins are pore-forming toxins that solubilize lipids by disrupting phospholipid membranes. They are notable for their ability to lyse red blood cells. *P. aeruginosa* secretes several hemolysins, including phospholipases, lipases, and lecithinase. Phospholipase C hydrolyzes phospholipids such as phosphatidylcholine and sphingomyelin. It also degrades the phosphatidylcholine component of lecithin, which is a major component of lung surfactant, and has been shown to impair lung function during acute or chronic lung infections (15, 64, 84, 85).

Rhamnolipids

Rhamnolipids are biosurfactants that reduce liquid surface tension. Rhamnolipid production allows *P. aeruginosa* to swim across solid or semi-solid surfaces in coordinated groups through a process called swarming motility. Rhamnolipids are also cytotoxic to competing bacterial cells and eukaryotic host cells, and interfere with normal cilia function in the lung (86-89).

Exotoxin A

An extremely toxic compound secreted by *P. aeruginosa* is exotoxin A, which inhibits protein translation in eukaryotic host cells. Depending on the concentration, when injected into mammalian hosts it causes tissue necrosis, neutropenia, shock, and death (15, 90, 91).

Pyocyanin

The pigment pyocyanin gives *P. aeruginosa* its distinctive blue-green color. Pyocyanin is a redox-active phenazine that generates toxic quantities of ROS that can kill other microbes and damage host cells. This mechanism is particularly potent in the lung where pyocyanin oxidizes glutathione (GSH), which is naturally present at high quantities, leading to ROS generation and lung damage (92-96).

Siderophores

Iron is an essential nutrient for most microorganisms, including *P. aeruginosa*. As a defense against invading microorganisms, hosts limit the availability of free iron in the body by sequestering it with iron-binding molecules, such as heme, transferrin, and lactoferrin. To obtain iron during infection, *P. aeruginosa* secretes two siderophores, pyochelin and pyoverdine. These are iron-chelating molecules that compete with host iron-binding molecules to bind and transport iron into the cell. Siderophore production is essential in numerous models of *P. aeruginosa* infection. (97-99)

Slime layer

The outermost component of the *P. aeruginosa* cell is the slime layer. This sticky coating is composed of exopolysaccharides, nucleic acids, hyaluronic acid, lipids, and proteins. It

may help protect the cell from desiccation and phagocytosis and also may aid attachment and biofilm formation. Mucoid *P. aeruginosa* mutants from CF lung infections overproduce the exopolysaccharide alginate (15, 52, 53, 56).

LPS

The outer membrane of Gram-negative bacteria has two leaflets; the inner leaflet is composed of phospholipids, the outer leaflet is composed of LPS (also known as endotoxin). LPS consists of lipid A (the endotoxic portion), core polysaccharides, and outer O antigens. LPS provides the outer membrane with structural integrity and increases the negative charge. It is also highly immunogenic; purified LPS alone can induce systemic shock and death. *P. aeruginosa* can remodel the number and structure of its O antigens. Over the course of chronic CF lung infection, *P. aeruginosa* strains tend to reduce the number of O antigens (LPS rough phenotype) which may help it evade the host immune response (54-56).

Flagella

Flagella are long, whip-like extracellular structures that rotate rapidly like a propeller to allow microorganisms to swim. *P. aeruginosa* has a single, polar flagellum. In some acute infections, like burn wound infections, flagella are important for fitness as they aid in dissemination and chemotaxis. However, flagella are also highly immunogenic and can be recognized by phagocytes. In chronic infections, like CF lung infections, mutants frequently lose their flagella, which may aid in immune evasion (1, 4, 50, 51).

Pili

Type IV pili are hair-like cellular structures sprouting from the surface of the cell's poles. Repeated extension and retraction of the pili, like a grappling hook, enables a form of

movement named twitching motility. Type IV pili may be useful to *P. aeruginosa* for exploring the environment, adhering to abiotic or biotic surfaces, and for biofilm formation. However, they are immunogenic and recognized by the immune system (56, 100, 101).

Secretion systems

P. aeruginosa encodes five different secretion systems (T1SS, T2SS, T3SS, T5SS, and T6SS), each with different structures and functions. These syringe-like cellular appendages, which are structurally similar to phage tails, are used to inject effector proteins into the extracellular environment or into the cytoplasm of bacteria or eukaryotic cells. Specifically, the T3SS and T6SS are capable of injecting effector toxins into eukaryotic host cells. Notably, the T3SS is an important fitness determinant for acute pneumonia infections, as it is used to disrupt lung epithelial tight junctions, allowing dissemination into the bloodstream (64, 102, 103).

Biofilm formation

P. aeruginosa exists in either a free-floating planktonic mode or a biofilm mode of growth, and there are major physiological differences between the two. A biofilm is like a “slime city” (104), where bacterial communities form sessile, aggregate-associated microcolonies covered in a protective coating of extracellular polymeric substances (EPS). The EPS is composed mainly of exopolysaccharides, extracellular DNA, proteins, and lipids. Bacteria growing in biofilms have significantly heightened resistance to ROS and phagocytosis, nutrient or oxygen limitation, and tolerance to antimicrobials (1, 64). Biofilms make it more difficult to eradicate *P. aeruginosa* from abiotic surfaces, such as surgical implants, catheters, and respirators (1). Biofilm formation is also an important component of chronic infections, such as chronic wound infections and CF lung infections (1, 31, 64). *P. aeruginosa* can form mixed-species polymicrobial biofilms with other microorganisms

in these infections, and such biofilms are more antibiotic resistant and virulent than single-species *P. aeruginosa* biofilms (29, 30, 33, 105, 106).

1.6 Quorum sensing and social behaviors[2]

Once thought to be solitary, independent organisms, we now know that bacteria are highly social and are capable of coordinating complex behaviors as a community via cell–cell communication (107). Social behaviors are mainly driven by either competition or cooperation. Cooperation occurs when a behavior benefits another individual (108). Bacteria are most cooperative toward clonal (genetically identical) relatives; since clonal bacteria share identical genes, they have a collective motivation to enhance their population's fitness (ability to survive and reproduce) by cooperating with each other (108). Social communication often regulates behaviors which are effective only at high cell density, such as the production and release of public goods. Public goods are extracellular products that can improve the fitness of neighboring bacteria, making them "social" traits (109). Examples include extracellular digestive proteases and siderophores. Social communication prevents inefficient public goods production at low population densities, when most secreted products would diffuse away rather than benefit the community (110).

The best understood form of bacterial communication is quorum sensing. Quorum sensing is mediated by diffusible signal molecules known as autoinducers (111). The characteristic autoinducer for quorum sensing in Gram-negative bacteria, and in *P. aeruginosa*, is the acyl homoserine lactone, or AHL. AHLs freely diffuse out of and into cells and accumulate in proportion to cell density. After reaching a critical concentration, they bind to and

[2] Parts of this subsection were adapted from the following reference: Michie, K.L., et al., *Bacterial tweets and podcasts# signaling# eavesdropping# microbialfightclub.* Molecular and biochemical parasitology, 208(1), 41-48. DOI: 10.1016/j.molbiopara.2016.05.005. Copyright © Elsevier B.V 2016. Reused with permission. I was the primary author of this work.

activate their cognate cytoplasmic receptors, causing a conformational change in the receptors that allows them to bind DNA and alter the transcription of target genes (111). Receptor-AHL activation also induces a positive feedback loop by increasing the transcription of AHL-synthesis genes, therefore resulting in rapid extracellular accumulation of AHL and a synchronized change in gene expression and behavior in the population. *P. aeruginosa* has three complex and interconnected quorum sensing systems: *las*, *rhl*, and *pqs.* (112, 113).

In *P. aeruginosa*, many genes associated with virulence are under the control of quorum sensing, such as motility (114), biofilm formation (114), antibiotic resistance (115), stress responses (115), and virulence factor production (1, 113). Virulence factors controlled by quorum sensing include extracellular proteases (83, 116), pyocyanin (94), exotoxin A (90), rhamnolipids (86), siderophores (97), and T6SS (103). Because so many different virulence factors are regulated by quorum sensing, it is not surprising that quorum sensing deficient *P. aeruginosa* mutants are often severely attenuated in laboratory models of infection, including lung and soft tissue models (117-119). However, a notable exception is that in the late stages of CF lung infection, *P. aeruginosa* isolates often evolve inactivating mutations in quorum sensing genes (58, 59). Therapeutic interventions aimed at inhibiting quorum sensing are attractive avenues for investigation, and have shown some promise in laboratory models (120-122). One key advantage of quorum sensing inhibitors is that they are unlikely to drive selective pressure for resistance against them, because unlike conventional antibiotics, quorum sensing inhibitors do not kill or inhibit the growth of bacteria, they only suppress virulence gene expression (123-125).

1.7 Laboratory models of *P. aeruginosa* infection

Since human experimentation is unethical, better understanding the infection biology of *P. aeruginosa* necessitates the use of laboratory models. There are a wide variety of commonly used *P. aeruginosa* laboratory models, from cell-free *in vitro* systems to large mammals. Every model has different advantages and disadvantages in terms of cost, ease of use, genetic tractability, ethical considerations, and which aspects of human infection biology are best recapitulated. While no model can perfectly represent a human infection, it is important to consider each model's limitations, which aspects are biologically relevant, and how relevance can be improved.

1.7.1 In vitro and ex vivo model systems

Simple *in vitro* models using culture tubes and undefined complex media, such as LB broth, have been used to elucidate countless important discoveries about *P. aeruginosa* physiology. These systems are relatively inexpensive, easy to manipulate, and can be carried out on large scales. However, there are several drawbacks which may often be overlooked. Notably, the nutritional environment does not reflect a natural environment, there is no spatial structure, and *P. aeruginosa* grows to unrealistically high population densities. Some *in vitro* systems have attempted to better simulate the nutritional composition of human infection environments and introduce host factors. Synthetic cystic fibrosis sputum medium (SCFM) was designed to mimic the nutritional and physical properties of expectorated sputum from CF patients (43). Physiological parameters of *P. aeruginosa*, such as growth rate and gene expression, are similar in SCFM compared with expectorated human CF sputum. Importantly, SCFM has a similar viscosity to human sputum, which provides spatial structure (5, 43, 126). Likewise, a wound-like medium (WLM) was designed to mimic the nutritional environment of a human chronic wound (106,

127). *P. aeruginosa* can grow as a mixed-species biofilm in WLM, and in the presence of *S. aureus*, which clots blood, the WLM even forms spatially structured blood clots (106, 127).

Macrophages and neutrophils are important components of the innate immune defense against *P. aeruginosa* infections. Researchers wishing to study interactions between *P. aeruginosa* and phagocytes can use *in vitro* co-culture systems with these cell types. Neutrophils are short-lived and must be extracted from healthy human volunteers (128), while macrophages can either be freshly extracted or cultured from immortalized cell lines (129, 130). Alternatively, *P. aeruginosa* can be co-cultured with the amoeba *Dictyostelium discoideum*, a natural predator of *P. aeruginosa*. Interactions between *P. aeruginosa* and *Dictyostelium* replicate interactions with phagocytes, and are useful for high-throughput genetic screens of *P. aeruginosa* traits important for resisting phagocytosis and killing by phagocytic cells. It is also useful for screening host phagocyte genes that are important for resistance to *P. aeruginosa* infection. Compared to phagocytes, *Dictyostelium* is easier to grow and genetically manipulate (131-133).

To study interactions between *P. aeruginosa* and particular tissue types, *P. aeruginosa* can be cultured with primary or immortalized cell lines. Primary cells are taken fresh from a living or recently deceased organism and cultured *in vitro*. Primary cells more closely retain the characteristics of intact tissue, but they have a limited lifespan outside the body, making them challenging to obtain and grow. Immortalized cell lines have undergone repeated passaging or genetic manipulation in order to allow them to replicate continuously *in vitro*. They are more convenient to use, more reproducible, and can also be further genetically manipulated to study host genes of interest. However, they often have significant genetic and physiological differences compared to primary cells or parental tissue (134, 135). Commonly used cell types include normal and CFTR knock-

out ciliated lung epithelial cells (89, 136, 137), corneal epithelial cells (138, 139), and skin fibroblasts or keratinocytes (140, 141). These *in vitro* co-culture systems are useful for studying mechanisms of *P. aeruginosa* tissue colonization, the impact of virulence factors on host cell survival, and host cell inflammatory responses to *P. aeruginosa* infection.

Ex vivo models involve co-culturing *P. aeruginosa* in sections of whole organ tissue. Two major advantages of an *ex vivo* organ system are that the tissue slices retain their complex three-dimensional spatial structure, and it allows for cross-talk between all of the different cell types present in a whole organ. An *ex vivo* pig lung model uses pig lungs obtained from commercial butchers. *Ex vivo* pig lungs are physiologically similar to human lungs, are relatively inexpensive, and raise fewer ethical concerns, since the lungs from pigs raised for food are usually discarded (142, 143). Other similar models use rabbit or goat corneas sourced from butchers (144, 145). Organ sections can also be acquired from human donors, including corneas from cadavers (144) and excised skin leftover from surgical procedures (146).

1.7.2 Plant and invertebrate model systems

Plant and invertebrate laboratory models feature whole multicellular organisms with intact but rudimentary immune systems. They are relatively inexpensive, quick and easy to use, high-throughput, genetically tractable, and without ethical restrictions. Therefore, these systems can allow for larger sample sizes than what is feasible with mammalian models. Validating the usefulness of these models, there is strong overlap in the genes necessary for *P. aeruginosa* to cause disease in plants, invertebrates, and mammals.

In nature, *P. aeruginosa* is known to colonize plants and is sometimes a plant pathogen (3, 147). Laboratory plant models of *P. aeruginosa* pathogenesis include the classic model organism *Arabidopsis thaliana* (103, 148-150), as well as mung bean (151), alfalfa (152),

and store-bought lettuce (149). An advantage of plant models is that they allow qualitative (plant growth, tissue damage) and quantitative (bacterial loads) measures of disease progression. These infections can also be relatively long-lived, for example up to 5 or 10 days. Of these models, *Arabidopsis* is the most well characterized, but mung beans grow faster. Store-bought lettuce requires no growing time, but the infections are short (24hrs).

There are several invertebrate laboratory models of *P. aeruginosa* infection, including the nematode *Caenorhabditis elegans* (148, 153-155), the fruit fly *Drosophila melanogaster* (30, 71, 156) and the greater wax moth *Galleria mellonella* (54, 157, 158). *C. elegans* is a soil organism that naturally feeds on bacteria. One advantage of the *C. elegans* model is that fluorescently tagged bacteria colonizing the gut can be easily imaged with fluorescent microscopy. However, the *Drosophila* immune system and tissue structure have more elements in common with mammals (159, 160). Greater wax moth larvae are relatively large (250mg) and can be easily seen without the aid of a microscope, making it easier to inject the bacteria, control bacterial inoculum sizes, and identify dead larvae. One limitation of all three invertebrate systems is that these hosts die very quickly from *P. aeruginosa* infection (usually 24-48hrs, but can survive up to 4 days).

1.7.3 Vertebrate model systems

Vertebrate model systems are more similar to humans in several important ways. For instance, they have similar organ and tissue structures and both innate and adaptive immunity is present. However, vertebrate model systems require strict ethical regulations, specialized facilities, personnel training, and are significantly more expensive. Popular models include zebrafish (*Danio rerio*) (54, 161), mice (*Mus musculus*) (148, 157, 162), rats (*Rattus norvegicus*) (163-167), and pigs (*Sus scrofa domesticus*) (168-171).

Zebrafish are non-mammalian vertebrate models with several useful characteristics. They reproduce quickly in large numbers, their genome is well characterized and relatively tractable, and many mutants are readily available. There are also fewer ethical restraints; experiments performed on zebrafish embryos under 5 days post-fertilization are legally considered *in vitro* experiments (54). Notably, zebrafish embryos are transparent, making it easy to visualize fluorescently labeled bacteria or host cell proteins in whole embryos using fluorescence microscopy (54, 161).

Mice are the most widely used mammalian model of *P. aeruginosa* infection. Four of these infection models, the chronic wound (4, 29), abscess (172, 173), burn wound (4, 174), and acute pneumonia models (175, 176), are discussed in further detail in Chapter 2. Additional models include keratitis (162, 177), intraperitoneal (178, 179), and foreign body surgical implant (180-182). The mouse genome is very well characterized, with many genetic tools, inbred mice and mutant mice available to researchers, such as diabetic (183, 184), CF (169, 185), and immune-deficient mice (177, 186-189). This is a major advantage, since comorbidities and host genetics can significantly impact susceptibility to *P. aeruginosa* infection (187, 190-192). However, there are important physiological differences between mice and humans that are worth considering. For instance, there are species-specific differences in the sensitivity of toll-like receptor 4 (TLR4) to recognize different forms of LPS, with mouse TLR4 tending to be more promiscuous (192, 193). Another difference is that in humans, skin wounds heal primarily by granulation and re-epithelialization, while in mice they heal primarily by contraction (194, 195). Third, since *P. aeruginosa* is an opportunistic pathogen, young and healthy immune-competent mice are generally resistant to *P. aeruginosa* infection. Consequently, mouse models often require high inoculating doses that likely do not recapitulate natural human routes of infection.

While rats are closely related to mice, rats are bigger, making it is easier to take multiple blood draws, work with small organs, perform delicate surgery, and monitor physiological parameters like pulse, temperature, and breathing rate. These characteristics may be desirable for certain infection models, such as ureter stent (165), orthopedic surgical wounds (167), inner ear (90) or septicemia (196). Compared to mice, rat physiology is better characterized and may be closer to humans in some respects (197, 198). However, rats can be more difficult to handle, are more expensive, require more space to house, and the available genomic resources are not yet as developed as they are for mice (198, 199).

The *P. aeruginosa* infection model that is the largest, and arguably the most similar to humans, is the pig. Humans are evolutionarily more closely related to pigs than to rats or mice, and pig anatomy, histology, and metabolism resembles that of humans (200). *P. aeruginosa* infection models include septic shock (170, 201), acute pneumonia (171, 202), and surgical wounds (203, 204). As previously discussed, CF mutant mice have been developed; however, how well they recapitulate the CF disease manifestations that occurs in humans is limited. For instance, it is difficult to establish a long-lasting chronic lung infection (205). CF pig models have been developed that more closely replicate the constellation of disease pathologies seen in human CF patients, including the characteristic inflammation, mucus buildup, and chronic bacterial infection. Studies using CF pigs have been used to identify novel therapeutic targets that weren't apparent in mouse models (168, 169). However, maintaining and experimenting on laboratory pigs requires large and specialized housing facilities, equipment, and training. Genetic resources are also limited. Combined, laboratory experiments involving pig models are very expensive and only allow for small sample sizes.

THE ROLE OF PSEUDOMONAS AERUGINOSA GLUTATHIONE BIOSYNTHESIS IN LUNG AND SOFT TISSUE INFECTION[3]

1.8 Background and significance

To survive in both the environment and in the host, *P. aeruginosa* must cope with redox stress. Glutathione (GSH) is a major cellular regulator of redox homeostasis (206, 207). It is a low molecular weight thiol-containing tripeptide (L-γ-glutamyl-L-cysteinyl-glycine) that can function as a reversible reducing agent by either directly interacting with reactive oxygen (ROS) and nitrogen (RNS) species or indirectly by serving as an enzymatic cofactor (207, 208). GSH is produced by most Gram-negative bacteria, by a few Gram-positive bacteria, and it is ubiquitous and essential in eukaryotic cells (206, 207, 209). Bacteria that do not biosynthesize GSH often produce functionally similar molecules, such as mycothiol or bacillithiol (210-212). In addition to protection from oxidative and nitrosative stress, GSH is involved in many important cellular functions, such as detoxification of electrophilic compounds, lipid peroxides, toxic metabolites and xenobiotics; regulation of cellular osmolality and pH (206, 213); and metal homeostasis (206, 207).

[3] This chapter was adapted from the following reference: Michie, K.L., et al., *The Role of Pseudomonas aeruginosa Glutathione Biosynthesis in Lung and Soft Tissue Infection.* Infection and Immunity, 2020 IAI.00116-20; DOI: 10.1128/IAI.00116-20. Copyright © American Society for Microbiology 2020. Reused with permission. I was the primary author of this work.

In *P. aeruginosa*, genetic defects in GSH biosynthesis result in a myriad of altered phenotypes both *in vitro* and *in vivo* that suggest an important role during infection. GSH biosynthesis has been shown to affect quorum sensing (214), T3SS and T6SS (176), production of the secondary metabolites pyocyanin and pyoverdine (71, 215), motility (71, 176, 215), biofilm formation (71, 176, 215), sensitivity to oxidative and nitrosative stress (71, 176, 215), and sensitivity to antibiotics (216, 217). GSH-deficient *P. aeruginosa* mutants have attenuated virulence in *Drosophila* (71) and *C. elegans* infection models (155), as well as a mouse model of acute pneumonia (176). Glutathione-deficient mutants in other bacterial species are also attenuated for virulence in mouse models of infection, including *Salmonella enterica* in an intraperitoneal model (218), *Listeria monocytogenes* in an intravenous model (208), and *Burkholderia pseudomallei* in an acute pneumonia model (219).

A large number of *in vitro* and *in vivo* models are used to study *P. aeruginosa* virulence, and it is clear that the traits required for *P. aeruginosa* fitness in these models can vary (4-6). This may be due to differences in nutrient availability, innate immune defenses, or other environmental factors, such as oxygen tension or pH. However, the role of GSH for *P. aeruginosa* pathogenesis in mammalian infection, particularly in different sites of infection, is still unclear. In this study, we first examined how GSH deficiency affects *P. aeruginosa*'s growth rate and susceptibility to antimicrobials *in vitro*. We then explored how GSH deficiency affects the fitness of *P. aeruginosa* in four mouse models of infection, including surgical wound, abscess, burn wound, and acute pneumonia models.

1.9 *P. aeruginosa* requires GSH for normal growth *in vitro*

In *P. aeruginosa*, GSH biosynthesis is catalyzed by a two-step reaction. In the rate-limiting first step, γ-glutamylcysteine synthetase, the product of the *gshA* gene, produces γ-

glutamylcysteine. In the second step, GSH is produced from γ-glutamatecysteine by glutathione synthetase, the product of the *gshB* gene (206, 207). To study the importance of GSH biosynthesis in *P. aeruginosa* biology, we constructed a *gshA* deletion mutant (Δ*gshA*) in the *P. aeruginosa* strain PAO1 background. We chose to inactivate *gshA* and not *gshB* not only because it disrupts the first step in glutathione biosynthesis, but also because *gshB* mutants still produce γ-glutamylcysteine, which can partially compensate for GSH (220). This is likely the reason why *P. aeruginosa gshA* mutants generally have a more severe growth rate and antimicrobial tolerance defect than *gshB* mutants (71, 221).

Previous studies have shown that *P. aeruginosa* Δ*gshA* has a growth defect in minimal media, but growth rates are restored to wild-type (WT) levels in LB broth (215). However, an explanation for the differences in growth rate for *gshA* mutants in the two media was unclear. To address this question, we measured the growth rates of *P. aeruginosa* WT and Δ*gshA* in several media. We tested MOPS (3-(N-morpholino)propanesulfonic acid) minimal medium supplemented with 20 mM glucose (MOPS-glucose), MOPS-glucose containing 1 mM GSH, MOPS-glucose containing yeast extract (5 g/L), MOPS-glucose containing tryptone (10 g/L), chemically defined media (CDM) (222), and LB broth. We selected 1 mM GSH because this concentration is within the range of typical intracellular GSH concentrations (215, 223-225). We chose 5 g/L yeast extract and 10 g/L of tryptone as these are the concentrations present in LB. Finally, CDM is a rich chemically defined media that contains all amino acids and nucleotides and many metabolites essential for growth, but it does not contain GSH (222).

Consistent with previous studies (215), we observed a growth rate defect for *P. aeruginosa* Δ*gshA* compared to the WT in MOPS-glucose, but not in LB (**Figure 1**). While it was previously hypothesized that the reason for this difference in growth rate was stress caused by nutritional restriction in minimal media (215), we discovered that *P. aeruginosa*

Δ*gshA* also exhibited a growth rate defect in CDM, a rich defined medium, as well as MOPS-glucose + tryptone. These data indicate that nutritional stress is unlikely to be the cause of the growth rate defect for *P. aeruginosa* Δ*gshA* in MOPS-glucose. Importantly, the growth rate of the mutant was restored to WT levels with the addition of GSH or yeast extract. GSH is abundant in yeast cells (226), thus the growth rate of *P. aeruginosa* Δ*gshA* is likely restored to WT levels in LB due to the presence of GSH in yeast extract.

These results underscore the importance of using a medium that does not contain GSH when studying GSH biosynthesis, since the presence of GSH in growth medium such as LB can confound interpretation of experimental results. For example, compared to WT, GSH-deficient *P. aeruginosa* mutants reportedly produce less biofilm when grown in M9 minimal media (215) compared to LB (71), likely because of the high levels of GSH in the yeast extract component of LB (226). Furthermore, unbuffered GSH added to media at high concentrations, such as 10 mM, can significantly lower the pH of the media and induce an acid shock response in bacteria (209). Finally, even bacteria grown in the same media, but in different culture vessels or culture volumes, display greatly different oxidative stress responses (227). Taken together, the experimental growth environment should be carefully considered, and differences in growth conditions between laboratories likely explain conflicting findings.

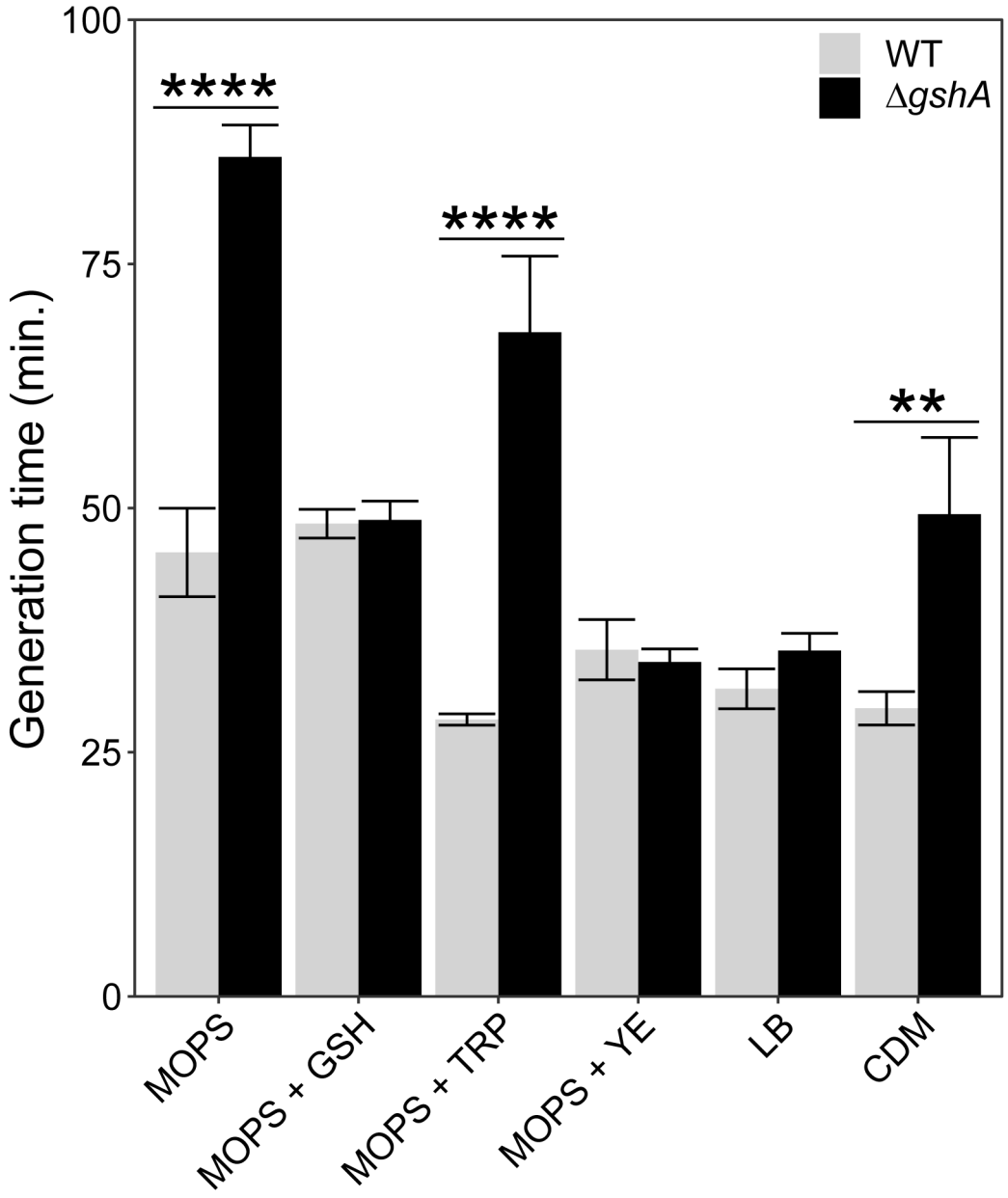

Figure 1. Growth rates of *P. aeruginosa* WT and Δ*gshA* in different media. n = 3-5. *P* value ** < 0.01, **** < 0.0001 using two-way ANOVA followed by Bonferroni's multiple comparisons test with 95% confidence interval. Error bars represent 1 standard error. GSH = glutathione, TRP = tryptone, YE = yeast extract, CDM = chemically defined media.

1.10 *P. aeruginosa* requires GSH for protection against some disinfectants and antibiotics

GSH has been implicated in tolerance to several antimicrobials. To kill bacteria during infection, neutrophils and macrophages produce ROS such as hydrogen peroxide (H_2O_2) and hypochlorous acid (HOCl) (228, 229). GSH is one of the cell's primary mechanisms for protection against ROS (206, 207), and GSH-deficient *P. aeruginosa* mutants are sensitive to ROS-generating agents including methyl viologen and paraquat (71, 215). Several recent studies have also argued that different classes of bactericidal antibiotics, but not bacteriostatic antibiotics, can generate ROS and kill bacteria through secondary mechanisms (196, 230). In some Gram-negative bacteria, GSH also helps maintain cellular osmolality by regulating intracellular K+ (206, 213) and mutants that are deficient in either GSH biosynthesis or in K+ transport are hypersusceptible to antimicrobial peptides (AMPs) (231-234).

To explore the role of GSH biosynthesis in protection from different antimicrobials in *P. aeruginosa*, we performed disc diffusion assays with a panel of disinfectants and antibiotics (**Table 1**). We grew *P. aeruginosa* WT and Δ*gshA* on MOPS-glucose + tryptone agar plates with or without 1 mM GSH, representing permissive and non-permissive conditions for the Δ*gshA* mutant, respectively. We tested two disinfectants: hydrogen peroxide and bleach (NaOCl), and six antibiotics: polymyxin B, colistin, ciprofloxacin, carbenicillin, tetracycline, and chloramphenicol. Polymyxin B and colistin are both bactericidal AMPs (64), ciprofloxacin and carbenicillin are both bactericidal antibiotics, and tetracycline and chloramphenicol are bacteriostatic antibiotics.

As shown in **Table 1**, *P. aeruginosa* Δ*gshA* had a larger zone of inhibition (ZOI) compared to the WT when exposed to hydrogen peroxide or bleach, and the ZOI was restored to WT

levels with the addition of GSH. *P. aeruginosa* Δ*gshA* was also more susceptible to the bactericidal antibiotic ciprofloxacin; however, this enhanced susceptibility was not chemically complemented by addition of GSH. *P. aeruginosa* Δ*gshA* was also slightly more resistant to the bactericidal antibiotic carbenicillin (*P* = 0.079). Finally, we observed no difference in the ZOI for *P. aeruginosa* Δ*gshA* compared to WT when treated with the AMPs polymyxin B and colistin or the bacteriostatic antibiotics chloramphenicol and tetracycline.

Taken together, these results show that *P. aeruginosa* GSH is critical for protection from ROS. In previous transposon sequencing (Tn-seq) experiments that assessed the fitness of thousands of *P. aeruginosa* mutants simultaneously upon exposure to antimicrobials, a similar fitness defect for *P. aeruginosa gshA* mutants was observed upon exposure to bleach, but not to H_2O_2 (221). This lack of a fitness defect upon exposure to H_2O_2 was likely due to rapid detoxification of H_2O_2 by *P. aeruginosa* catalases, which prevented identification of a number of functions important for *P. aeruginosa* H_2O_2 tolerance in that study (221). The importance of GSH for tolerance to ROS raises the possibility that GSH biosynthesis inhibitors may be a reasonable therapeutic strategy for enhancing bacterial clearance by host-generated ROS or certain antibiotics. However, this approach would likely require development of GSH biosynthesis inhibitors that are bacteria specific, as common non-specific GSH inhibitors, such as buthionine sulfoximine (BSO) (223) or diethylmaletate (DEM) (235), are also toxic to eukaryotic host cells.

Table 1. *P. aeruginosa* zones of inhibition following exposure to 8 antimicrobials. The average zone of inhibition (measured in millimeters ± standard error of the mean) for *P. aeruginosa* WT and Δ*gshA* with or without 1 mM glutathione (GSH) added to the media. n = 3-8 for each condition. *P* values < 0.05 by using two-way ANOVA followed by Bonferroni's multiple comparisons test with 95% confidence interval are indicated in bold.

Antimicrobial	**GSH**	**WT**	**Δ*gshA***	***P* value**
Hydrogen peroxide	-	38.0 ± 0.9	49.6 ± 1.9	**<0.0001**
	+	38.3 ± 1.1	39.3 ± 1.2	>0.9999
Bleach	-	37.0 ± 2.1	47.4 ± 1.3	**0.0002**
	+	21.3 ± 1.8	22.3 ± 2.2	>0.9999
Polymyxin B	-	13.8 ± 0.2	16.0 ± 0.4	>0.9999
	+	13.8 ± 0.4	15.2 ± 0.6	>0.9999
Colistin	-	15.0 ± 0.3	18.1 ± 0.6	0.4750
	+	14.9 ± 0.3	16.0 ± 0.6	>0.9999
Ciprofloxacin	-	28.4 ± 0.9	35.8 ± 1.6	**<0.0001**
	+	27.9 ± 0.8	36.6 ± 1.6	**<0.0001**
Carbenicillin	-	19.9 ± 1.5	14.3 ± 0.6	0.0789
	+	17.6 ± 1.1	14.4 ± 1.3	>0.9999
Tetracycline	-	10.9 ± 0.8	8.8 ± 2.7	>0.9999
	+	10.6 ± 0.7	12.3 ± 0.7	>0.9999
Chloramphenicol	-	14.3 ± 1.6	14.3 ± 1.2	>0.9999
	+	13.3 ± 1.0	13.1 ± 0.8	>0.9999

The slight increase in tolerance to carbenicillin (**Table 1**) is likely due to the slower growth rate of *P. aeruginosa* Δ*gshA* in MOPS-glucose + tryptone (**Figure 1**), as it is known that slower growing cells are more resistant to the beta-lactam class of antibiotics (236, 237). This phenotype was mitigated by the addition of GSH, although this was due to an increase in tolerance of WT *P. aeruginosa* to carbenicillin in the presence of GSH. Thus, the mechanisms controlling carbenicillin tolerance and GSH is more complex than that observed for ROS. The mechanism of ciprofloxacin hypersusceptibility also appears complex, as tolerance of *P. aeruginosa* Δ*gshA* was not restored by addition of GSH. Finally, *P. aeruginosa* Δ*gshA* showed no change in tolerance to AMPs as has been observed in other bacteria (231), although this does agree with recent Tn-seq data showing that inactivation of *gshA* had no effect on *P. aeruginosa* fitness in the presence of polymyxin B (221).

1.11 GSH biosynthesis provides a fitness benefit to *P. aeruginosa* in a mouse model of acute pneumonia, but is dispensable in surgical wound, abscess, and acute burn wound infections

As discussed in Chapter 1, *P. aeruginosa* is a versatile pathogen that can infect multiple body sites, among the most common of which are soft tissues and lungs. *P. aeruginosa* is one of the most common organisms isolated from human chronic wound infections, burn wound infections, and hospital-associated acute pneumonia, and the presence of *P. aeruginosa* in these infections is also associated with increased infection severity and mortality (33, 41, 63, 64, 238). Previous studies (71, 155, 176, 214, 215), as well as our *in vitro* experiments, suggest an important role for GSH biosynthesis for *P. aeruginosa* during infection. Here, we comprehensively assessed the fitness of *P. aeruginosa* WT and Δ*gshA* in four mouse models of infection: the surgical wound, abscess, acute burn wound, and acute pneumonia models.

We first tested two non-lethal soft tissue infection models. The surgical wound mouse model involves surgically removing a full-thickness area of skin from the shaved backs of the mice, applying a semipermeable bandage over the wound, and administering the bacterial inoculum to the wound topically underneath the bandage (4, 29, 239, 240). The abscess model involves a subcutaneous injection of bacteria into the shaved inner thigh of the mice (241, 242). For both models, we infected mice with ~10^6 CFUs of *P. aeruginosa* WT or Δ*gshA* and enumerated bacterial loads after 4 and 3 days post-infection for the surgical wound and abscess models, respectively. Results from these experiments revealed no significant difference between bacterial loads for the Δ*gshA* mutant compared to the WT in the surgical wound model (**Figure 2A**) or in the abscess model (**Figure 2B**).

We next tested two lethal mouse infection models, the acute burn wound and acute pneumonia models. The mouse burn wound model (4, 174) involves exposing the shaved backs of mice to 90°C water for 10 seconds, creating a uniform third-degree burn. The acute pneumonia model (175, 243) involves a non-invasive intratracheal administration of bacteria directly into the lung. We infected mice with ~10^3 CFU and 2.5x10^7 CFU *P. aeruginosa* WT and Δ*gshA* for the burn model and the pneumonia model, respectively. Survival was monitored over a period of seven days.

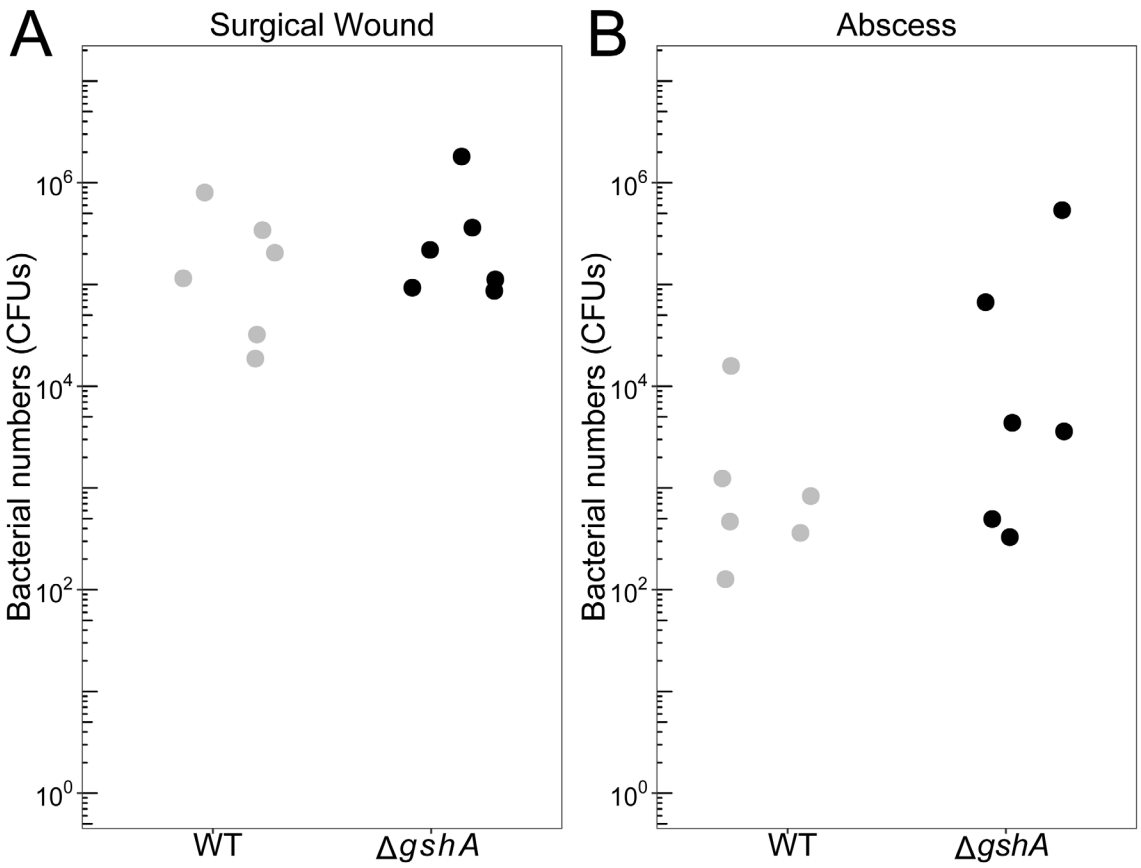

Figure 2. Surgical wound and abscess mouse infection models. Mice were infected with approximately 1x10^6 CFUs of *P. aeruginosa* WT or Δ*gshA* in the (A) surgical wound and (B) abscess mouse models of infection. Mice were sacrificed at 4 and 3 days post-infection, respectively. Mouse infections were performed with three mice in each group and repeated independently twice, n = 6.

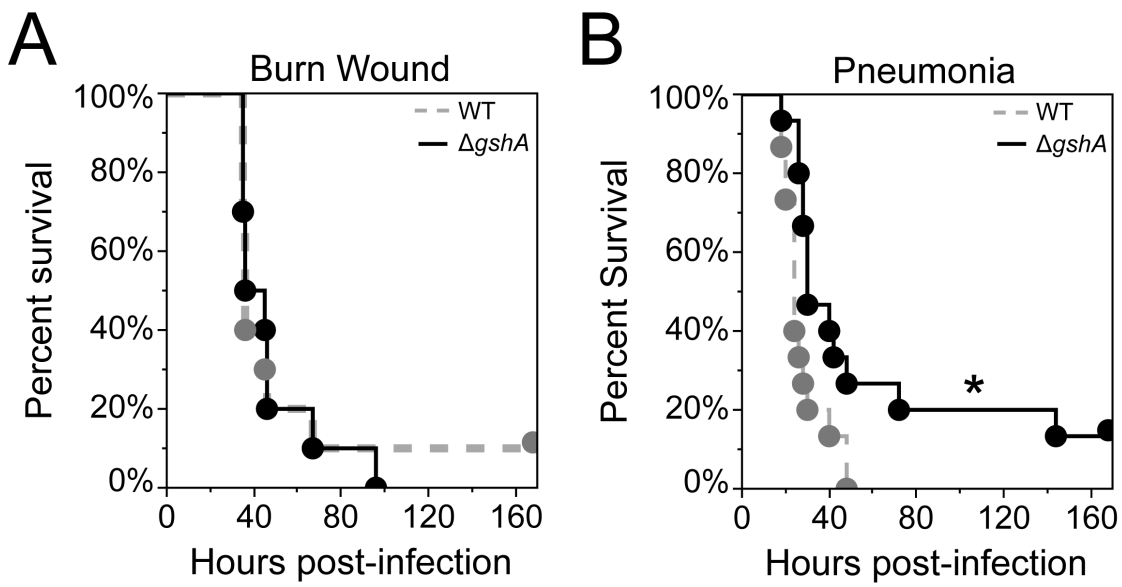

Figure 3. Burn wound and acute pneumonia infection models. (A) For the mouse burn wound infection model, mice were infected with approximately $1x10^3$ CFUs of WT or Δ*gshA P. aeruginosa*. Experiments were performed with five mice in each group and repeated independently twice, n = 10. (B) For the mouse acute pneumonia infection, mice were infected with approximately $2.5x10^7$ CFUs (2X LD_{50}) of *P. aeruginosa*. Mouse infections were performed with five mice in each group and repeated independently three times, n = 15. All mice were monitored for 7 days or until moribund and humanely euthanized. Results are represented as Kaplan-Meier survival curves; differences in survival were calculated by the log-rank test. *, $P < 0.05$.

As shown in **Figure 3A**, there was no significant difference in survival between mice infected with *P. aeruginosa* WT or Δ*gshA* in the burn wound model. However, in the pneumonia model (**Figure 3B**) we observed a modest but statistically significant increase in survival for mice infected with *P. aeruginosa* Δ*gshA* compared to the WT. The pneumonia model data are consistent with a previous study showing decreased bacterial loads in the lung for *P. aeruginosa* Δ*gshA* in a mouse acute pneumonia model (176). The increased importance of GSH biosynthesis for *P. aeruginosa* in the lung and not soft tissue is likely explained by the fact that GSH-deficient *P. aeruginosa* mutants have reduced expression of T3SS (176) which is important for lung pathogenesis (64), as discussed in Chapter 1.5.

1.12 Discussion

While *P. aeruginosa* Δ*gshA* does show a statistically significant decrease in lethality in the pneumonia model, the effect is quite modest compared to other mutants that are considered attenuated in this model, such as *rhlR* (175) and *aroA* (244). These results, along with the lack of an infection phenotype for *P. aeruginosa* Δ*gshA* in the burn, surgical wound and abscess mouse models reveal that GSH biosynthesis plays little if any role in virulence in commonly used mouse models of *P. aeruginosa* infection. This result is somewhat surprising given the role of GSH in the pathogenesis of other bacteria, the high susceptibility of *P. aeruginosa* Δ*gshA* to ROS (**Table 1**), as well as the heightened inflammatory responses, oxidative stress and tissue GSH depletion that are characteristic of the mouse models that we used (18, 19, 34-36, 245).

One simple explanation for our results is that *P. aeruginosa* can scavenge sufficient bioavailable glutathione from the host in these infection models, despite the lowered tissue

GSH levels associated with infection, thus mitigating the Δ*gshA* phenotype. This explanation is supported by previous Tn-seq studies showing that *P. aeruginosa gshA* mutants were more fit in the burn and surgical wound mouse models than in a minimal MOPS-succinate medium without added GSH (4). These studies also indicate that the *gshA* mutant is not *trans*-complemented by the other *P. aeruginosa* mutants in the infection, thus GSH does not appear to be a social good that is shared amongst community members (as discussed in Chapter 1.6) (4). It should be noted that we followed commonly used methodology in our experiments including method of inoculation and inoculating dose. Thus, while we think it is unlikely based on the diversity of models and inoculating doses used, it is possible that altering these parameters could change the outcome of our experiments and reveal a role for GSH biosynthesis in *P. aeruginosa* pathogenesis.

Due to its potent antioxidant properties, there is increasing interest in using GSH as a treatment strategy for a variety of human pathologies. Uncontrolled oxidative stress is a key pathophysiological feature of chronic wounds (246), burn wounds (34), and pneumonia (245, 247). Experimental rodent and human clinical studies have shown that administration of GSH can result in significantly improved healing, reduced tissue damage, and lower mortality in chronic wounds (248, 249), burn wounds (35, 250, 251), and pneumonia (252-254). However, it is unclear how administration of GSH in human subjects will affect the physiology of *P. aeruginosa* during infection. While our *in vitro* data suggest that inhibiting GSH biosynthesis may render *P. aeruginosa* more susceptible to ROS, addition of GSH can restore tolerance to the *gshA* mutant and in some cases alter the tolerance of WT *P. aeruginosa* (**Table 1**). Thus, GSH administration may in fact promote unwanted *P. aeruginosa*-mediated infection phenotypes. Further studies are necessary to elucidate the safety and efficacy of GSH administration during *P. aeruginosa*

infection. In conclusion, our results provide new and complementary data regarding the role of GSH in *P. aeruginosa* virulence.

1.13 Materials and methods

Bacterial strains and growth media.

P. aeruginosa strain PAO1 was obtained from Colin Manoil (University of Washington). The PAO1 Δ*gshA* deletion mutant was constructed as previously described (5). Briefly, ~700-bp fragments flanking the *gshA* gene were amplified by PCR with Phusion hot start II DNA polymerase (Thermo Scientific, Waltham, MA) to replace the coding sequence with the sequence 5′-GCGGCCGCC-3′ flanked by the native start codon. The PCR primers were 5'-TTCTGCAGGTCGACTCTAGACGAGAAGGTCGAAGGCCAGC-3' and 5'-CCGGCTTGGCTCGGGATTCCTTGTGATCGCGT-3' for the upstream region and 5'-GAATCCCGAGCCAAGCCGGCGCGCC-3' and 5'-GAATTCGAGCTCGAGCCCGGGCTTGCTGGACGCATCCGGC-3' for the downstream region. These two amplicons and the suicide vector pEXG2 (255) were assembled using Gibson assembly as described previously (256), transformed initially into *Escherichia coli* DH5α λpir, and then transformed into *E. coli* SM10 λpir for conjugation into *P. aeruginosa* strain PAO1. Successful transconjugates were selected for with gentamicin followed by selection on sucrose to obtain the chromosomal deletion. This mutation was then verified by PCR. For routine growth, *P. aeruginosa* strains were grown on LB agar plates overnight. Unless otherwise stated, overnight *P. aeruginosa* cultures from single colonies on the LB agar plates were grown in 3-(N-morpholino)propanesulfonic acid acid (MOPS)-buffered minimal medium with 20mM glucose (MOPS-glucose), which does not contain GSH.

Growth curves

P. aeruginosa WT PAO1 or Δ*gshA* were grown overnight in either MOPS-glucose, MOPS-glucose + 1mM GSH (L-Glutathione reduced, Sigma), MOPS-glucose + 5g/L yeast extract (Sigma), MOPS-glucose + 10g/L Bacto tryptone (Fisher), LB broth (Fisher), or a rich, chemically defined medium (CDM) (222). Subcultures were diluted in the same medium to an OD_{600} of 0.05 and grown in culture tubes at 37°C shaking. OD_{600} measurements were recorded by diluting subculture samples to between 0.09 and 0.5. The generation times were calculated using OD_{600} measurements taken during exponential growth.

Disc diffusion assays

Overnight *P. aeruginosa* cultures were grown in MOPS-glucose, adjusted to an OD of 0.4, and swabbed onto MOPS-glucose + tryptone agar plates (MOPS-glucose supplemented with 10g/L Bacto tryptone, Fisher) with or without added 1mM GSH. Sterile quarter-inch filter discs were placed on the center of each plate, and 20 µL of each compound tested was pipetted onto the disc. Stock concentrations of each antibiotic (Polymyxin B, Sigma; Colistin, Sigma; Ciprofloxacin, Sigma; Carbenicillin, Alfa Aesar; Tetracycline, Sigma; Chloramphenicol, IBI Scientific) were dissolved at concentrations of 1 mg/ml. For the disinfectants, 3% hydrogen peroxide or 0.85% sodium hypochlorite was used. An additional 20 µL of hydrogen peroxide was added onto the hydrogen peroxide plates after 7 hr of growth. Plates were incubated at 37°C overnight. Two measurements of the diameter of the zone of inhibition were recorded for each plate and averaged.

Mouse infections

All mouse procedures were carried out in strict accordance with established guidelines at each respective university following recommendations in the Guide for the Care and Use of Laboratory Animals (257) of the National Institute of Health as well as local, state, and

federal laws. For all mouse experiments, *P. aeruginosa* strains were struck on LB agar plates, grown overnight in LB broth, then subcultured in LB broth to logarithmic phase growth. Bacterial inoculums were diluted to the appropriate OD_{600} in PBS.

For the mouse acute thermal injury infection model (also referred to as the “mouse burn wound model’) (4, 174), all animals were treated humanely and in accordance with protocol number 96020 approved by the Institutional Animal Care and Use Committee (IACUC) at Texas Tech University Health Sciences Center in Lubbock, TX. Adult 6-8 week-old female Swiss Webster mice (Charles River Laboratories, Inc.) weighing between 20 and 25 grams, were anesthetized by intraperitoneal injection of 100 mg/kg sodium pentobarbital (Nembutal; Diamondback Drugs). Their backs were then shaved and the remaining hair was removed with a depilatory agent (Nair). Prior to injury, 0.5 mg/kg buprenorphine (ZooPharm) was administered subcutaneously for pain management. A 15% total body surface area, third-degree, full-thickness thermal injury was induced by submerging an exposed area of the dorsal surface in a 90°C water bath for 10 seconds. Mice were then given a subcutaneous injection of 500 µl physiological saline for fluid support. 100 µl of approximately 10^3 CFU of either *P. aeruginosa* PAO1 WT or Δ*gshA* were injected subcutaneously directly underneath the freshly injured tissue. The animals were then monitored for 7 days post-injury and infection for signs of sepsis (lethargy, weight-loss, tremors, etc.). In the event that mice became moribund, they were euthanized by intraperitoneal injection of 200 µl (390 mg/ml) Fatal-Plus (Vortech Pharmaceuticals, Ltd.) and included in the experimental results. Surviving mice were similarly euthanized after the 7-day experimental end-point.

For the mouse surgical incision infection model (also referred to as the “mouse chronic wound model”) (4, 29), Female 6-8 week-old adult Swiss Webster mice weighing between 20 and 25 grams were anesthetized by intraperitoneal injection of 100 mg/kg sodium

pentobarbital. Their backs were then shaved and the remaining hair was removed with a depilatory agent. Prior to injury, animals were given 0.5 mg/kg buprenorphine subcutaneously for pain management. A dorsal, 1.5 x 1.5 cm excisional skin wound to the level of the panniculus muscle was administered. Wounds were then covered with a transparent, semipermeable polyurethane dressings (OPSITE dressings). 100 µl of ~$1x10^6$ CFU of bacterial cells were injected under the dressing on top of the wound to establish the infection. The adhesive dressing prevents contractile healing and ensures that these wounds heal by deposition of granulation tissue, much like human wounds. After four days post-infection the animals were sacrificed by intraperitoneal injection of 200 µl (390 mg/ml) Fatal-Plus and wounds were harvested. Wounds were homogenized in PBS for 30 seconds in BeadBug tubes with 2.8-mm steel beads (Sigma-Aldrich) using a Mini-Beadbeater-16 (BioSpec Products). Bacterial loads in the wounds were enumerated by serial dilution and plating on Pseudomonas Isolation Agar (Sigma).

For the mouse acute pneumonia model (175, 243), all animals were treated humanely and in accordance with protocol number DAR-201700441 approved by the IACUC at Emory University in Atlanta, GA. Adult 6-8 week-old female BALB/c mice (Jackson Laboratories, Bar Harbor, ME) were anesthetized by an intraperitoneal injection of 200 µl of a mixture of (80 mg/kg) ketamine and (10mg/kg) xylaxine (Med-Vet International). Mice were infected by non-invasive intratracheal instillation of 50 µl of ~$2.5x10^7$ CFU ($2xLD_{50}$) of *P. aeruginosa* PAO1 WT or Δ*gshA*. The animals were then monitored for 7 days post-infection for survival. In the event that mice became moribund, they were humanely euthanized by CO_2 asphyxiation and included in the experimental results. Surviving mice were similarly euthanized after the 7-day experimental end-point.

For the mouse abscess model (241, 242), all animals were treated humanely and in accordance with protocol number 00136 approved by the IACUC of The University of

Texas at Austin (Austin, TX) and protocol number A17086 approved by the IACUC of Georgia Institute of Technology (Atlanta, GA). Adult 6-8 week-old female Swiss Webster mice (Charles River Laboratories, Inc.) were anesthetized with inhaled isoflurane (1-3% for maintenance; up to 5% for induction) in oxygen from a precision vaporizer. While anesthetized, their inner thigh was shaved and any remaining hair removed with a depilatory agent (Nair). A 75% ethanol solution was used to clean the area prior to infection. Abscesses were initiated by injecting 100 µL of approximately $1x10^6$ CFU of *P. aeruginosa* PAO1 WT or Δ*gshA* subcutaneously into the inner thigh. Mice were monitored for signs of sepsis, and in the event that mice became moribund, they were humanely euthanized by CO_2 asphyxiation. Three days post-infection, mice were euthanized by CO_2 asphyxiation and abscesses were harvested. Abscesses were homogenized in PBS for 30 seconds in BeadBug tubes with 2.8-mm steel beads (Sigma-Aldrich) using a Mini-Beadbeater-16 (BioSpec Products). Bacterial loads were enumerated by serial dilution and plating on Pseudomonas Isolation Agar (Sigma).

TRANSCRIPTOMIC AND PROTEOMIC SIGNATURES OF GROWTH RATE IN *PSEUDOMONAS AERUGINOSA* GROWN IN CHEMOSTATS

1.14 Background and significance

Bacteria live in diverse, continuously fluctuating environments. To survive, they must be able to adapt to rapid changes in environmental conditions such as temperature, pH, osmolarity, oxygen level, nutrient availability, and the presence of stressors like toxins and antibiotics. Accordingly, bacteria have evolved sophisticated systems for sensing their environment and adjusting their cellular growth rate to suit their current environmental conditions (258-260). Many important aspects of cellular physiology change with respect to growth rate (also known as generation time). For example, cellular morphology and macromolecular composition vary greatly with growth rate; compared to slow-growing cells, fast-growing cells are larger and contain more DNA, RNA, protein, lipids, carbohydrates, and ribosomes (258, 261, 262). Importantly, clinically-relevant cellular behaviors are also dependent on generation time, such as production of virulence factors (263, 264), stress resistance (265-267) and antibiotic susceptibility (268-270). However, despite the importance of the relationship between growth rate and cellular physiology, most laboratory experiments are performed during only the rapid logarithmic phase of growth, leaving cellular physiology at slower growth rates is less well understood.

During infection, bacteria are thought to grow at a wide range of doubling times depending on the stage of infection, activity of the immune system, and nutrient availability. These

growth rates are likely slower than the rapid, maximal growth rates achieved in standard laboratory cultures. Determining the rate of bacterial growth during infection is not trivial, but several approaches have been used, including use of superinfecting phage (271), radio isotope labeling (262), and quantitative fluorescence in situ hybridization (FISH) (272-274). Depending on the infecting organism, culturing conditions, type of infection and measurement technique, recorded bacterial generation times during infection range from 1 to 10 hours, or they are found to be non-growing (262, 271-273). This is in contrast to the *in vitro* maximal generation times for the same organisms ranging between about 0.5 and 1 hr (262, 271-273). This information emphasizes the importance of better understanding both how quickly bacteria grow in the host during infection and also how bacterial physiology changes with growth rate.

Knowing, and controlling for, the impact of growth rate on cellular physiology is also critically important for more accurately interpreting experimental results. Experimental conditions of interest often inadvertently affect cellular growth rate; for example, experiments involving changes in media composition, oxygen availability, and exposure to stressors will also cause a change in growth rate. However, without a growth-rate control, it is often difficult if not impossible to distinguish between the physiological effects caused by the experimental condition of interest and those caused by changes in growth rate. This problem is particularly pronounced in high-throughput –omics experiments, such as differential transcriptome or proteome profiling. For example, in an RNA-seq experiment comparing yeast subjected to a variety of stressful conditions, many genes were initially identified as part of a general stress tolerance response (275). However, when compared to yeast grown in the same media but at different growth rates, most of these “stress tolerance genes” were actually strongly correlated with slow growth (276). Furthermore, in many published datasets, the cellular growth rate is often unmeasured

and left undefined as simply “logarithmic phase growth”, making it difficult to compare data across experiments. For these reasons, it is important to carefully consider the effect of growth rate when interpreting experimental results.

Precisely controlling growth rate in the laboratory can be challenging. Common methods of altering bacterial growth rate include varying media composition (258, 277), temperature (278, 279), or adding stressors (280, 281). However, changing each of these conditions will also cause alterations in cellular physiology that are independent of growth rate. Furthermore, use of traditional closed culture systems, such as culture tubes or flasks, results in measurements that are imprecise and variable. This is because the environment in a closed-culture system is constantly in flux. Following initial inoculation, bacteria grow at a maximal rate, but as nutrients are depleted, the pH changes and toxic metabolic byproducts accumulate, causing growth to slow and cells transition to stationary phase. A more precise method to control cellular growth is the use of a continuous culture system called a chemostat (282-285). In a chemostat, bacteria grow at a near steady-state equilibrium where both the cellular density and growth rate is kept constant over an indefinite period of time. The media contains a growth-limiting concentration of an essential nutrient, which allows the bacterial density to be kept near-constant. The bacterial growth rate is thus proportional to the media flow rate. Previous studies have demonstrated that cellular physiological responses during growth in a chemostat are more consistent and reproducible than growth in culture tubes or flasks (282).

As discussed in section 1.7, there are many laboratory models of bacterial infection, including *in vitro*, invertebrate and vertebrate models. However, every model has its own limitations in how accurately it replicates human infections. One powerful advantage of RNA-seq is that it can be used on bacteria sampled directly from human infections. RNA-seq works by capturing a gene expression “snapshot” from bacterial populations. RNA-

seq data from human infection samples performed in this lab (286, 287) and in others (288-290) have been used to infer attributes of the human infection environment (such as oxygen or iron availability) and to identify functions that may be important for bacterial fitness during infection. However, one issue when interpreting RNA-seq data is that there is a general assumption that mRNA expression is proportional to protein expression. For example, if we observe increased mRNA expression for a gene in a human infection sample, we assume that the corresponding protein expression will also be higher. However, due to disparate rates of mRNA and protein degradation, as well as mechanisms of post-transcriptional, translational, and post-translational regulation, for a given gene the corresponding mRNA and protein levels may be weakly correlated (291-294). Importantly, these correlations are not static, and can vary by strain (292) or growth phase (291).

For this study, we sought to characterize global patterns of gene and protein expression over a broad range of growth rates in *P. aeruginosa*. We generated a carefully controlled benchmark dataset by culturing *P. aeruginosa* in MOPS-succinate minimal medium at several defined growth rates using a chemostat. Bacteria were sampled 3.3-, 6.0-, 13.8-, and 25.3-hr doubling times, and mRNA and protein abundances were quantified using RNA-seq and proteomics mass spectrometry, respectively. From our analysis we observe only modest correlations between mRNA and protein expression, and these correlations differ by growth rate. Both mRNA and protein expression are impacted by growth rate, but there are distinct effects on each. There tends to be more variation in the mRNA data compared to the protein data. Globally, for a given individual gene, the mRNA has a greater range and variation in expression across growth rates than the protein. At the same time, differences in the protein-to-mRNA ratio for a given gene are driven largely by protein expression rather than mRNA expression.

These results demonstrate that the assumption of a 1:1 protein to mRNA ratio doesn't hold. Rather, the relationship between mRNA and protein expression, and how they are affected by changes in cellular growth rate, are complex.

1.15 mRNA and protein expression levels cluster by growth rate

Commercially available chemostats are typically very expensive. For this study, we modified a previous design (282) for a simple assembly built from common laboratory glassware and equipment that should be affordable for most laboratories. Using this chemostat, we grew *P. aeruginosa* strain PA14, a clinical human chronic wound isolate, in MOPS minimal medium containing 10mM succinate as the sole carbon and energy source (MOPS-succinate). We started with MOPS-succinate minimal media because *P. aeruginosa* succinate metabolism is relatively simple, well characterized, and reproducible (4, 221, 286). We sampled bacteria maintained at 3.3-, 6.0-, 13.8-, and 25.3-hr doubling times. This range spans the doubling times that *P. aeruginosa* is likely to grow at during human infection (262, 271-273). We collected 16 samples for RNA-seq analysis (4 from each growth rate) and 10 samples for proteomics mass spectrometry analysis (3 samples from the two extremes and 2 for the middle growth rates). Mass spectrometry was performed on cell pellets, so secreted proteins were not included in our analysis. All bacterial cultures were allowed to acclimate to the chemostat conditions for two days (confirmed by steady OD_{600}) before collection. All samples were collected at least one day apart. To minimize batch effects, mRNA and protein samples were collected from separate chemostat batches, and samples from the same growth rate were collected from at least two different chemostat batches (except protein samples from the middle two growth rates).

First, to explore global relationships between growth rate and mRNA or protein expression, we performed a principal component analysis (PCA). To normalize by sampling depth, raw mRNA and protein sample counts were scaled to 1,000,000, then log2 transformed. As demonstrated in **Figure 4**, for both the mRNA and protein data, samples tend to cluster by growth rate. The proportion of variance across the dataset that is explained by PC1 and PC2 was also very high: 44.1% and 23.5%, respectively for the mRNA data, and 30.6% and 13.1%, respectively for the protein data. For the mRNA data, samples of bacteria grown at the extreme growth rates (3.3- or 25.3-hr doubling times) clustered the most tightly together, while the middle growth rates (6.0- and 13.8-hr doubling times) had greater variability. The cumulative value for PC1 and PC2 is also higher for the mRNA samples (67.6%) compared to protein (43.7%). Taken together, these results suggest that for *P. aeruginosa*, alterations in growth rate alone, while keeping other environmental conditions constant, results in significant changes in global mRNA and protein expression. Furthermore, in general there is more variability in mRNA expression compared to protein expression in relationship to changing growth rate.

1.16 mRNA and protein are only modestly correlated, and vary with growth rate

As mentioned previously, the general assumption when interpreting RNA-seq data is that the relationship between mRNA and protein expression is 1:1. To explore how well this assumption holds, we next sought to compare and contrast patterns of mRNA and protein expression across growth rates. For this analysis, and all subsequent analyses, we used depth-normalized, log2 transformed counts for mRNA and protein, and included only genes with non-zero counts for both mRNA and protein samples (3903 genes). First, we examined the distribution of the protein (**Figure 5A**) and mRNA (**Figure 5B**) expression level for each gene averaged across all 4 growth rates. The median expression value for protein is 4.3, while the median expression value for mRNA is 6.4. We can see that even

after normalization, the protein samples tended to have lower counts compared to the mRNA. However, the range of protein expression across all genes appears more uniform or stable, while the peak for the mRNA is much more pronounced, and the overall distribution appears more variable. Specifically, for protein, the 1st and 3rd quarter expression values for protein are 2.27 and 6.44, respectively, while for mRNA they are 5.24 and 6.51. Put another way, the sample quantile 5% and 95% probabilities for protein are 0.52 and 9.84, respectively; for mRNA they are 3.39 and 9.74, respectively. Next, we calculated the Spearman's rank correlation coefficient (SpR) between mRNA and protein expression levels for *P. aeruginosa* averaged across all growth rates (**Figure 6**). We observe only a modest correlation (SpR = 0.59) between protein and mRNA. This means that generally for a given gene as mRNA expression increases, the corresponding protein also increases. However, there is considerable noise and outliers. To examine how these correlations may be affected by growth rate, we calculated the SpR for mRNA and protein samples separated by growth rate (**Figure 7**). While overall the SpR were similar across growth rates, the fastest growth rate (3.3-hr doubling) had the highest correlation (SpR = 0.63), while one of the middle growth rates, 6.0-hr doubling, had the lowest correlation (SpR = 0.54). These results suggest that for a given gene, mRNA and protein levels are often not 1:1, and these correlations can be affected by the rate at which a cell is dividing.

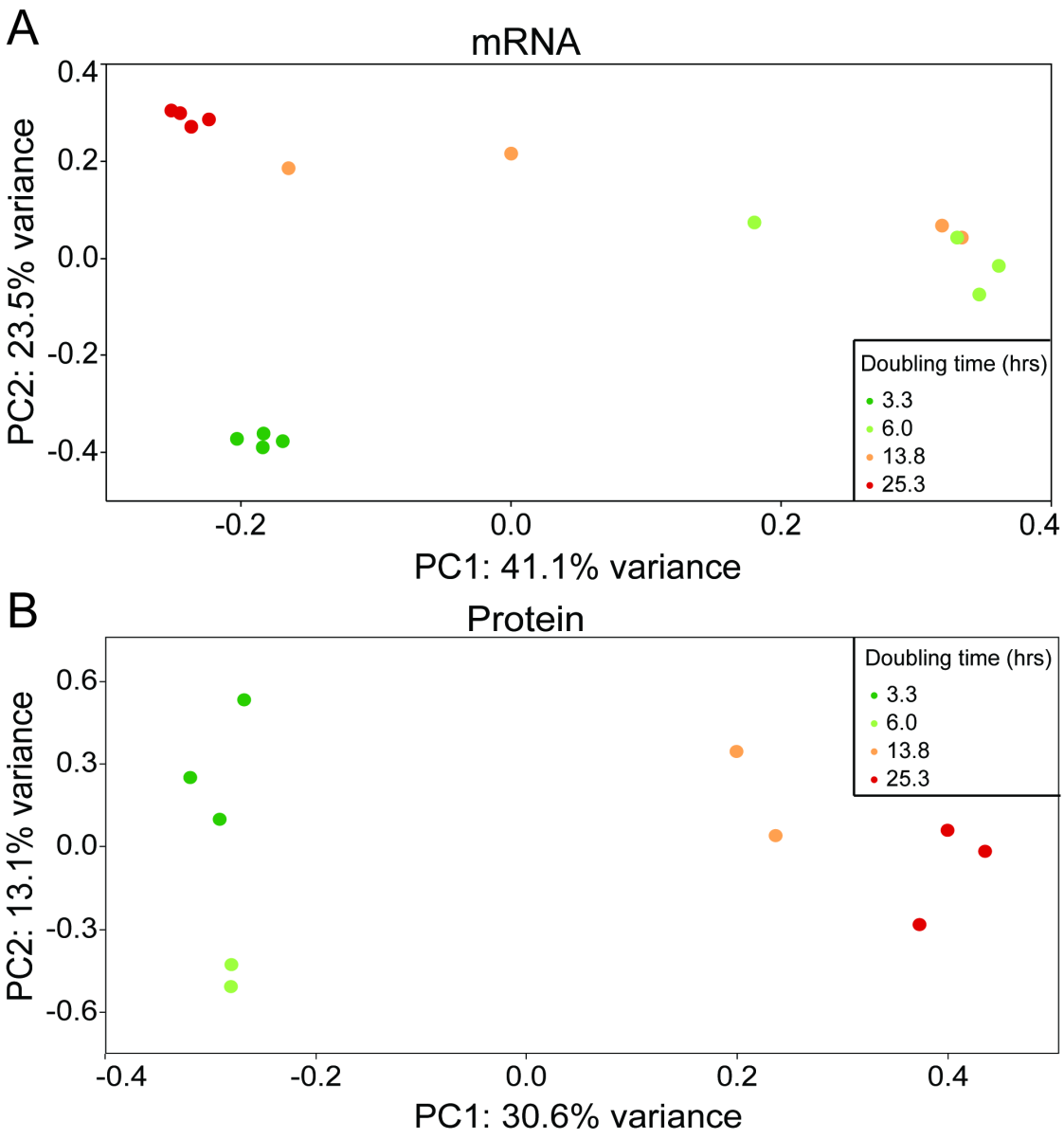

Figure 4. PCA of mRNA and protein chemostat samples. PCA was performed on (A) mRNA (B) and protein levels normalized by count depth and log2 transformed.

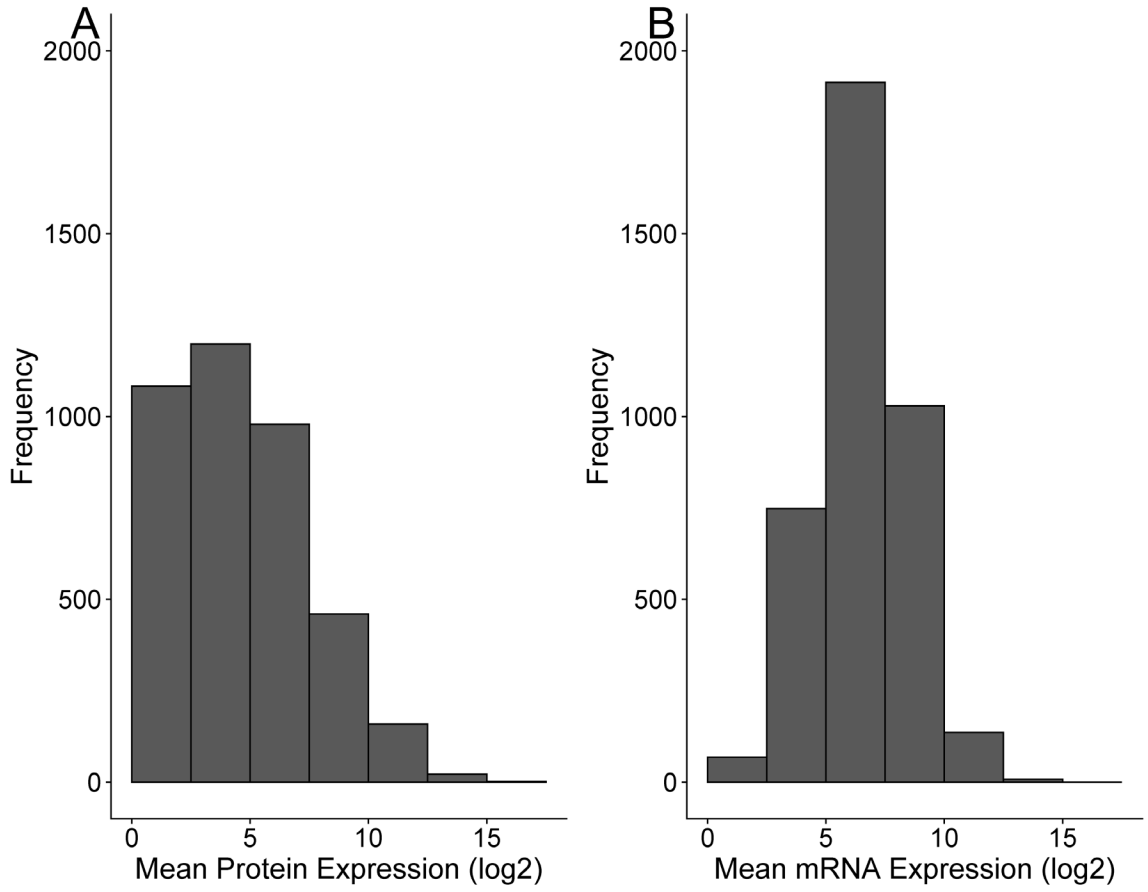

Figure 5. Distribution of mean expression levels. For each gene, protein and mRNA expression counts were normalized by depth, log2 transformed, and averaged across all 4 growth rates.

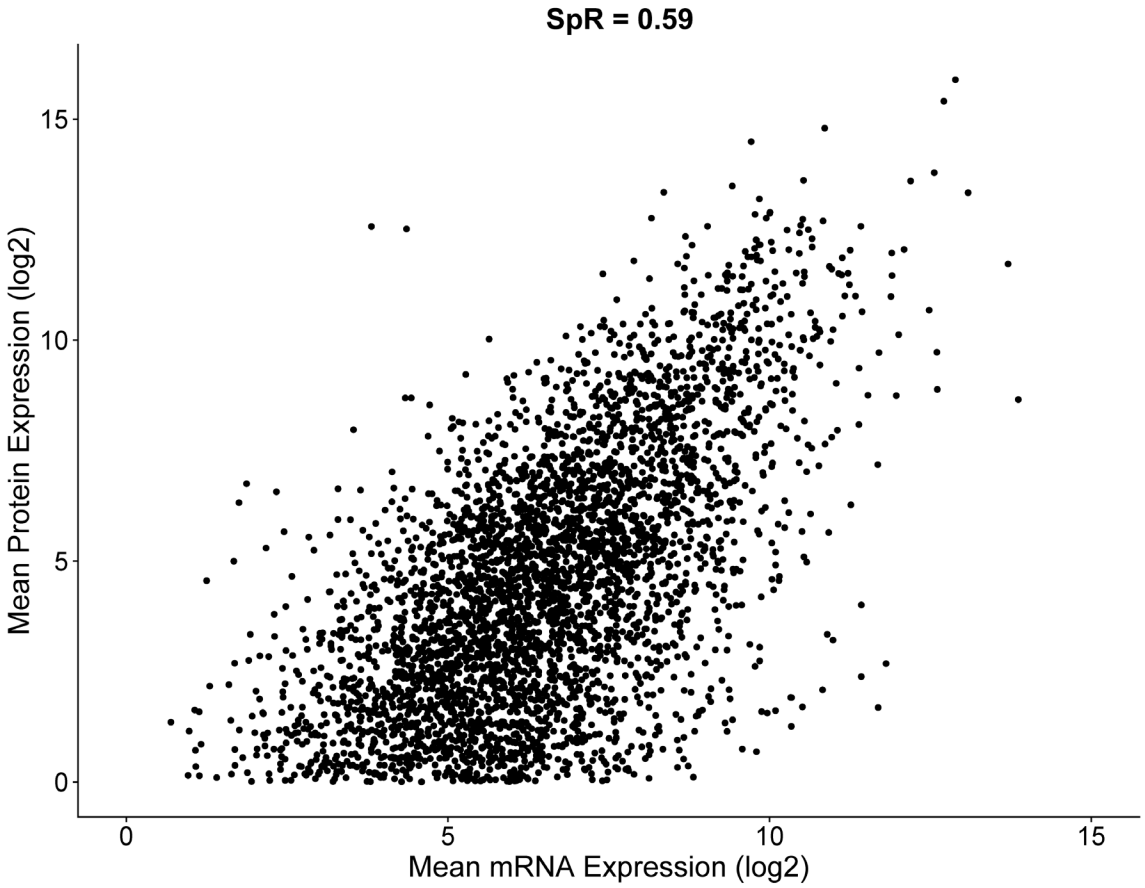

Figure 6. Correlation between average mRNA and protein expression. Each point represents a gene. For each gene, protein and mRNA expression counts were normalized by depth, log2 transformed, and averaged across all 4 growth rates. The Spearman's rank correlation coefficient (SpR) between mRNA and protein is indicated in the graph’s tittle.

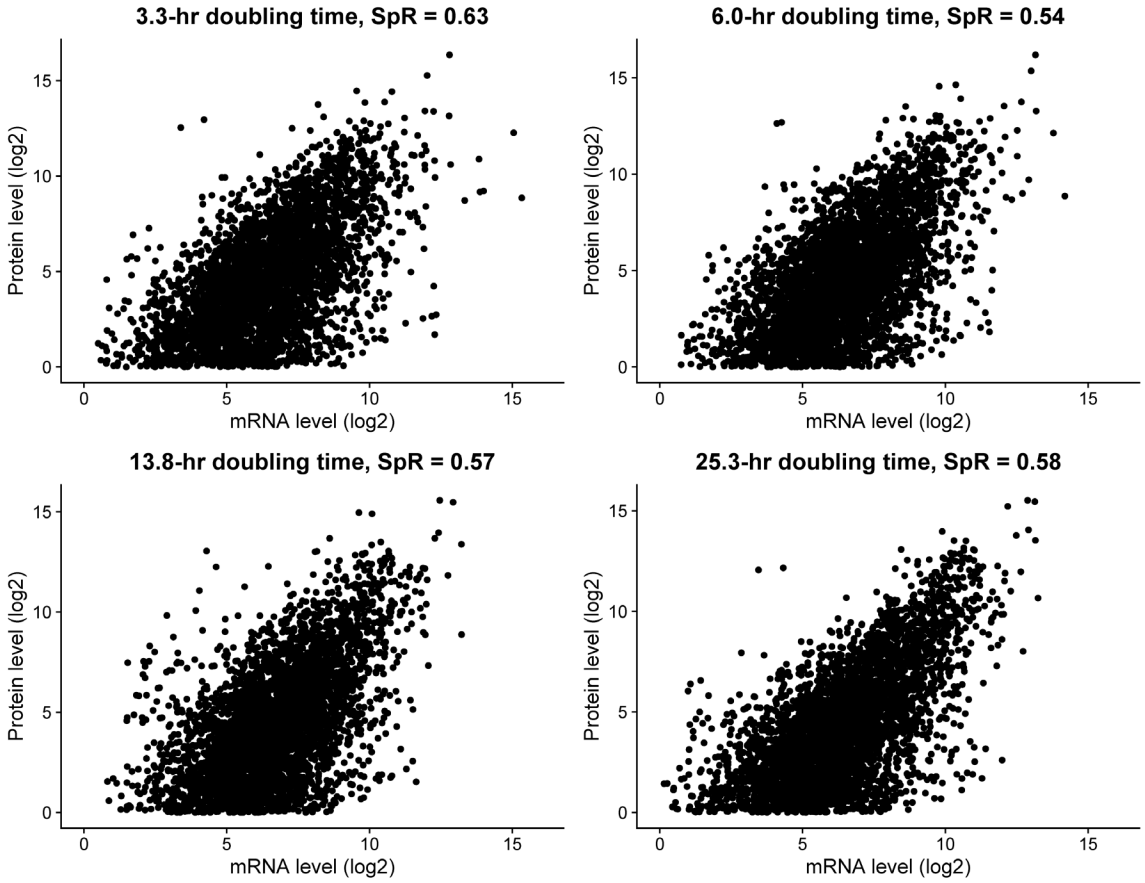

Figure 7. mRNA and protein expression are only modestly correlated, and vary with growth rate. Each point represents a gene. mRNA and protein counts were normalized by depth and log2 transformed. Graphs are ordered from fastest to slowest growth rates (A-D). The Spearman's rank correlation coefficient (SpR) between mRNA and protein levels for each growth rate are indicated in each graph’s tittle.

1.17 Variables affecting mRNA-to-protein ratios

We next attempted to identify variables that may explain the discrepancy between mRNA and protein correlations. In theory, for each gene we could apply a conversion factor to the mRNA in order to predict the corresponding protein level. A simple conversion factor could be the ratio of protein expression to mRNA expression. To calculate this ratio, we subtracted the log2 mRNA expression level from the log2 protein expression level, and averaged this value across the 4 growth rates. A distribution of these protein-to-mRNA ratios is shown in **Figure 8**. 2917 genes, or 74%, had the absolute value of the log2 fold-change (|L2FC|) > 1, indicating that for most genes, there is at least a two-fold difference in expression between the corresponding mRNA and protein. The median protein-to-mRNA ratio is -1.9, meaning that for over half of genes, the mean RNA expression level was higher than the mean protein expression level. This is consistent with results from **Figure 5**, which showed generally higher RNA expression than protein expression. There is also a considerable range of protein-to-mRNA ratios, from $2^{-10.0}$ to $2^{8.7}$, or between a ~1000 and 400-fold difference.

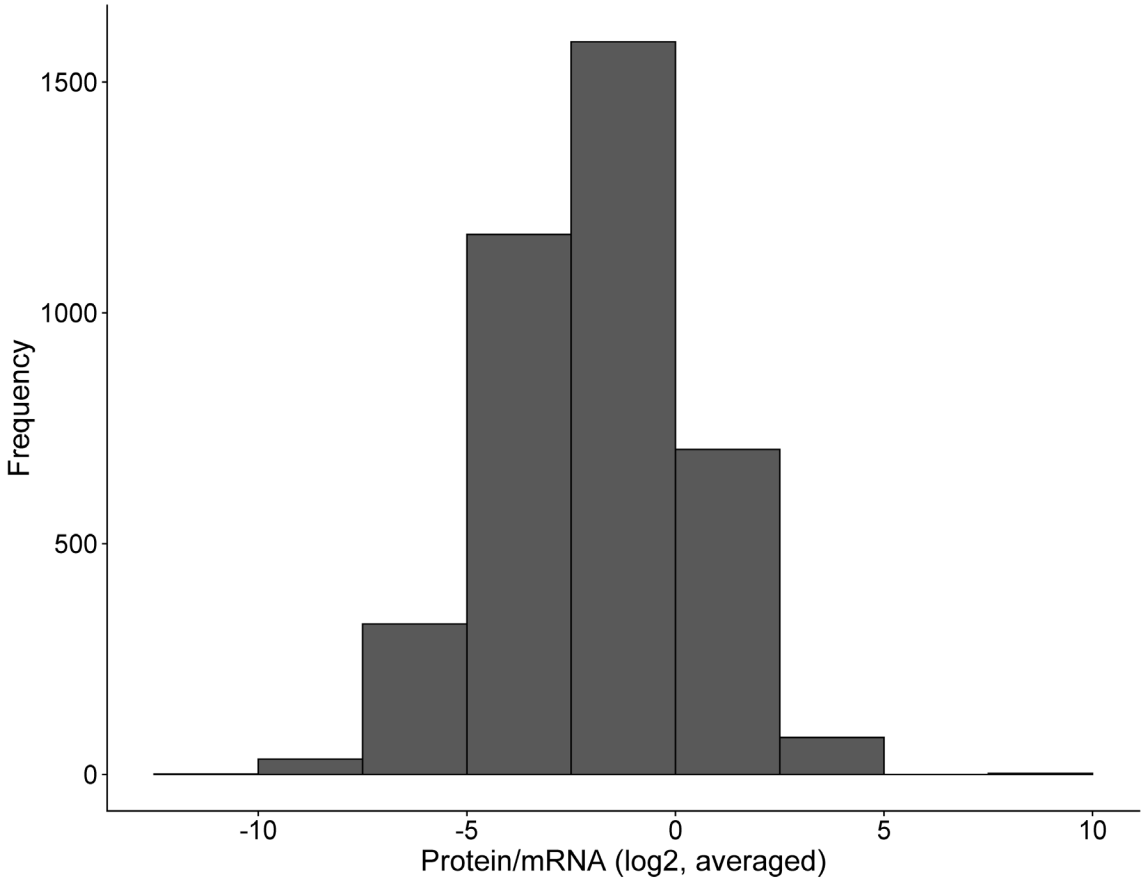

Figure 8. Ratio between protein and mRNA expression levels. For each gene, the log2 transformed mRNA expression values were subtracted from the log2 transformed protein values, then averaged across all 4 growth rates.

To explore this relationship further, we plotted mean protein (**Figure 9A**) or mRNA (**Figure** 9**B**) expression against the ratio of protein-and-mRNA expression, or the "conversion factor". Strikingly, there is a strong SpR between the protein/mRNA ratio and mean protein expression (SpR = 0.76), but not for mRNA expression (SpR = -0.02). These results indicate that for a given gene, as protein expression increases, so too does the ratio between protein and mRNA levels. This relationship is not a mathematical artefact due to protein expression being present on both axes, because the mRNA expression is not always proportional to the protein expression. In other words, if the difference between protein and mRNA was constant, then even if the mean protein expression was higher, then the slope between mean protein expression and protein/mRNA would be zero.

To investigate what variables may be driving this relationship, we next examined the range of protein or mRNA expression levels across growth rates. The range represents the degree to which mRNA or protein expression varies between growth rates for a given gene. To calculate the range for each gene, we subtracted the minimum expression value from the maximum expression value across the 4 growth rates for either mRNA or protein. As shown in **Figure 10**, the dynamic range for mRNA is much greater than that for protein. 2206 (57%) genes have an mRNA range <1, or less than a 2-fold change across all growth rates. In contrast, 3443 genes (88%) have a protein range <1. The largest single mRNA range is $2^{6.4}$ (84-fold) while the largest protein range is $2^{4.8}$ (28-fold). This means that overall, changes in growth rate result in greater variation in mRNA expression than protein expression.

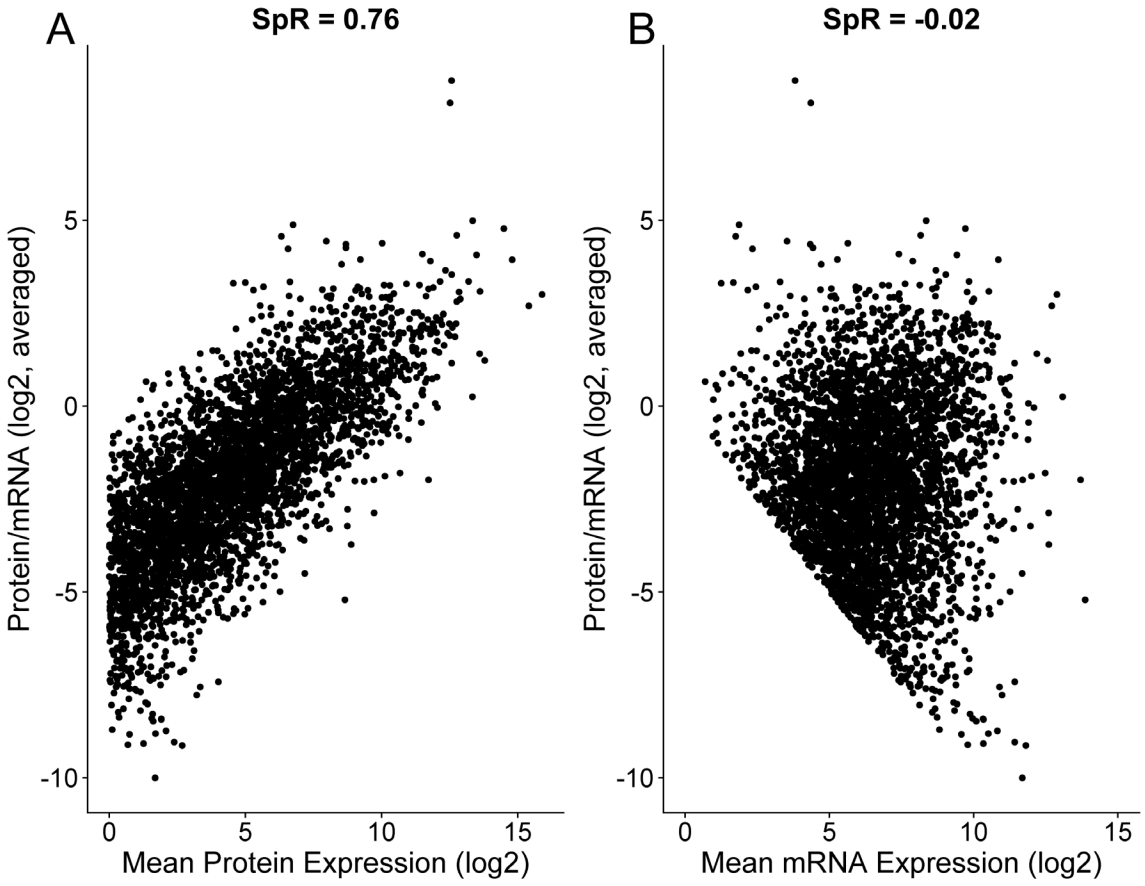

Figure 9. Mean protein or mRNA expression levels vs. the ratio of protein-to-mRNA. Each point represents a gene. For each gene, protein and mRNA expression counts were normalized by depth, log2 transformed, and averaged across all 4 growth rates. The ratio of protein-to-mRNA was calculated by subtracting the log2 transformed mRNA from the log2 transformed protein, then averaged across all 4 growth rates.

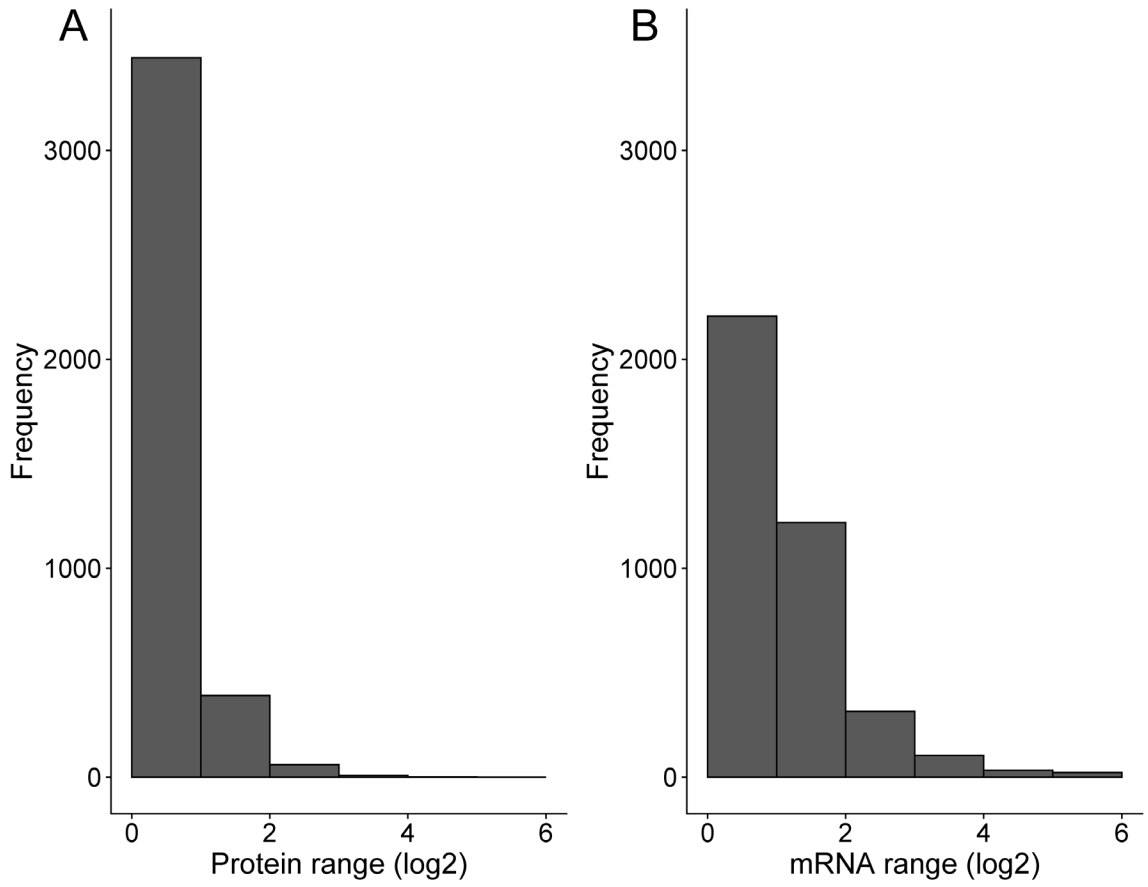

Figure 10. The range of protein and mRNA expression within a gene across growth rates. Protein and mRNA expression values were normalized by depth, log2 transformed, and averaged across all 4 growth rates. The range was calculated for each gene by subtracting the minimum expression value was from the maximum expression value among the 4 growth rates.

Knowing that changes in growth rate cause a greater variation in mRNA expression than protein expression, we next wanted to assess the effect that growth rate has on the protein-to-mRNA ratio. We calculated a new variable that represents the change in the protein-to-mRNA ratio with respect to growth rate, or the proportional variation in the conversion factor. As in **Figure 8**, for each gene we subtracted the log2 mRNA expression level from the log2 protein expression level to get the protein-to-mRNA ratio. We then subtracted the maximum protein-to-mRNA ratio from the minimal protein-to-mRNA ratio between the 4 growth rates for each gene. A distribution of the proportional variation in the correlation factor values is shown in **Figure 11**. 1647 genes (42%) had a value > 1, meaning that the difference in mRNA-to-protein ratios across the 4 growth rates is greater than 2-fold. In other words, for a given gene, a cell's generation time can often impact the correlation between protein and mRNA.

To explore this relationship further, we then plotted the interaction between the proportional variation in the correlation factor and the protein range (**Figure 12A**) or mRNA range (**Figure 12B**). Interestingly, there is a strong correlation with the mRNA range (SpR = 0.78), but not with the protein range (SpR = -0.17). This indicates that it is mainly the variation in mRNA expression across growth rates, rather than protein expression, that is driving the variation in protein-to-mRNA ratios.

Finally, a correlation matrix, summarizing the interactions between all of the variables discussed thus far (mean protein and mRNA expression, protein and mRNA range, protein-to-mRNA ratio, and proportional variation in protein-to-mRNA ratio), is presented in **Figure 13**.

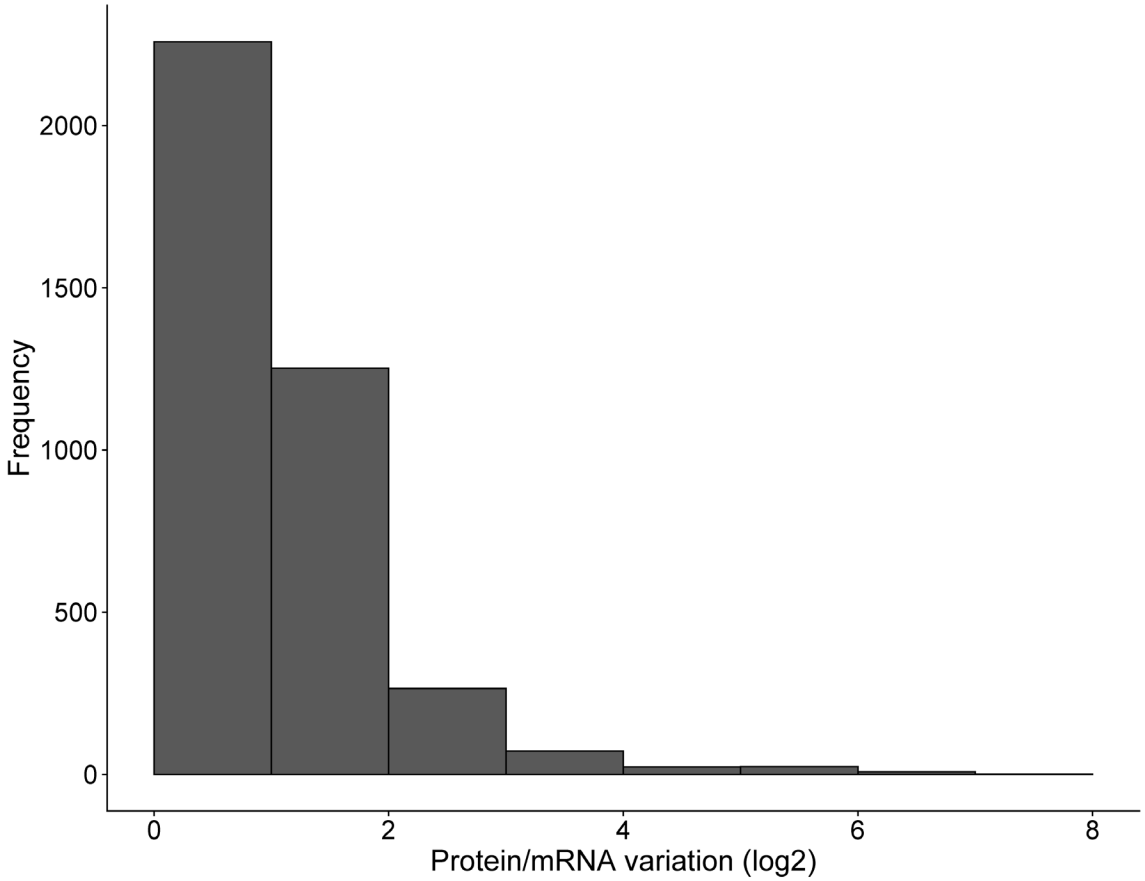

Figure 11. Variation in protein-to-mRNA ratios across growth rates. For each gene, the protein-to-mRNA ratio was calculated by subtracting the log2 mRNA expression level from the log2 protein expression level. The maximum protein-to-mRNA ratio was then subtracted from the minimal protein-to-mRNA ratio across the 4 growth rates to determine the final proportional variation in protein-to-mRNA ratio for each gene.

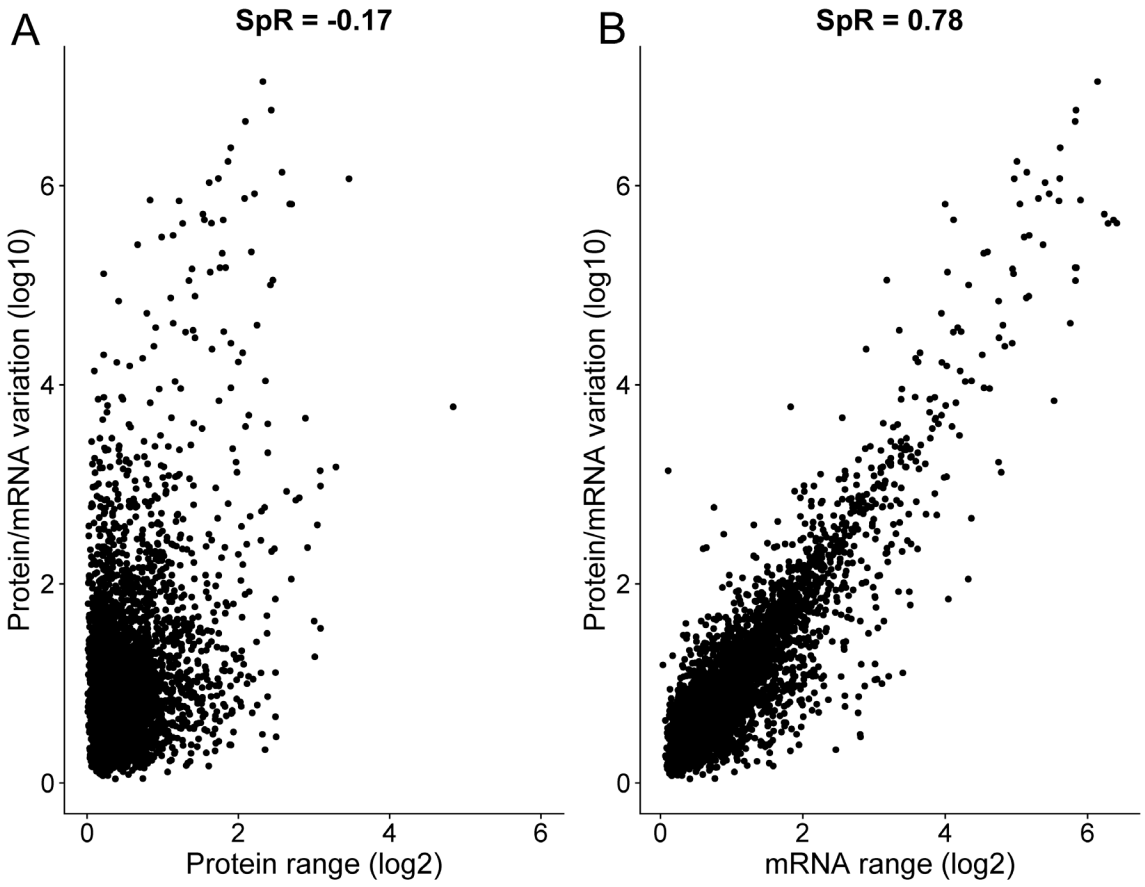

Figure 12. The relationship between range and variation in protein-to-mRNA ratio. The protein or mRNA ranges were calculated for each gene by subtracting the minimum expression value was from the maximum expression value between the 4 growth rates. Protein and mRNA expression values were normalized by depth, log2 transformed, and averaged across all 4 growth rates. The protein-to-mRNA ratios were calculated by subtracting the log2 mRNA expression level from the log2 protein expression level. The variation in protein-to-mRNA ratios was determined by subtracting the maximum protein-to-mRNA ratio from the minimal protein-to-mRNA ratio between the 4 growth rates for each gene.

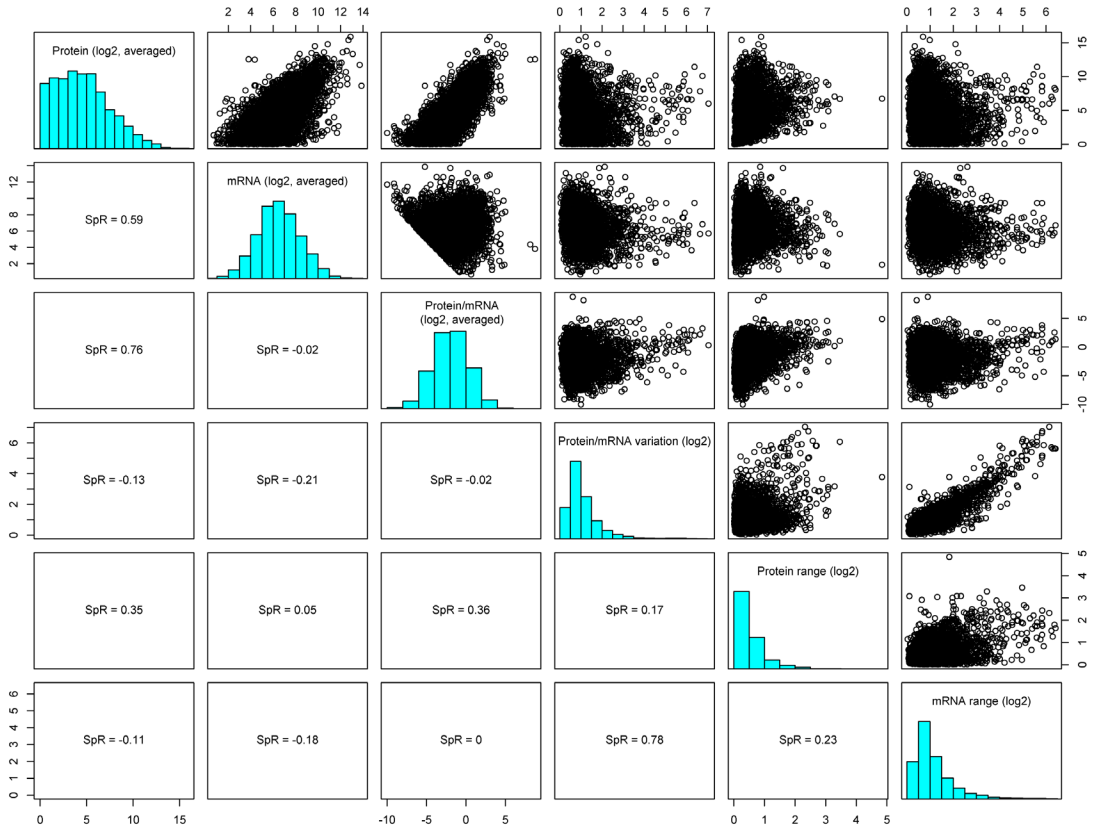

Figure 13. Correlation matrix summary of results. See Figures 5-12 for description of all variables.

1.18 Discussion

RNA-seq is a powerful tool for profiling gene expression, and it can even be used on bacteria sampled directly from human infections (286, 287). However, it has limitations. When interpreting RNA-seq data, changes in mRNA expression are assumed to result in proportional changes in protein expression. As our results have shown, mRNA and protein levels are only somewhat correlated, and these correlations can change with growth rate. As shown in **Figure 7 and 8**, when averaging across all of the growth rates, the SpR was 0.59. When the data is separated by growth rate, we observed a maximum SpR of 0.63 (3.3-hr doubling) and a minimum SpR of 0.54 (6.0-hr doubling). The correlations that we calculated are consistent with those reported in other studies (291, 292).

We then explored how variables, such as the mean protein and mRNA expression, the range of protein and mRNA expression, protein-to-mRNA ratio, and proportional variation in protein-to-mRNA ratio, may explain the incongruity between mRNA and protein correlations. As shown in **Figure 5**, when averaged across all growth rates, there is more variation in mRNA expression than protein expression, with the mRNA having a higher median and sharper peak than the protein. However, the range of expression across the genome and averaged across growth rates is higher for protein than mRNA. Likewise, as shown in **Figure 10**, there is a stark contrast in the mRNA range, or the difference in mRNA expression within a gene across growth rates, compared to the protein range. This variation in mRNA expression across growth rates appears to be driving the variance in protein-to-mRNA ratios across growth rates (**Figure 12**). In contrast, it is the mean protein expression, rather than the mean mRNA expression, that is strongly correlated with the protein-to-mRNA ratio (**Figure 9)**.

We calculated protein-to-mRNA ratios, or conversion factors, for roughly 3900 *P. aeruginosa* genes. These conversion factors could potentially be used to more accurately predict protein abundance from RNA-seq data, especially if the growth rate is known. However, caution should be used, as over 40% of these conversion factors vary by more than two-fold across our growth rates (**Figure 11**). One limitation of our dataset is that we performed mass spectrometry on cell pellets, so secreted proteins weren't included. Future studies could involve collecting filtered chemostat media in order to include secreted proteins. Another limitation of our dataset is that we only used one strain and one media condition. We know from previous experiments in our laboratory that the mRNA-to-protein ratios between *P. aeruginosa* strain PA14 and the laboratory strain PAO1 are generally highly conserved (292). However, nutrient availability has a major impact on gene expression (276, 295, 296). These conversion factors could be further refined by expanding our dataset to include chemostat conditions with different media and *P. aeruginosa* strains. With this approach we could identify genes with conversion factors that are conserved across strain, media condition, and growth rate.

1.19 Materials and methods

Chemostat assembly

Our chemostat design is based on a previously described system (282) with minor modifications. The fresh media was contained in a 4 L glass Erlenmeyer flask (Pyrex). A rubber stopper (No. 10, Fisher) was fitted to the mouth of the flask. Three holes, approximately 5.9 mm in diameter, were drilled into the stopper. Two holes were fitted with short 12 cm glass tubes topped with air venting filter sterilizers (0.2 µm pore size, 50 mm diameter, VWR) to allow gas exchange and prevent vacuuming. The third hole was fitted with a long 40 cm glass tube from which to draw the media. Polytetrafluoroethylene

capillary tubing (Millipore) connected the media reservoir flask to the chemostat growth chamber. The tubing was hooked up to a 4 channel peristaltic pump (Watson Marlow), allowing precise control over the media flow rate.

A 300 ml Berzelius beaker without a spout (Kimble) was used as the chemostat growth chamber. A rubber stopper (No. 13-1/2, Fisher) was fitted to the mouth of the beaker. Four holes were drilled into this stopper. The first hole, 6.0 mm in diameter, was fitted with a 1 ml syringe (BD) with the plunger removed. Capillary tubing was inserted into the syringe and sealed in place with silicone aquarium sealant (VWR). The second hole, 16.5 mm, was fitted with a 15 ml polypropylene conical (Corning). The lower half of the conical was cut off, allowing bacterial culture samples to be obtained by unscrewing the conical lid and inserting a serological pipette into the growth chamber. The third hole, 6.7 mm, was fitted with a glass tube blown into a “J” shape to serve as the waste outflow tube. The surface of the waste tube was level with the 100 ml mark of the growth chamber. Capillary tubing was connected from the waste tube to a separate 4 L Erlenmeyer flask for waste collection. The fourth hole, 8.41 mm, was fitted with a 12 mm O.D. x 20 mm fritted gas dispersion tube (Chemglass). The gas dispersion tube was connected by capillary tubing to an air venting filter sterilizer, which in turn was connected to an aquarium air pump (Fusion Air Pump 200). This system pumps fresh, sterilized air to the growth chamber and creates a positive pressure in the chamber, which is necessary for expelling waste from the waste tube. The end of the fritted tube was lowered into the media in the growth chamber, constantly bubbling the media and allowing for continuous aeration and mixing.

Bacterial strains and growth media

Pseudomonas aeruginosa strain UCBPP-PA14 (PA14) was obtained from the MGH-ParaBioSys:NHLBI Program for Genomic Applications, Massachusetts General Hospital

and Harvard Medical School, Boston, MA (http://pga.mgh.harvard.edu). For each individual chemostat batch, bacteria were cultured from frozen glycerol stocks by streaking for isolation on LB agar plates and incubated at 37ºC overnight. For chemostat growth, bacteria were cultured in morpholinepropanesulfonic acid (MOPS) buffered minimal medium with 10 mM succinic acid as the sole carbon and energy source (MOPS-succinate). All chemostat components including the MOPS buffed base were autoclaved for sterilization. After autoclaving, filter-sterilized $FeSO_4$, $MgsO_4$, and succinic acid were added aseptically to the MOPS buffed base. Media was pumped through the chemostat and left at room temperature overnight to confirm system sterility. A single *P. aeruginosa* colony was then picked and aseptically inoculated into the media in the chemostat growth chamber. Bacteria were then allowed to grow overnight at room temperature in order to reach a sufficient density. The chemostat was then transferred and maintained in a 37ºC warm room. The peristaltic pump was turned on and set to the appropriate flow rate. The bacteria were allowed to acclimate in the chemostat for 48 hrs before sampling. One sample was collected per day. The culture densities were determined by measuring the OD_{600} with a spectrophotometer. To mitigate batch effects, RNA-seq and mass spec samples were collected from separate chemostat batches. Bacterial generation times were calculated by dividing chemostat growth chamber volume (100ml) by the media flow rate.

RNA-seq sample collection and library preparation

To mitigate batch effects, for each growth rate samples were collected from at least two separate chemostat batches. For each individual RNA-seq sample, 5 ml of chemostat culture was collected and mixed well with 20 ml of the RNA preservative RNAlater (Sigma). Samples were stored at 4ºC for 24hrs to allow the solution to fully permeate the cells, and then stored at -80 ºC. RNA-seq libraries were prepared as previously described (221) with

minor modifications. Briefly, to extract RNA, samples were pelleted at 4°C, supernatant removed, and resuspended in 300 µl RNase-free TE buffer and 12 µl lysozyme (50 mg/ml, Thermo). To enzymatically lyse cells, samples were incubated at 37°C for 30 minutes. 1ml of RNA-Bee (Fisher) was added to each sample followed by transfer to 2 ml Bead Bug tubes containing 0.1-mm beads (Sigma). To homogenize the cells, tubes were bead beaten 3x for 30 seconds and chilled on ice for 1 minute in-between bead beatings. Cells were then transferred to 1.5 ml tubes with 0.2 ml chloroform (Fisher) added. Samples were vortexed vigorously for 1 minute, followed by storage on ice for 5 minutes. To separate the phases, samples were centrifuged at 13,000g for 30 minutes at 4°C. The aqueous phase was removed and transferred to fresh 1.5 ml tubes with added 0.5 ml isopropanol (Sigma) and 2 µl linear acrylamide (Sigma). Samples were stored at -80 ºC overnight to precipitate the RNA. Samples were thawed on ice and centrifuged at 13,000g for 30 minutes at 4°C to pellet the RNA. Pellets were washed with 75% ethanol twice, allowed to air dry for 5 minutes, and then resuspended in 50 µl RNAse-free water (Fisher). RNA concentration was assessed using a Nanodrop spectrophotometer (Thermo Scientific).

RNA-seq libraries were prepared as previously described (297). Briefly, ribosomal RNA was depleted using the MICROBExpress bacterial mRNA enrichment kit (Sigma). mRNA was then fragmented using the NEBNext Magnesium RNA Fragmentation module (NEB) with minor modifications. During the fragmentation step, samples were incubated at 4°C for two minutes. During the ethanol precipitation step, samples were incubated at -80°C overnight. Sequencing libraries were prepared using the NEB Library Preparation kit E7300. Libraries were then purified using the Qiagen QIAquick purification kit. To isolate libraries of the correct size, the NEB QC Check and Size Selection using 6% polyacylamide gel E7300 protocol was used with minor modifications. 10 µl of gel loading dye was added to 25 µl of each sample. A pre-cast 5% TBE gel was used (Bio-Rad), and

each sample was loaded in 1 well. During gel electrophoresis, the voltage was set to 65V to account for the thinner gel. Samples were eluted from the gel by rotating end-to-end for at least two hours at 37°C. Samples were never vortexed, only inverted. The concentration and purity of final libraries was assessed using the Qubit dsDNA HS assay kit (Thermo) and the High Sensitivity Bioanalyzer kit (Agilent).

Proteomics mass spectrometry sample collection and preparation

To mitigate batch effects, for the 3.3-hr and 25.3-hr doubling times, of which there were three samples each, samples were collected from two separate chemostat batches. Since there were only two samples analyzed at the 13.8-hr and 6.0-hr doubling times, these samples were collected on subsequent days from the same chemostat batch. For each individual sample, 5 ml of chemostat culture (OD_{600} = ~0.7) was collected on ice, followed immediately by centrifugation at 4ºC at 14,000g for 5 minutes. The supernatant was removed and cells were washed once in 1 ml of 4 ºC sterile PBS. Cells were pelleted again, supernatant removed, and cell pellets were stored at -80 ºC.

Samples were processed for global proteome mass spectrometry analysis by the Georgia Institute of Technology's Systems Mass Spectrometry Core Facility following previously described methods (298). Briefly, frozen cell pellets were lysed on ice with chilled urea lysis buffer. Extracted proteins were reduced, alkylated and sequentially digested with LysC for 2 hours and with trypsin overnight. Peptides were desalted by solid phase extraction (SPE) using SepPak cartridges and labeled with the TMT10plex isobaric labels (ThermoFisher Scientific). The TMT-labeled peptides were pooled and desalted again using the SepPak cartridges. The peptide mixture was first separated by high pH reverse phase chromatography using a Beckman System Gold HPLC system with a Zorbax 300 Extended C18 column (Agilent). A total of 120 fractions were collected and pooled into

10 fractions as previously described (299). Both the unfractionated and the 10 pooled fractions were analyzed by nano-LC/MS-MS using Dionex nanoLC system coupled to a Q Exactive Plus mass spectrometer (Thermo Scientific) as previously described (300) with the following modifications. Reverse phase chromatography was performed using an in-house packed column (40 cm long X 75 µm ID X 360 OD, Dr. Maisch GmbH ReproSil-Pur 120 C18-AQ 1.9 µm beads) and a 120 min. gradient. MS settings included MS1 scans (70,000 resolution, 3 × 106 AGC, and 20 ms maximal ion time) and 12 data-dependent MS2 scans (35,000 resolution, 5 × 104 AGC, 120 ms maximal ion time, HCD, 30% normalized collision energy, 1.6 m/z isolation window with 0.3 m/z offset, and 20 s dynamic exclusion).

RNA-seq bioinformatic analyses

RNA-seq reads were trimmed using Cutadapt version 1.8.1 with default parameters and a minimum read length cut-off of 18 bases (301). Reads were then mapped to the current NCBI PA14 genome assembly (GCA_000014625.1 ASM1462v1) with Bowtie 2.2.3 using the default parameters (302). Gene counts were tallied to the coding sequences (CDS) using the R package Subread 2.0.0 with the strand specific option (-s 1) enabled (303) using the current GFF file downloaded from The Pseudomonas Genome Database (304).

Proteomics mass spectrometry bioinformatics analyses

Proteome Discoverer v2.1 (Thermo Fisher Scientific) and Mascot (Matrix Science) v2.6 were used to process raw data files. Data was aligned with the Pseudomonas.com PA14 proteome and the common repository of adventitious proteins (cRAP) v1.0. Protein identification allowed an MS tolerance of ± 10 ppm and an MS/MS tolerance of ± 0.8 Da ppm along with permission of up to 2 missed tryptic cleavages. Quantification was

achieved by calculating the sum of centroided reporter ions within a ± 2 millimass unit (mmu) window around the expected *m*/*z* for each of the four TMT reporter ions.

All comparative analyses were performed with R (305). The R package MSnbase (306) was used for processing proteomics data. Briefly, this entailed missing value removal (instances where a protein was identified but not quantified in all channels were rejected from further analysis), log2-transformation of the raw data, followed by sample normalization; utilizing the 'diff.median' method in MSnbase. Protein differential abundance was evaluated using the Limma package (307). Differences in protein abundances were statistically determined using the Student's t-test with variances moderated by Limma's empirical Bayes method. P-values were adjusted for multiple testing by the Benjamini Hochberg method (308). Proteins were considered as increased or decreased in abundance, only when their log2 fold change was >1 or <−1, respectively, and their P value was <0.05.

CONCLUSIONS AND FUTURE DIRECTIONS

1.20 The Role of *Pseudomonas aeruginosa* Glutathione Biosynthesis in Lung and Soft Tissue Infection

1.20.1 Summary of results

P. aeruginosa is a leading public health threat, particularly in immunocompromised people and in hospital settings (1, 10, 15). It is a versatile bacterium capable of infecting multiple body sites, including the skin and soft tissues. However, current antibiotic therapies are insufficient for treating these infections, necessitating a better understanding of *P. aeruginosa* infection biology. In this work, we focused on the role of GSH for *P. aeruginosa* during infection. GSH is a major cellular antioxidant that is involved in a variety of cellular processes, including protection from oxidative stress, toxins, and regulation of pH and osmolarity (206, 207). *In vitro* experiments have shown that GSH is involved in many different cellular processes that are important for infection, including motility, biofilm formation, toxin production, and quorum sensing (71, 155, 176, 214, 215). However, the role of GSH biosynthesis during mammalian infection, particularly in different sites of infection, was unclear.

We found that GSH is critical for normal *P. aeruginosa* growth *in vitro*. *P. aeruginosa* Δ*gshA* grown in minimal media without GSH had a severe growth rate defect, but the growth rate was restored to WT levels with the addition of exogenous GSH (**Figure 1**). We speculate that the conflicting results in published literature regarding GSH-mediated phenotypes may be due to inadvertent use of media that contains GSH, such as LB broth. Using disc diffusion assays, we then showed that GSH biosynthesis provides *P. aeruginosa* with protection against some antimicrobials, including hydrogen peroxide,

bleach and ciprofloxacin (**Table 1**). Finally, we also studied the role of *P. aeruginosa* GSH biosynthesis in four mouse infection models: surgical wound, abscess, burn wound, and acute pneumonia. We discovered that *P. aeruginosa* Δ*gshA* was slightly less virulent in the acute pneumonia infection model but was equally virulent in the three other models (**Figure 2, 3**). Future directions building off of this work could 1) elucidate the role of GSH in regulating cellular pH and osmolarity in *P. aeruginosa*, 2) explore additional mouse models of infection, 3) test the efficacy of combination GSH inhibitor and antibiotic therapy *in vivo*, 4) elucidate the mechanism for why GSH biosynthesis provides *P. aeruginosa* a fitness benefit in the lungs and 5) explore the effect of exogenous GSH therapy on *P. aeruginosa* infection.

1.20.2 Role of GSH biosynthesis for pH and osmolarity regulation in P. aeruginosa

The ability to resist pH and osmotic stress is important for bacterial survival in the environment and in the host during infection. In some Gram-negative bacteria, GSH plays an important role in controlling intracellular osmolarity and pH by regulating the closing of K+ channels (206). *E. coli* with mutations in GSH biosynthesis genes, or in GSH-regulated K+ channel genes, leak K+ into the extracellular environment and cannot grow in low K+ media (213). Similarly, in *Rhizobium tropici,* GSH biosynthesis mutants are hypersusceptible to osmotic and acid shock (309). AMPs, a component of the innate immune system, create pores in bacterial membranes, causing leakage of cellular contents, osmotic shock, and death. In *Yersinia enterocolitica* (233), *Neisseria meningitides* (231), and *Salmonella typhimurium* (232) mutants in GSH biosynthesis or K+ transport are hypersusceptible to AMPs. However, to our knowledge, the role of GSH in protecting *P. aeruginosa* from pH or osmotic shock has not been explicitly tested.

Follow-up experiments, similar to those conducted in **Figure 1,** could test how pH or osmotic shock affect the growth rate of *P. aeruginosa* Δ*gshA*. Both WT and *P. aeruginosa* Δ*gshA* would be grown in MOPS-glucose, and the growth rate of the bacteria would be monitored over time using a spectrophotometer. To test the effect of osmotic stress, the bacteria could be grown in varying concentrations of K+. Likewise, to measure the effect of pH stress, the bacteria could be grown in MOPS minimal media adjusted to a range of different pH. To chemically complement the mutant, the bacteria would also be grown with or without exogenous GSH added to the medium. These growth rates would be compared to growth in normal MOPS-glucose, since *P. aeruginosa* Δ*gshA* already has a growth rate defect in MOPS-glucose. More in-depth procedures could also be used to measure intracellular K+ and pH levels in the Δ*gshA* mutant compared to the WT. Radiolabeled weak acids or fluorescent dyes have been used to measure intracellular pH (309, 310), while intracellular K+ levels could be quantified using flame photometry (213, 309).

Results from these experiments would further elucidate the physiological role of GSH in *P. aeruginosa*. If we find that *P. aeruginosa* Δ*gshA* has a growth rate defect upon exposure to low pH, this may help explain why *P. aeruginosa* Δ*gshA* is severely attenuated for virulence in *Drosophila* (71) and *C. elegans* infection models (155). In these two models, *P. aeruginosa* colonizes the low pH environment of the gut. If we find that *P. aeruginosa* Δ*gshA* is resistant to osmotic stress, this may help explain why we observed *P. aeruginosa* Δ*gshA* resistance to AMPs (**Table 1**). Such a result may suggest that either GSH does not play a role in regulating osmotic stress upon exposure to AMPs, or there may exist additional redundant systems. Finally, if *P. aeruginosa* Δ*gshA* is found to be resistant to both osmotic and pH stress, that may also help explain why it was not severely attenuated in mice; mammalian blood is highly osmotic and oxidative (311), and bloodstream

dissemination is a key attribute of some infection types, including burn wound and acute pneumonia infections.

1.20.3 Additional mouse models of infection

We limited the number of mouse models that we investigated to four because of ethical considerations. Since *P. aeruginosa* Δ*gshA* was less fit in only one of the mouse models that we tested (acute pneumonia, **Figure 3**), it is unlikely that *P. aeruginosa* Δ*gshA* would be severely attenuated in a different mouse model of infection. However, if this work were investigated further, there are two more compelling mouse models to test: intraperitoneal (IP) and intravenous (IV) (179, 312, 313). Both are models of *P. aeruginosa* sepsis, which is a clinically relevant route of infection (174, 201). The IP model involves an injection of bacteria into the body cavity through the abdomen, while the IV model features administration of bacteria directly into the bloodstream through the tail vein. As mentioned previously, mammalian blood is hostile to bacterial growth because it is osmotic and oxidative, and it contains anti-bacterial components of the innate immune system such as complement and AMPs (311). GSH-deficient *Yersinia pestis* mutants display a severe growth defect in both whole defibrinated blood and in heat-treated serum (233). GSH biosynthesis mutants of *Salmonella enterica* were attenuated in an IP mouse model (218), and GSH-deficient *Listeria monocytogenes* mutants were attenuated in an IV mouse model (208).

Results from testing *P. aeruginosa* Δ*gshA* mutants in either an IP or IV mouse model would more directly assess *P. aeruginosa*'s requirement for GSH biosynthesis in the blood. While bloodstream dissemination is characteristic of late stage burn wound and acute pneumonia *P. aeruginosa* infections, *P. aeruginosa* Δ*gshA* may have been able to acquire host GSH from the tissues before migrating to the bloodstream, which may have

helped it survive in the blood. In contrast, sepsis is the main clinical feature of IP and IV infections, and in the IV model, *P. aeruginosa* Δ*gshA* is subjected to the blood immediately. It would also be possible to test this hypothesis *in vitro* first. Similar to the experiments conducted in **Figure 1**, *P. aeruginosa* Δ*gshA* and WT could be grown in MOPS-glucose with added whole blood or serum, and their growth rate could be monitored over time. If the *P. aeruginosa* Δ*gshA* mutant demonstrates a growth rate defect in the presence of whole blood or individual blood components *in vitro*, then that evidence would suggest a role for GSH biosynthesis for *P. aeruginosa* in the blood.

1.20.4 Combination GSH inhibitors and antibiotic therapy

P. aeruginosa infections are notoriously difficult to treat due to *P. aeruginosa*'s high innate tolerance to antimicrobials. Therefore, new treatments are urgently needed (1, 66). As we demonstrated in **Table 1**, *P. aeruginosa* Δ*gshA* is hypersusceptible to the antibiotic ciprofloxacin. Future work could assess the potential of combination therapy using GSH inhibitors and ciprofloxacin together as a novel *P. aeruginosa* treatment strategy. This antibiotic is clinically relevant, as oral ciprofloxacin is widely used to treat a variety of human *P. aeruginosa* infections, including lung and soft tissue infections (314, 315). There is a precedent for this strategy; some experimental cancer therapies use GSH inhibitors in combination with chemotherapeutic agents (316, 317). Furthermore, we hypothesized that *P. aeruginosa* Δ*gshA* may have been able to scavenge GSH from the host in order to offset any GSH-related fitness defects. GSH inhibitors would deplete intracellular GSH levels from both *P. aeruginosa* and from the host, which may help sensitize *P. aeruginosa* to ciprofloxacin and to the immune system. However, since mammalian cells also require GSH (207), it would be necessary to find a balance between harming the bacteria while sparing the host.

First, we would determine whether GSH inhibitors can induce heightened ciprofloxacin susceptibility in WT *P. aeruginosa in vitro*. GSH inhibitors include buthionine sulfoximine (BSO) (223) or diethylmaletate (DEM) (235). Similar to the experiments conducted in **Table 1,** we could perform disc diffusion assays on MOPS-glucose + tryptone plates with WT *P. aeruginosa* and ciprofloxacin + GSH inhibitors, as well as treatment with ciprofloxacin alone and GSH inhibitors alone as controls. We would expect to see WT *P. aeruginosa* hypersusceptible to ciprofloxacin + GSH inhibitors, similar to *P. aeruginosa* Δ*gshA* treated with ciprofloxacin. Alternatively, WT *P. aeruginosa* could be pre-treated with GSH inhibitors before plating and ciprofloxacin exposure.

Before testing in mice, we could then try an *in vitro* cell culture system (89, 136, 137). We could co-culture WT *P. aeruginosa* with lung epithelial cells (or other appropriate cell types) and treat them as before with ciprofloxacin + GSH inhibitors, ciprofloxacin alone, or GSH inhibitors alone. Here, we would determine which concentrations, if any, of ciprofloxacin + GSH inhibitors would be effective in killing *P. aeruginosa* without causing severe stress to the lung cells. We would also want to achieve a significantly higher *P. aeruginosa* killing in the ciprofloxacin + GSH inhibitors group compared to treatment with ciprofloxacin alone. *P. aeruginosa* viability would be assessed using serial dilution and plate counts. Lung cell health in treated vs. untreated cultures could be assessed by comparing lung cell viability, histology, ciliary beating, and transepithelial electrical resistance (TEER), which measures the integrity of the epithelial tight junctions (318).

Since we know that *P. aeruginosa* Δ*gshA* is more susceptible to ciprofloxacin *in vitro* (**Table 1**), we next could examine whether *P. aeruginosa* Δ*gshA* is more susceptible than the WT to ciprofloxacin treatment *in vivo*. Because *P. aeruginosa* Δ*gshA* was modestly less fit than the WT in the acute pneumonia model (**Figure 3**), we would start these follow-up experiments in the acute pneumonia model as well. Ciprofloxacin has previously been

used in this infection model (319, 320). We would infect mice with WT or *P. aeruginosa* Δ*gshA* as before, and either treat mice with ciprofloxacin or leave them untreated as a control. To assess the efficacy of the treatment, we would measure viable bacterial loads in the lungs over time and compare lung histology as a measure of lung damage. Histological indicators of lung damage include leukocyte infiltration, edema, blood clotting, and tissue necrosis. We would expect to see enhanced clearing of *P. aeruginosa* Δ*gshA* than the WT in the ciprofloxacin treated mice. A range of ciprofloxacin dosing concentrations may also be necessary to establish a dose-response curve. Alternatively, we could perform competition assays with WT or *P. aeruginosa* Δ*gshA*. We would infect mice with equal proportions of WT and *P. aeruginosa* Δ*gshA*, then either leave mice untreated or treat with ciprofloxacin. We could measure the final proportions of WT and *P. aeruginosa* Δ*gshA* using qPCR. We could expect the proportion of WT:Δ*gshA* to be significantly higher in the ciprofloxacin treated group compared to the control.

Finally, we would test combination therapy of ciprofloxacin + GSH inhibitors *in vivo.* We would infect mice with WT *P. aeruginosa* and treat with ciprofloxacin alone, GSH inhibitors alone, and ciprofloxacin + GSH inhibitors. As before, we would measure bacterial loads in the lungs over time and assess lung histology. To check for host toxicity caused by GSH inhibitor treatment, we would also treat uninfected mice with GSH inhibitors + ciprofloxacin and then evaluate indicators of mouse health, such as the presence of white spots on the liver (a sign of hepatocellular necrosis), and changes in body weight or behavior (scruffy fur, lethargy, rapid breathing, etc.) (257). If combination therapy with ciprofloxacin + GSH inhibitors is significantly more efficacious at killing *P. aeruginosa* in the mouse lung than ciprofloxacin alone, then these results would provide a first proof-of-concept of the potential benefit of the therapy. It may then be worth investigating further for its safety and efficacy in humans. However, this model has its limitations. A lack of toxicity in mice does

not always correlate with a lack of toxicity in humans (321). Furthermore, mice tend to metabolize drugs, including antibiotics, faster than humans, which can make it difficult to compare appropriate dosing (321).

1.20.5 Mechanisms for GSH biosynthesis fitness benefit in the lung

As demonstrated in **Figure 3**, *P. aeruginosa* Δ*gshA* was modestly less fit in the acute pneumonia mouse infection model, but it was as fit as the WT in the surgical wound, burn wound, and abscess models. It is not obvious why *P. aeruginosa* Δ*gshA* does not suffer from a significant fitness defect in these three models. For instance, oxidative stress is extensively involved in the pathophysiology of burns (see section 1.3.3). Immediately following a burn there is severe immune suppression, quickly followed by heightened inflammatory responses, activation of phagocytic cells, and subsequent production of ROS (34-36). Extracellular concentrations of GSH in the blood and soft tissues are normally low (250, 322), and tissue levels of GSH are further depleted by the increased oxidative activity (251, 323). Furthermore, work in our lab has previously shown that flagellar motility is a fitness requirement for *P. aeruginosa* in burn wound infections (4), as *P. aeruginosa* uses flagellar motility to invade the bloodstream and become septic, leading to shock and death. However, GSH deficiency inhibits flagellar motility (71, 176, 215). Increased inflammatory responses, oxidative stress and tissue GSH depletion are similarly characteristic of chronic wound infections (18, 19). Future work could be directed at investigating the mechanisms for why GSH provides a fitness benefit for *P. aeruginosa* in the lung, but not in the soft tissues.

One explanation may be differences in the infection environment. Extracellular concentrations of GSH in the tissues are typically very low; however, Alveolar fluid contains unusually high concentrations of extracellular GSH as a protectant against the

relatively high oxygen tension and oxidative stress present in the lung (207, 322). Under aerobic conditions, pyocyanin, a redox-active phenazine secreted by *P. aeruginosa* (see section 1.5), directly oxidizes GSH and produces hydrogen peroxide, depleting available GSH in the process (92, 93). Oxygen availability also affects pyocyanin production; *P. aeruginosa* PAO1 produces little pyocyanin under anaerobic conditions {Arai, 2011 #412}. While determining oxygen availability during infection, particularly at different sites of infection, is an area of active investigation and debate, it is likely that *P. aeruginosa* is exposed to more oxygen in the lung than in the soft tissues {Wessel, 2014 #405}{Stacy, 2016 #67}. Therefore, under aerobic conditions in the lung, *P. aeruginosa* may be stimulated to produce more pyocyanin, which in turn can oxidize host GSH. This reaction would deplete the pool of available reduced GSH and also produce hydrogen peroxide as a byproduct. As shown in **Table 1**, *P. aeruginosa* Δ*gshA* is hypersensitive to oxidative stress, which would further hinder *P. aeruginosa* Δ*gshA*'s survival in the lung.

To test this hypothesis, we could determine the degree of GSH scavenging in the lung compared to the soft tissues. We could make a double mutant in both GSH biosynthesis and GSH import. The genes involved in GSH import in *P. aeruginosa* are unclear, but there are homologs in other bacteria {Vergauwen, 2010 #413}{Pittman, 2005 #414}, and a genetic screen could be performed to identify the GSH importer genes. We would then infect mice with *P. aeruginosa* Δ*gshA* and GSH importer double mutants in all four mouse models of infection. If we discover that the double mutants are less fit in the soft tissues, then this would indicate that *P. aeruginosa* Δ*gshA* is able to scavenge host GSH and offset its GSH biosynthesis deficiency. Likewise, the degree of fitness loss for the double mutant in the lung would indicate the degree that *P. aeruginosa* Δ*gshA* was able to scavenge GSH from the lung. In other words, if we do not find a significant fitness defect for the double mutant compared to the single *P. aeruginosa* Δ*gshA* mutant in the lung, this would

indicate that host GSH was not available to *P. aeruginosa* Δ*gshA* in the lung, likely because it was depleted due to the action of pyocyanin.

An alternative test to this hypothesis is to explore the effect of catalase on *P. aeruginosa* Δ*gshA* fitness. Catalase is an enzyme that breaks down hydrogen peroxide into oxygen and water. *P. aeruginosa* makes several catalases, including the major, constitutively expressed catalase produced by the *katA* gene (324). We would first test if overproduction of catalase would protect *P. aeruginosa* Δ*gshA* from hydrogen peroxide. We would create WT and *P. aeruginosa* Δ*gshA katA* overexpression strains carrying *katA* expression plasmids. As before in **Table 1**, we would perform hydrogen peroxide disc diffusion assays with WT::*katA* and Δ*gshA*::*katA* strains. We would expect to see *P. aeruginosa WT::katA* less susceptible to hydrogen peroxide than the parent WT, and to see *P. aeruginosa* Δ*gshA::katA* also having reduced susceptibility to hydrogen peroxide, similar to or even surpassing the parent WT. We would then test these strains in the acute pneumonia mouse model as before in **Figure 3**. We would record mouse survival, but could also go more in-depth and record bacterial CFUs in the lungs over time or compare lung histology. If hydrogen peroxide is killing *P. aeruginosa* Δ*gshA*, then we would expect *P. aeruginosa* Δ*gshA*::*katA* to be better protected from hydrogen peroxide and have lethality or bacterial loads restored to WT levels. It is important to test *P. aeruginosa WT::katA* as well, as it may be more fit than the parent WT during infection because it is better protected from the hydrogen peroxide produced by the immune system. Alternatively, we could infect mice with *P. aeruginosa* WT or Δ*gshA* and treat the mice with exogenous catalase. In this case, we would also expect catalase treatment to protect *P. aeruginosa* Δ*gshA*, restoring lethality or bacterial loads to WT levels. However, exogenous catalase treatment may also be protective for the host.

A second approach to testing this hypothesis is knocking out pyocyanin production. We could create a *P. aeruginosa* Δ*gshA,* Δ*phzM* double mutant, and a Δ*phzM* single mutant (95). The absence of pyocyanin production in the Δ*phzM* mutants would be confirmed *in vitro* (215). We would then infect mice with *P. aeruginosa* WT; Δ*gshA;* Δ*gshA,* Δ*phzM*; and Δ*phzM*. It is important to test the *P. aeruginosa* Δ*phzM* single mutant as a control, since pyocyanin is a virulence factor that is toxic to the host, and deleting it will likely reduce *P. aeruginosa*'s virulence (94, 96). If pyocyanin production is key to the *P. aeruginosa* Δ*gshA* fitness defect, then we would expect to see the *P. aeruginosa* Δ*gshA,* Δ*phzM* double mutant more fit than the Δ*gshA* single mutant. However, the fitness loss in the single *P. aeruginosa* Δ*phzM* mutant may be so severe that it overshadows any fitness gains in the *P. aeruginosa* Δ*gshA,* Δ*phzM* double mutant.

One caveat to this hypothesis is that previous studies have shown that *P. aeruginosa* Δ*gshA* produces less pyocyanin than the WT in tryptic soy broth (215). However, it is not known if *P. aeruginosa* Δ*gshA* produces less pyocyanin in the lung during acute pneumonia infections. It is possible that *P. aeruginosa* Δ*gshA* is able to compensate for its inability to biosynthesize GSH by importing host GSH, which is available in alveolar fluid. Or, the reduced pyocyanin levels produced by *P. aeruginosa* Δ*gshA* may still be sufficient to generate a harmful amount of hydrogen peroxide. To address this concern, we could infect mice as in **Figure 3** with *P. aeruginosa* WT, Δ*gshA*, or uninfected controls, and measure lung pyocyanin and hydrogen peroxide concentrations. We could measure pyocyanin in whole lung homogenates using a spectrophotometric test or high-pressure liquid chromatography (HPLC) (215, 325). Hydrogen peroxide could also be quantified using a spectrophotometric test on captured exhaled breath (326, 327). As a control, we would expect to find higher pyocyanin and hydrogen peroxide levels in *P. aeruginosa* WT infected mice than uninfected mice. We may find that *P. aeruginosa* Δ*gshA* produces

pyocyanin and induces hydrogen peroxide stress at similar levels as the WT, supporting the hypothesis. However, if both pyocyanin and hydrogen peroxide levels are significantly lower in *P. aeruginosa* Δ*gshA* infected mice compared to *P. aeruginosa* WT infected mice, then those results would weaken support for this hypothesis.

A second hypothesis for why *P. aeruginosa* requires GSH for fitness in the lung, but not in the soft tissues, is that GSH may modulate virulence factors that are more important for fitness in the lung. The requirement of T3SS for virulence in the mouse lung is well documented (64, 102, 178). The T3SS (see section 1.5) enables *P. aeruginosa* to inject host cells with toxins. These toxins can disrupt the lung epithelial barrier, allowing the bacteria to invade the bloodstream and become septic (64). Importantly, GSH-deficient *P. aeruginosa* mutants have reduced T3SS expression (176). While T3SS appears strongly correlated with virulence in the lung, its importance in the soft tissues is less well understood, and the fitness benefit of T3SS in these different sites of infection hasn't been compared directly. In our previous Tn-seq study, we observed increased T3SS expression and lower T3SS mutant abundance in burn and surgical wound mouse models compared to growth in MOPS-succinate (4). A recent study showed that a T3SS and alginate double mutant had significantly lower bacterial loads in a rabbit ear model, however, single T3SS mutants weren't tested (328). T3SS mutants were also less fit in a mouse abscess model of infection (173).

To test this hypothesis, we would use all four mouse models (acute pneumonia, burn wound, surgical wound, and abscess) and infect mice with either *P. aeruginosa* WT or a T3SS mutant (for example, Δ*pcrV)* (178). We would then compare bacterial loads between each site of infection. If T3SS is more important for fitness in the lung compared to the soft tissues, then we would expect the difference in bacterial loads for *P. aeruginosa* WT compared to *P. aeruginosa* Δ*pcrV* to be more severe in the lung than in the soft tissues.

However, if this hypothesis is incorrect and T3SS isn't especially more important in the lung, then these studies would still better elucidate the role of T3SS for virulence in different sites of infection.

1.20.6 *Effect of exogenous GSH therapy on P. aeruginosa infection*

Excessive oxidative stress is a component of many different human pathologies, including chronic wounds (246), burn wounds (34), pneumonia (245, 247) and cystic fibrosis (329, 330). Because of its robust antioxidant abilities, low toxicity and low cost, exogenous GSH therapy may be an attractive treatment option (207). Rodent experiments and human clinical trials have demonstrated that exogenous GSH treatment can significantly improve healing, reduce tissue damage, and lower mortality in chronic wounds (248, 249), burn wounds (35, 250, 251), and pneumonia (252-254). However, laboratory experiments regarding the effect of GSH therapy on injured tissue are usually conducted with uninfected tissue, so it is unknown how exogenous therapy may affect *P. aeruginosa* physiology and influence the severity of infection. Our data in **Table 1** show that adding GSH to WT *P. aeruginosa* reduced its susceptibility to bleach and carbenicillin. Previous studies have also shown that *P. aeruginosa* WT exposed to exogenous GSH induced increased T3SS expression (176) and altered susceptibility to some antibiotics (217). Therefore, while exogenous GSH therapy may be beneficial for host cells, it may simultaneously promote unwanted *P. aeruginosa* phenotypes and potentially exacerbate infection. Therefore, further studies may attempt to elucidate the safety and efficacy of GSH administration in different types of *P. aeruginosa* infection.

To test this hypothesis, we could repeat our four mouse infection models (surgical wound, burn wound, abscess, and pneumonia) with *P. aeruginosa* WT or uninfected controls, and then treat mice with GSH or leave untreated as a control. We could measure host health

outcomes, such as survival (burn and pneumonia), histology, wound size (burn and chronic wound), and mouse physiological parameters (weight change, behavior). We would also measure *P. aeruginosa* bacterial loads over time as an indicator of the effect of exogenous GSH on *P. aeruginosa* survival. We may find that GSH treated groups have improved health outcomes compared to untreated groups, regardless of *P. aeruginosa* infection, which would indicate safety and efficacy of the treatment. Or, we may find that *P. aeruginosa* survives better in GSH treated animals, which may negate or even worsen any beneficial effect that exogenous GSH treatment may have. In that case, human clinical trials using exogenous GSH therapy should examine presence or absence of *P. aeruginosa* as a factor that could influence treatment outcomes.

In conclusion, results from these future directions may further our understanding of the role of GSH in *P. aeruginosa* physiology, and may inform future treatment strategies.

1.21 Transcriptomic and Proteomic Signatures of Growth Rate in *Pseudomonas aeruginosa* Grown in Chemostats

1.21.1 Summary of results

Bacteria use many complex, interconnected systems for adjusting their growth rate to suit their environmental conditions. The growth rate, or doubling time, has significant impacts on cellular physiology, from cell size, to ribosomal abundance, to stress tolerance, to antibiotic resistance (258, 267, 268). A few studies have provided insight into the range of doubling times that *P. aeruginosa* likely grows at during infection, and these growth rates are likely slower than the rapid logarithmic phase growth usually studied under laboratory conditions (262, 271-273). Because growth rate affects so many aspects of cellular physiology, better understanding the effect of growth rate will improve interpretations of RNA-seq data.

We used a chemostat, which allows the cellular density and growth rate to be precisely controlled while keeping other environmental factors near-constant (282-285). We cultured *P. aeruginosa* strain PA14 in MOPs succinate minimal medium at a wide range of four different doubling times, and mRNA and protein abundances were quantified using RNA-seq and proteomics mass spectrometry, respectively. We found that there are differing relationships between growth rate, mRNA expression, protein expression, and protein-to-mRNA ratios. There is a modest correlation between mRNA and protein levels, and these vary slightly with growth rate (**Figure 7 and 8**). We also observed greater variation in mRNA expression compared to protein expression. The variation in mRNA expression across growth rates is strongly correlated with the variance in protein-to-mRNA ratios across growth rates (**Figure 5, Figure 12**), while mean protein expression is strongly correlated with the protein-to-mRNA ratio (**Figure 9**).

These results show that the assumption of a 1:1 correlation between mRNA and protein is not accurate for interpreting RNA-seq data. Instead, it may be feasible to apply a "conversion factor", based on the protein-to-mRNA ratio for each gene. We have characterized conversion factors for roughly 3900 *P. aeruginosa* genes. Over half of these are stable across growth rates (**Figure 11**). However, the reliability of our conversion factors is limited by our use of only one strain and type of media. These conversion factors could be further refined by including different strains, media conditions, and even bacterial species.

1.21.2 Building a computational model for predicting growth rate in human infection

While RNA-seq is a powerful tool for profiling a "snapshot" of global gene expression, and it is one of a few techniques that can be used on bacteria sampled from human infections, is has limitations. When interpreting RNA-seq data, relative differences in gene expression

levels in the condition of interest are compared to those of *in vitro* conditions. However, environmental conditions often impact multiple genetic pathways simultaneously, making it difficult to discern the importance of individual physiological functions from changes in gene expression. Furthermore, because these comparisons are relative, it is difficult to draw conclusions about absolute qualities of the infection environment itself. For example, we currently cannot determine important characteristics such as bacterial growth rate, density, oxygen availability, or nutrient availability at the site of infection from RNA-seq data alone. In our laboratory, future directions for this work are aimed at 1) expanding the dataset to include a greater variety of experimental conditions, and then 2) building a computational model for predicting bacterial growth rate during human infection.

1.21.2.1 Expanding the dataset with respect to media composition, strain, and species

Here we presented a benchmark dataset of carefully controlled chemostat conditions that included four different generation times, one type of media, and a single strain of *P. aeruginosa*. Naturally, this dataset can be expanded in many different directions with regards to media composition, strain, and even species. These additional factors are all complementary and can build upon each other. Ultimately, expanding our dataset in this way will help better define a conserved, core set of genes that are differentially expressed with growth rate independent of other factors. It will also be a powerful dataset to use as an *in vitro* comparison in other RNA-seq experiments. Finally, this information will also further our understanding of basic bacterial physiology at the transcriptional level.

We started with MOPS-succinate minimal media because *P. aeruginosa* succinate metabolism is relatively simple, well characterized, and reproducible (4, 221, 286). However, since gene expression is highly impacted by nutrient availability (276, 295, 296), future experiments using different types of media would allow us to more precisely identify

the genes that are differentially expressed with growth rate, independent of the limiting nutrient. It would also allow us to explore the interactions between other metabolic pathways and growth rate. One approach is to change the nature of the limiting nutrient, such as carbon, nitrogen, or phosphorus limitation (276, 295). A different approach is to use complex media such as diluted brain heart infusion broth (BHI) or SCFM. BHI is an animal-protein-based rich undefined laboratory media, while SCFM (as described in section 1.7.1) is designed to mimic human CF sputum. Importantly, these media types, particularly SCFM, more closely resemble the nutritional environment of the host during infection. We also know from previous *in vitro* work that the *P. aeruginosa* transcriptional profile in BHI or SCFM is very different than in minimal medium (43, 286).

In these experiments we used only *P. aeruginosa* strain PA14, which is a widely used clinical strain isolated from a human chronic wound. However, natural human infections are usually composed of a mixture of strains (51, 331). While our previous work has shown that mRNA-to-protein ratios for a given gene are largely conserved between strains (in that case, *P. aeruginosa* PAO1 and PA14), differences between strains can cause variations in clinically relevant phenotypes, such as antibiotic resistance (292). For these reasons, our future directions include repeating these experiments with different strains of *P. aeruginosa*, such as PAO1, the most well-characterized laboratory strain, or PAB1, a CF human clinical isolate. We could directly compare responses in these strains to PA14 by growing them in the same media, MOPS-succinate. We could also provide a potentially dramatically different transcriptional profile by growing them in diluted BHI or SCFM.

As described in section 1.3, some infection types, such as chronic wounds and CF lung infections, are composed of polymicrobial communities, rather than a single species. Furthermore, it is probable that many genetic pathways with expression levels dependant on growth rate are conserved across living organisms, similar to how mechanisms of

general stress response are highly conserved (260, 276). While the focus of this work was on *P. aeruginosa*, our laboratory is interested in expanding this dataset to include two other clinically relevant bacteria: *Mycobacterium abscessus* (MAB) and *Aggregatibacter actinomycetemcomitans*. *A. actinomycetemcomitans* is a Gram-negative, facultative anaerobe that is associated with aggressive periodontitis (332, 333). One major advantage of studying oral pathogens is that it is relatively easy to collect human clinical samples. *Mycobacterium abscessus* is part of the *Mycobacterium abscessus* complex (MAB), a group of rapid growing, multi-drug resistant nontuberculous mycobacteria (NTM) known to commonly infect CF patients (334, 335). As before, we would culture these bacterial species in precisely controlled chemostat conditions. We plan to grow two clinical CF strains of *Mycobacterium abscessus* in SCFM, and one strain of *A. actinomycetemcomitans* in diluted BHI and in CDM (described in section 2.2). This information will allow us to identify genes that are differentially expressed in response to growth rate that are conserved across bacterial species.

1.21.2.2 Building a computational model for predicting growth rate in human infection

Performing RNA-seq on bacteria sampled directly from humans has the potential to reveal information about bacterial physiology during human infection without relying on laboratory models that may not recapitulate all aspects of a human infection. However, until recently, human sample RNA-seq has rarely been done due to technical challenges. The amount of bacterial RNA relative to human RNA is often very low, and the throughput and cost of sequencing technologies were prohibitive. Previous studies mainly used samples that were relatively easy to obtain and contained a greater proportion of bacterial RNA to host RNA, such as human stool or urine (288-290). Our laboratory has recently developed an RNA-seq protocol applicable for a diverse range of human samples, including expectorated CF sputum and chronic wounds (286, 287). Using this protocol to

continue to expand the number and diversity of human infection RNA-seq samples will greatly improve our knowledge of bacterial physiology during infection. However, while standard differential expression analysis allows us to identify which genes are expressed differently between *in vitro* and human samples, it can be difficult to interpret how these transcriptional differences relate to the bacterium's infection environment and complex physiological functions.

One method to address these shortcomings is flux-balance analysis (FBA) (336). FBA uses precise metabolic network reconstructions to mathematically calculate the flow of metabolites through a system and predict cellular behavior, such as oxygen consumption or growth rate. However, FBA is only as accurate as the underlying metabolic models, and thus can only be used to predict a small set of highly characterized phenotypes. A second, more common approach is the use of biomarker genes. Expression of a biomarker gene is directly linked to an environmental variable (337). For example, we have used expression of the biomarker gene cbb3-2 to indicate low oxygen availability (< ~2%) in *P. aeruginosa* aggregates (338). However, biomarker genes are not precisely quantitative, and might only be accurate for classifying environmental qualities into binary categories, such as presence/absence, or low/high availability of an environmental factor. Their use is also restricted to simple and well-characterized variables; they may not be accurate for features that are influenced by many complex variables simultaneously, such as growth rate.

Future work in our laboratory aims to build a machine learning framework to quantify bacterial growth rate directly from gene expression data. This framework is based on a recently developed method used in *Saccharomyces cerevisiae* (339). In that work, researchers successfully built a computational model based on a small number of genes to accurately predict the growth rate of *S. cerevisiae, Saccharomyces bayanus* and

Schizosaccharomyces pombe, in different media conditions. Similarly, we will use our chemostat gene expression data to fit a multivariable LASSO (least absolute shrinkage and selection operator) regression model (340). LASSO regression analysis uses both feature selection and regularization in order to penalize solutions that require many features (genes) in order to avoid overfitting and improve prediction accuracy and interpretability. A regression analysis aims to model the relationship between a dependant variable and one or more independent variables, in this case to predict growth rate from gene expression data. Overfitting occurs when a model is not generalizable to other datasets. We want our model to be robust and avoid overfitting, since human sample RNA-seq involves many different complex factors, for example host comorbidities, presence of co-infecting microbes, antibiotic treatment, etc. Feature selection is the process of narrowing down the number of genes to include in the model. Regularization shrinks the coefficient estimates towards zero, penalizing complex models with many features. These processes help build an accurate model with the minimal number of genes possible, since too many genes can cause overfitting.

To develop and test our model, we will expand our current dataset with a wide variety of carefully controlled chemostat conditions that vary with respect to media, strain, and species, as described in the previous section. The key to establishing a precise relationship between variables like growth rate and media composition to gene expression is to specifically vary one variable at a time, so that any transcriptional changes observed can be attributed to that perturbation. Therefore, we could include samples with only one variable altered compared to our original dataset, such as *P. aeruginosa* strain PA14 grown in SCFM, or strain PAB1 grown in MOPS-succinate. Furthermore, in order to validate our model, we also want to include samples with dramatically different transcriptional profiles, such as *M. abscessus* grown in SCFM. Taken together, we will be

able to determine a core set of genes with expression dependent on growth rate independent of other factors.

We will test the accuracy and robustness of our model for predicting bacterial growth rate from RNA-seq data using *k*-fold cross validation and bootstrap randomization. *k*-fold cross validation involves repeatedly randomly dividing the dataset into new test or training samples, training the model on the new training samples, and assessing how accurately it predicts the new test samples. Bootstrap randomization involves randomly shuffling the dataset and re-running the LASSO algorithm to obtain pseudo p-values. After assessing model accuracy using chemostat data, we will then validate the model using RNA-seq data previously generated in our lab where the generation time of *P. aeruginosa* is known. We will then use our model to estimate *P. aeruginosa* growth rate from animal models and human infection samples.

Should LASSO not perform well, elastic net may be used as an alternative. Elastic net is also a regularized regression model, but it adds ridge regression into the feature penalization function, which may be helpful for dealing with many genes with similar patterns of gene expression. However, if our model is still not capable to accurately quantifying growth rate from human samples, it is likely that we will at least be able to classify growth rate into arbitrary categories, such as slow, medium, or fast growth.

In conclusion, completion of these future directions will result in both a large, carefully controlled dataset of bacterial transcriptional profiles, and a robust computational framework for predicting *P. aeruginosa* growth rate during human infection. Since growth rate impacts many aspects of cellular physiology, particularly antibiotic resistance, this information will improve our understanding of fundamental cell biology and may inform future treatment strategies.

1.22 Final discussion

In conclusion, this research has elucidated fundamental aspects of *P. aeruginosa* physiology. We assessed the role of GSH biosynthesis for *P. aeruginosa* during infection, and found that it confers a modest fitness benefit in the lung, but not in the soft tissues. We also explored how growth rate impacts *P. aeruginosa* mRNA and protein expression, and identified conversion factors that could be used to more accurately predict protein abundance from RNA-seq data. However, many questions remain unknown, and this work could be further refined. Follow-up studies could provide insight into the mechanism of GSH biosynthesis in the lung and determine the safety and efficacy of combination therapy with GSH biosynthesis inhibitors and antibiotics. Likewise, our conversion factors could be made more robust and accurate by expanding our dataset with respect to strain, media composition, and even bacterial species. The research presented in this dissertation is one small contribution to the global effort to better understand, and ultimately treat, *P. aeruginosa* infections.

REFERENECES

1. Moradali, M.F., S. Ghods, and B.H. Rehm, *Pseudomonas aeruginosa lifestyle: a paradigm for adaptation, survival, and persistence.* Frontiers in cellular and infection microbiology, 2017. **7**: p. 39.

2. Ringen, L.M. and C.H. Drake, *A study of the incidence of Pseudomonas aeruginosa from various natural sources.* Journal of bacteriology, 1952. **64**(6): p. 841.

3. Crone, S., et al., *The environmental occurrence of Pseudomonas aeruginosa.* APMIS, 2019.

4. Turner, K.H., et al., *Requirements for Pseudomonas aeruginosa acute burn and chronic surgical wound infection.* PLoS genetics, 2014. **10**(7): p. e1004518.

5. Turner, K.H., et al., *Essential genome of Pseudomonas aeruginosa in cystic fibrosis sputum.* Proceedings of the National Academy of Sciences, 2015. **112**(13): p. 4110-4115.

6. Ibberson, C.B., et al., *Co-infecting microorganisms dramatically alter pathogen gene essentiality during polymicrobial infection.* Nature microbiology, 2017. **2**(8): p. 17079.

7. Jovcic, B., et al., *Emergence of NDM-1 metallo-β-lactamase in Pseudomonas aeruginosa clinical isolates from Serbia.* Antimicrobial agents and chemotherapy, 2011. **55**(8): p. 3929-3931.

8. Mataseje, L., et al., *Colistin-nonsusceptible Pseudomonas aeruginosa sequence type 654 with blaNDM-1 arrives in North America.* Antimicrobial agents and chemotherapy, 2016. **60**(3): p. 1794-1800.

9. Potron, A., L. Poirel, and P. Nordmann, *Emerging broad-spectrum resistance in Pseudomonas aeruginosa and Acinetobacter baumannii: mechanisms and*

epidemiology. International journal of antimicrobial agents, 2015. **45**(6): p. 568-585.

10. Iglewski, B., *Pseudomonas*. 4th ed. Medical Microbiology, ed. S. Baron. 1996, Galveston, TX.

11. Klockgether, J., et al., *Pseudomonas aeruginosa genomic structure and diversity.* Frontiers in microbiology, 2011. **2**: p. 150.

12. Blanc, D., et al., *Faucets as a reservoir of endemic Pseudomonas aeruginosa colonization/infections in intensive care units.* Intensive care medicine, 2004. **30**(10): p. 1964-1968.

13. Engelhart, S., et al., *Pseudomonas aeruginosa outbreak in a haematology–oncology unit associated with contaminated surface cleaning equipment.* Journal of Hospital Infection, 2002. **52**(2): p. 93-98.

14. Strand, C.L., et al., *Nosocomial Pseudomonas aeruginosa urinary tract infections.* Jama, 1982. **248**(13): p. 1615-1618.

15. Bodey, G.P., et al., *Infections caused by Pseudomonas aeruginosa.* Reviews of infectious diseases, 1983. **5**(2): p. 279-313.

16. Frimmersdorf, E., et al., *How Pseudomonas aeruginosa adapts to various environments: a metabolomic approach.* Environmental microbiology, 2010. **12**(6): p. 1734-1747.

17. Health, U.D.o., et al., *ANTIBIOTIC RESISTANCE THREATS in the United States, 2013.[online] CDC*. 2019.

18. Sen, C.K., et al., *Human skin wounds: a major and snowballing threat to public health and the economy.* Wound repair and regeneration, 2009. **17**(6): p. 763-771.

19. Lazarus, G.S., et al., *Definitions and guidelines for assessment of wounds and evaluation of healing.* Archives of dermatology, 1994. **130**(4): p. 489-493.

20. Control, C.f.D. and Prevention, *National diabetes statistics report: estimates of diabetes and its burden in the United States, 2014.* Atlanta, GA: US Department of Health and Human Services, 2014. **2014**.

21. Davies, C.E., et al., *Use of 16S ribosomal DNA PCR and denaturing gradient gel electrophoresis for analysis of the microfloras of healing and nonhealing chronic venous leg ulcers.* J Clin Microbiol, 2004. **42**(8): p. 3549-57.

22. Dowd, S.E., et al., *Survey of bacterial diversity in chronic wounds using pyrosequencing, DGGE, and full ribosome shotgun sequencing.* BMC Microbiol, 2008. **8**: p. 43.

23. Dowd, S.E., et al., *Polymicrobial nature of chronic diabetic foot ulcer biofilm infections determined using bacterial tag encoded FLX amplicon pyrosequencing (bTEFAP).* PLoS ONE, 2008. **3**(10): p. e3326.

24. Gjødsbøl, K., et al., *Multiple bacterial species reside in chronic wounds: a longitudinal study.* International wound journal, 2006. **3**(3): p. 225-231.

25. Kirketerp-Møller, K., et al., *Distribution, organization, and ecology of bacteria in chronic wounds.* Journal of clinical microbiology, 2008. **46**(8): p. 2717-2722.

26. Price, L.B., et al., *Community analysis of chronic wound bacteria using 16S rRNA gene-based pyrosequencing: impact of diabetes and antibiotics on chronic wound microbiota.* PLoS One, 2009. **4**(7): p. e6462.

27. Wolcott, R.D., et al., *Analysis of the chronic wound microbiota of 2,963 patients by 16S rDNA pyrosequencing.* Wound Repair Regen, 2016. **24**(1): p. 163-74.

28. Fazli, M., et al., *Nonrandom distribution of Pseudomonas aeruginosa and Staphylococcus aureus in chronic wounds.* J Clin Microbiol, 2009. **47**(12): p. 4084-9.

29. Dalton, T., et al., *An in vivo polymicrobial biofilm wound infection model to study interspecies interactions.* PloS one, 2011. **6**(11): p. e27317.

30. Korgaonkar, A., et al., *Community surveillance enhances Pseudomonas aeruginosa virulence during polymicrobial infection.* Proceedings of the National Academy of Sciences, 2013. **110**(3): p. 1059-1064.

31. Zhao, G., et al., *Biofilms and inflammation in chronic wounds.* Advances in wound care, 2013. **2**(7): p. 389-399.

32. Halbert, A.R., et al., *The effect of bacterial colonization on venous ulcer healing.* The Australasian journal of dermatology, 1992. **33**(2): p. 75-80.

33. Gjødsbøl, K., et al., *Multiple bacterial species reside in chronic wounds: a longitudinal study.* International wound journal, 2006. **3**(3): p. 225-231.

34. Parihar, A., et al., *Oxidative stress and anti-oxidative mobilization in burn injury.* Burns, 2008. **34**(1): p. 6-17.

35. Deniz, M., et al., *An effective antioxidant drug on prevention of the necrosis of zone of stasis: N-acetylcysteine.* Burns, 2013. **39**(2): p. 320-325.

36. Bertin-Maghit, M., et al., *Time course of oxidative stress after major burns.* Intensive care medicine, 2000. **26**(6): p. 800-803.

37. McManus, A., et al., *Twenty-five year review ofPseudomonas aeruginosa bacteremia in a burn center.* European journal of clinical microbiology, 1985. **4**(2): p. 219-223.

38. Coetzee, E., H. Rode, and D. Kahn, *Pseudomonas aeruginosa burn wound infection in a dedicated paediatric burns unit.* South African Journal of Surgery, 2013. **51**(2): p. 50-53.

39. Keen III, E.F., et al., *Prevalence of multidrug-resistant organisms recovered at a military burn center.* Burns, 2010. **36**(6): p. 819-825.

40. Geyik, M.F., et al., *Epidemiology of burn unit infections in children.* American journal of infection control, 2003. **31**(6): p. 342-346.

41. Sittig, K. and E.A. Deitch, *Effect of bacteremia on mortality after thermal injury.* Archives of Surgery, 1988. **123**(11): p. 1367-1370.

42. Tang, A.C., et al., *Current concepts: host–pathogen interactions in cystic fibrosis airways disease.* European Respiratory Review, 2014. **23**(133): p. 320-332.

43. Palmer, K.L., L.M. Aye, and M. Whiteley, *Nutritional cues control Pseudomonas aeruginosa multicellular behavior in cystic fibrosis sputum.* Journal of bacteriology, 2007. **189**(22): p. 8079-8087.

44. Pressler, T., et al., *Chronic pseudomonas aeruginosa infection definition: EuroCareCF working group report.* Journal of Cystic Fibrosis, 2011. **10**: p. S75-S78.

45. LiPuma, J.J., *The changing microbial epidemiology in cystic fibrosis.* Clinical microbiology reviews, 2010. **23**(2): p. 299-323.

46. *Cystic Fibrosis Foundation Patient Registry 2018 Annual Data Report* 2018; Available from: https://www.cff.org/Research/Researcher-Resources/Patient-Registry/2018-Patient-Registry-Annual-Data-Report.pdf.

47. Kerem, E., et al., *Pulmonary function and clinical course in patients with cystic fibrosis after pulmonary colonization with Pseudomonas aeruginosa.* The Journal of pediatrics, 1990. **116**(5): p. 714-719.

48. Kosorok, M.R., et al., *Acceleration of lung disease in children with cystic fibrosis after Pseudomonas aeruginosa acquisition.* Pediatric pulmonology, 2001. **32**(4): p. 277-287.

49. Henry, R.L., C.M. Mellis, and L. Petrovic, *Mucoid Pseudomonas aeruginosa is a marker of poor survival in cystic fibrosis.* Pediatric pulmonology, 1992. **12**(3): p. 158-161.

50. Huse, H.K., et al., *Parallel evolution in Pseudomonas aeruginosa over 39,000 generations in vivo.* MBio, 2010. **1**(4): p. e00199-10.

51. Smith, E.E., et al., *Genetic adaptation by Pseudomonas aeruginosa to the airways of cystic fibrosis patients.* Proceedings of the National Academy of Sciences, 2006. **103**(22): p. 8487-8492.

52. Schwarzmann, S. and J.R. Boring, *Antiphagocytic effect of slime from a mucoid strain of Pseudomonas aeruginosa.* Infection and immunity, 1971. **3**(6): p. 762-767.

53. Govan, J.R. and V. Deretic, *Microbial pathogenesis in cystic fibrosis: mucoid Pseudomonas aeruginosa and Burkholderia cepacia.* Microbiol. Mol. Biol. Rev., 1996. **60**(3): p. 539-574.

54. McCarthy, R.R., et al., *Cyclic-di-GMP regulates lipopolysaccharide modification and contributes to Pseudomonas aeruginosa immune evasion.* Nature microbiology, 2017. **2**(6): p. 1-10.

55. Goldberg, J.B. and G.B. Pier, *Pseudomonas aeruginosa lipopolysaccharides and pathogenesis.* Trends in microbiology, 1996. **4**(12): p. 490-494.

56. Stanislavsky, E.S. and J.S. Lam, *Pseudomonas aeruginosa antigens as potential vaccines.* FEMS microbiology reviews, 1997. **21**(3): p. 243-277.

57. Poole, K., *Pseudomonas aeruginosa: resistance to the max.* Frontiers in microbiology, 2011. **2**: p. 65.

58. Bjarnsholt, T., et al., *Quorum sensing and virulence of Pseudomonas aeruginosa during lung infection of cystic fibrosis patients.* PloS one, 2010. **5**(4).

59. LaFayette, S.L., et al., *Cystic fibrosis–adapted Pseudomonas aeruginosa quorum sensing lasR mutants cause hyperinflammatory responses.* Science advances, 2015. **1**(6): p. e1500199.

60. *Pneumonia*. 2018; Available from: https://www.mayoclinic.org/diseases-conditions/pneumonia/symptoms-causes/syc-20354204.

61. Jones, R.N., *Microbial etiologies of hospital-acquired bacterial pneumonia and ventilator-associated bacterial pneumonia.* Clinical infectious diseases, 2010. **51**(Supplement_1): p. S81-S87.

62. Peleg, A.Y. and D.C. Hooper, *Hospital-acquired infections due to gram-negative bacteria.* New England Journal of Medicine, 2010. **362**(19): p. 1804-1813.

63. Parker, C.M., et al., *Ventilator-associated pneumonia caused by multidrug-resistant organisms or Pseudomonas aeruginosa: prevalence, incidence, risk factors, and outcomes.* Journal of critical care, 2008. **23**(1): p. 18-26.

64. Sadikot, R.T., et al., *Pathogen–host interactions in Pseudomonas aeruginosa pneumonia.* American journal of respiratory and critical care medicine, 2005. **171**(11): p. 1209-1223.

65. Santajit, S. and N. Indrawattana, *Mechanisms of antimicrobial resistance in ESKAPE pathogens.* BioMed research international, 2016. **2016**.

66. Cox, G. and G.D. Wright, *Intrinsic antibiotic resistance: mechanisms, origins, challenges and solutions.* International Journal of Medical Microbiology, 2013. **303**(6-7): p. 287-292.

67. Cornforth, D.M. and K.R. Foster, *Antibiotics and the art of bacterial war.* Proceedings of the National Academy of Sciences, 2015. **112**(35): p. 10827-10828.

68. Ochs, M.M., et al., *Negative regulation of the Pseudomonas aeruginosa outer membrane porin OprD selective for imipenem and basic amino acids.* Antimicrobial agents and chemotherapy, 1999. **43**(5): p. 1085-1090.

69. Sun, J., Z. Deng, and A. Yan, *Bacterial multidrug efflux pumps: mechanisms, physiology and pharmacological exploitations.* Biochemical and biophysical research communications, 2014. **453**(2): p. 254-267.

70. Hassett, D.J., et al., *Quorum sensing in Pseudomonas aeruginosa controls expression of catalase and superoxide dismutase genes and mediates biofilm susceptibility to hydrogen peroxide.* Molecular microbiology, 1999. **34**(5): p. 1082-1093.

71. Wongsaroj, L., et al., *Pseudomonas aeruginosa glutathione biosynthesis genes play multiple roles in stress protection, bacterial virulence and biofilm formation.* PloS one, 2018. **13**(10): p. e0205815.

72. Tam, V., et al., *Prevalence of AmpC over-expression in bloodstream isolates of Pseudomonas aeruginosa.* Clinical microbiology and infection, 2007. **13**(4): p. 413-418.

73. Rejiba, S., et al., *Contribution of ParE mutation and efflux to ciprofloxacin resistance in Pseudomonas aeruginosa clinical isolates.* Journal of Chemotherapy, 2008. **20**(6): p. 749-752.

74. Partridge, S.R., et al., *Gene cassettes and cassette arrays in mobile resistance integrons.* FEMS microbiology reviews, 2009. **33**(4): p. 757-784.

75. Rodriguez-Mozaz, S., et al., *Occurrence of antibiotics and antibiotic resistance genes in hospital and urban wastewaters and their impact on the receiving river.* Water research, 2015. **69**: p. 234-242.

76. Hsu, J.-T., et al., *Prevalence of sulfonamide-resistant bacteria, resistance genes and integron-associated horizontal gene transfer in natural water bodies and soils adjacent to a swine feedlot in northern Taiwan.* Journal of hazardous materials, 2014. **277**: p. 34-43.

77. Nguyen, H.N.K., T.T.H. Van, and P.J. Coloe, *Antibiotic resistance associated with aquaculture in Vietnam.* Microbiology Australia, 2016. **37**(3): p. 108-111.

78. Bengtsson-Palme, J., et al., *Shotgun metagenomics reveals a wide array of antibiotic resistance genes and mobile elements in a polluted lake in India.* Frontiers in microbiology, 2014. **5**: p. 648.

79. Hong, D.J., et al., *Epidemiology and characteristics of metallo-β-lactamase-producing Pseudomonas aeruginosa.* Infection & chemotherapy, 2015. **47**(2): p. 81-97.

80. Poole, K., *Aminoglycoside resistance in Pseudomonas aeruginosa.* Antimicrobial agents and Chemotherapy, 2005. **49**(2): p. 479-487.

81. Doi, Y., et al., *High prevalence of metallo-β-lactamase and 16S rRNA methylase coproduction among imipenem-resistant Pseudomonas aeruginosa isolates in Brazil.* Antimicrobial agents and chemotherapy, 2007. **51**(9): p. 3388-3390.

82. Cross, A.S., *What is a virulence factor?* Critical Care, 2008. **12**(6): p. 196.

83. Hoge, R., et al., *Weapons of a pathogen: proteases and their role in virulence of Pseudomonas aeruginosa.* Current research, technology and education topics in applied microbiology and microbial biotechnology, 2010. **2**: p. 383-395.

84. Holm, B.A., et al., *Inhibition of pulmonary surfactant function by phospholipases.* Journal of Applied Physiology, 1991. **71**(1): p. 317-321.

85. Wargo, M.J., et al., *Hemolytic phospholipase C inhibition protects lung function during Pseudomonas aeruginosa infection.* American journal of respiratory and critical care medicine, 2011. **184**(3): p. 345-354.

86. Soberón-Chávez, G., F. Lépine, and E. Déziel, *Production of rhamnolipids by Pseudomonas aeruginosa.* Applied microbiology and biotechnology, 2005. **68**(6): p. 718-725.

87. Caiazza, N.C., R.M. Shanks, and G. O'toole, *Rhamnolipids modulate swarming motility patterns of Pseudomonas aeruginosa.* Journal of bacteriology, 2005. **187**(21): p. 7351-7361.

88. Jiang, L., et al., *Rhamnolipids elicit the same cytotoxic sensitivity between cancer cell and normal cell by reducing surface tension of culture medium.* Applied microbiology and biotechnology, 2014. **98**(24): p. 10187-10196.

89. Read, R.C., et al., *Effect of Pseudomonas aeruginosa rhamnolipids on mucociliary transport and ciliary beating.* Journal of Applied Physiology, 1992. **72**(6): p. 2271-2277.

90. Allured, V.S., et al., *Structure of exotoxin A of Pseudomonas aeruginosa at 3.0-Angstrom resolution.* Proceedings of the National Academy of Sciences, 1986. **83**(5): p. 1320-1324.

91. McEwan, D.L., N.V. Kirienko, and F.M. Ausubel, *Host translational inhibition by Pseudomonas aeruginosa Exotoxin A Triggers an immune response in Caenorhabditis elegans.* Cell host & microbe, 2012. **11**(4): p. 364-374.

92. Muller, M., *Pyocyanin induces oxidative stress in human endothelial cells and modulates the glutathione redox cycle.* Free Radical Biology and Medicine, 2002. **33**(11): p. 1527-1533.

93. O'Malley, Y.Q., et al., *Pseudomonas aeruginosa pyocyanin directly oxidizes glutathione and decreases its levels in airway epithelial cells.* American Journal of Physiology-Lung Cellular and Molecular Physiology, 2004. **287**(1): p. L94-L103.

94. Lau, G.W., et al., *The role of pyocyanin in Pseudomonas aeruginosa infection.* Trends in molecular medicine, 2004. **10**(12): p. 599-606.

95. Parsons, J.F., et al., *Structural and functional analysis of the pyocyanin biosynthetic protein PhzM from Pseudomonas aeruginosa.* Biochemistry, 2007. **46**(7): p. 1821-1828.

96. Lau, G.W., et al., *Pseudomonas aeruginosa pyocyanin is critical for lung infection in mice.* Infection and immunity, 2004. **72**(7): p. 4275-4278.

97. Visca, P., F. Imperi, and I.L. Lamont, *Pyoverdine siderophores: from biogenesis to biosignificance.* Trends in microbiology, 2007. **15**(1): p. 22-30.

98. Cornelis, P. and J. Dingemans, *Pseudomonas aeruginosa adapts its iron uptake strategies in function of the type of infections.* Frontiers in cellular and infection microbiology, 2013. **3**: p. 75.

99. Meyer, J.-M., et al., *Pyoverdin is essential for virulence of Pseudomonas aeruginosa.* Infection and immunity, 1996. **64**(2): p. 518-523.

100. Burrows, L.L., *Pseudomonas aeruginosa twitching motility: type IV pili in action.* Annual review of microbiology, 2012. **66**: p. 493-520.

101. Bucior, I., J.F. Pielage, and J.N. Engel, *Pseudomonas aeruginosa pili and flagella mediate distinct binding and signaling events at the apical and basolateral surface of airway epithelium.* PLoS pathogens, 2012. **8**(4).

102. Bleves, S., et al., *Protein secretion systems in Pseudomonas aeruginosa: a wealth of pathogenic weapons.* International Journal of Medical Microbiology, 2010. **300**(8): p. 534-543.

103. Lesic, á., et al., *Quorum sensing differentially regulates Pseudomonas aeruginosa type VI secretion locus I and homologous loci II and III, which are required for pathogenesis.* Microbiology, 2009. **155**(Pt 9): p. 2845.

104. Coghlan, A., *Slime city.* New Scientist, 1996. **151**(2045): p. 32-6.

105. Trejo-Hernández, A., et al., *Interspecies competition triggers virulence and mutability in Candida albicans–Pseudomonas aeruginosa mixed biofilms.* The ISME journal, 2014. **8**(10): p. 1974-1988.

106. Sun, Y., et al., *In vitro multispecies Lubbock chronic wound biofilm model.* Wound repair and regeneration, 2008. **16**(6): p. 805-813.

107. Michie, K.L., D.M. Cornforth, and M. Whiteley, *Bacterial tweets and podcasts# signaling# eavesdropping# microbialfightclub.* Molecular and biochemical parasitology, 2016. **208**(1): p. 41-48.

108. West, S.A., et al., *Social evolution theory for microorganisms.* Nature reviews microbiology, 2006. **4**(8): p. 597-607.

109. West, S.A., et al., *The social lives of microbes.* Annu. Rev. Ecol. Evol. Syst., 2007. **38**: p. 53-77.

110. Darch, S.E., et al., *Density-dependent fitness benefits in quorum-sensing bacterial populations.* Proceedings of the National Academy of Sciences, 2012. **109**(21): p. 8259-8263.

111. Fuqua, C., M.R. Parsek, and E.P. Greenberg, *Regulation of gene expression by cell-to-cell communication: acyl-homoserine lactone quorum sensing.* Annual review of genetics, 2001. **35**(1): p. 439-468.

112. Rumbaugh, K.P., J.A. Griswold, and A.N. Hamood, *The role of quorum sensing in the in vivo virulence of Pseudomonas aeruginosa.* Microbes and infection, 2000. **2**(14): p. 1721-1731.

113. Lee, J. and L. Zhang, *The hierarchy quorum sensing network in Pseudomonas aeruginosa.* Protein & cell, 2015. **6**(1): p. 26-41.

114. Shrout, J.D., et al., *The impact of quorum sensing and swarming motility on Pseudomonas aeruginosa biofilm formation is nutritionally conditional.* Molecular microbiology, 2006. **62**(5): p. 1264-1277.

115. Bjarnsholt, T., et al., *Pseudomonas aeruginosa tolerance to tobramycin, hydrogen peroxide and polymorphonuclear leukocytes is quorum-sensing dependent.* Microbiology, 2005. **151**(2): p. 373-383.

116. Gambello, M.J., S. Kaye, and B.H. Iglewski, *LasR of Pseudomonas aeruginosa is a transcriptional activator of the alkaline protease gene (apr) and an enhancer of exotoxin A expression.* Infection and immunity, 1993. **61**(4): p. 1180-1184.

117. Rumbaugh, K.P., et al., *Contribution of quorum sensing to the virulence ofpseudomonas aeruginosa in burn wound infections.* Infection and immunity, 1999. **67**(11): p. 5854-5862.

118. Pearson, J.P., et al., *Pseudomonas aeruginosa cell-to-cell signaling is required for virulence in a model of acute pulmonary infection.* Infection and immunity, 2000. **68**(7): p. 4331-4334.

119. Preston, M.J., et al., *Contribution of proteases and LasR to the virulence of Pseudomonas aeruginosa during corneal infections.* Infection and immunity, 1997. **65**(8): p. 3086-3090.

120. Wu, H., et al., *Synthetic furanones inhibit quorum-sensing and enhance bacterial clearance in Pseudomonas aeruginosa lung infection in mice.* Journal of Antimicrobial Chemotherapy, 2004. **53**(6): p. 1054-1061.

121. Hentzer, M., et al., *Attenuation of Pseudomonas aeruginosa virulence by quorum sensing inhibitors.* The EMBO journal, 2003. **22**(15): p. 3803-3815.

122. Luo, J., et al., *Baicalin inhibits biofilm formation, attenuates the quorum sensing-controlled virulence and enhances Pseudomonas aeruginosa clearance in a mouse peritoneal implant infection model.* PLoS One, 2017. **12**(4): p. e0176883.

123. Kalia, V.C., *Quorum sensing inhibitors: an overview.* Biotechnology advances, 2013. **31**(2): p. 224-245.

124. Allen, R.C., et al., *Targeting virulence: can we make evolution-proof drugs?* Nature Reviews Microbiology, 2014. **12**(4): p. 300-308.

125. Chen, F., et al., *Quorum quenching enzymes and their application in degrading signal molecules to block quorum sensing-dependent infection.* International journal of molecular sciences, 2013. **14**(9): p. 17477-17500.

126. Darch, S.E., et al., *Spatial determinants of quorum signaling in a Pseudomonas aeruginosa infection model.* Proceedings of the National Academy of Sciences, 2018. **115**(18): p. 4779-4784.

127. DeLeon, S., et al., *Synergistic interactions of Pseudomonas aeruginosa and Staphylococcus aureus in an in vitro wound model.* Infection and immunity, 2014. **82**(11): p. 4718-4728.

128. Haslett, C., et al., *Modulation of multiple neutrophil functions by preparative methods or trace concentrations of bacterial lipopolysaccharide.* The American journal of pathology, 1985. **119**(1): p. 101.

129. Leid, J.G., et al., *The exopolysaccharide alginate protects Pseudomonas aeruginosa biofilm bacteria from IFN-γ-mediated macrophage killing.* The Journal of Immunology, 2005. **175**(11): p. 7512-7518.

130. Helmke, R.J., V.F. German, and J.A. Mangos, *A continuous alveolar macrophage cell line: comparisons with freshly derived alveolar macrophages.* In vitro cellular & developmental biology, 1989. **25**(1): p. 44-48.

131. Cosson, P., et al., *Pseudomonas aeruginosa virulence analyzed in a Dictyostelium discoideum host system.* Journal of Bacteriology, 2002. **184**(11): p. 3027-3033.

132. Alibaud, L., et al., *Pseudomonas aeruginosa virulence genes identified in a Dictyostelium host model.* Cellular microbiology, 2008. **10**(3): p. 729-740.

133. Steinert, M. and K. Heuner, *Dictyostelium as host model for pathogenesis.* Cellular microbiology, 2005. **7**(3): p. 307-314.

134. Lidington, E., et al., *A comparison of primary endothelial cells and endothelial cell lines for studies of immune interactions.* Transplant immunology, 1999. **7**(4): p. 239-246.

135. Steiner, O., et al., *Comparison of immortalized bEnd5 and primary mouse brain microvascular endothelial cells as in vitro blood–brain barrier models for the study of T cell extravasation.* Journal of Cerebral Blood Flow & Metabolism, 2011. **31**(1): p. 315-327.

136. Kanthakumar, K., et al., *Mechanisms of action of Pseudomonas aeruginosa pyocyanin on human ciliary beat in vitro.* Infection and immunity, 1993. **61**(7): p. 2848-2853.

137. DiMango, E., et al., *Activation of NF-kappaB by adherent Pseudomonas aeruginosa in normal and cystic fibrosis respiratory epithelial cells.* The Journal of clinical investigation, 1998. **101**(11): p. 2598-2605.

138. Fleiszig, S., et al., *Pseudomonas aeruginosa invades corneal epithelial cells during experimental infection.* Infection and immunity, 1994. **62**(8): p. 3485-3493.

139. Fleiszig, S., et al., *Relationship between cytotoxicity and corneal epithelial cell invasion by clinical isolates of Pseudomonas aeruginosa.* Infection and immunity, 1996. **64**(6): p. 2288-2294.

140. Schmidtchen, A., et al., *Elastase-producing Pseudomonas aeruginosa degrade plasma proteins and extracellular products of human skin and fibroblasts, and inhibit fibroblast growth.* Microbial pathogenesis, 2003. **34**(1): p. 47-55.

141. Stipcevic, T., T. Piljac, and R.R. Isseroff, *Di-rhamnolipid from Pseudomonas aeruginosa displays differential effects on human keratinocyte and fibroblast cultures.* Journal of dermatological science, 2005. **40**(2): p. 141-143.

142. Harrison, F. and S.P. Diggle, *An ex vivo lung model to study bronchioles infected with Pseudomonas aeruginosa biofilms.* Microbiology, 2020. **162**.

143. Harrison, F., et al., *Development of an ex vivo porcine lung model for studying growth, virulence, and signaling of Pseudomonas aeruginosa.* Infection and immunity, 2014. **82**(8): p. 3312-3323.

144. Pinnock, A., et al., *Ex vivo rabbit and human corneas as models for bacterial and fungal keratitis.* Graefe's Archive for Clinical and Experimental Ophthalmology, 2017. **255**(2): p. 333-342.

145. Madhu, S.N., et al., *Ex vivo caprine model to study virulence factors in keratitis.* Journal of ophthalmic & vision research, 2018. **13**(4): p. 383.

146. Steinstraesser, L., et al., *A novel human skin chamber model to study wound infection ex vivo.* Archives of dermatological research, 2010. **302**(5): p. 357-365.

147. Green, S.K., et al., *Agricultural plants and soil as a reservoir for Pseudomonas aeruginosa.* Appl. Environ. Microbiol., 1974. **28**(6): p. 987-991.

148. Yorgey, P., et al., *The roles of mucD and alginate in the virulence of Pseudomonas aeruginosa in plants, nematodes and mice.* Molecular microbiology, 2001. **41**(5): p. 1063-1076.

149. Rahme, L.G., et al., *Use of model plant hosts to identify Pseudomonas aeruginosa virulence factors.* Proceedings of the National Academy of Sciences, 1997. **94**(24): p. 13245-13250.

150. Starkey, M. and L.G. Rahme, *Modeling Pseudomonas aeruginosa pathogenesis in plant hosts.* Nature protocols, 2009. **4**(2): p. 117.

151. Garge, S., S. Azimi, and S.P. Diggle, *A simple mung bean infection model for studying the virulence of Pseudomonas aeruginosa.* Microbiology, 2018. **164**(5): p. 764-768.

152. Silo-Suh, L., et al., *A simple alfalfa seedling infection model for Pseudomonas aeruginosa strains associated with cystic fibrosis shows AlgT (sigma-22) and RhlR contribute to pathogenesis.* Proceedings of the National Academy of Sciences, 2002. **99**(24): p. 15699-15704.

153. Tan, M.-W., S. Mahajan-Miklos, and F.M. Ausubel, *Killing of Caenorhabditis elegans by Pseudomonas aeruginosa used to model mammalian bacterial pathogenesis.* Proceedings of the National Academy of Sciences, 1999. **96**(2): p. 715-720.

154. Kirienko, N.V., et al., *Pseudomonas aeruginosa disrupts Caenorhabditis elegans iron homeostasis, causing a hypoxic response and death.* Cell host & microbe, 2013. **13**(4): p. 406-416.

155. Feinbaum, R.L., et al., *Genome-wide identification of Pseudomonas aeruginosa virulence-related genes using a Caenorhabditis elegans infection model.* PLoS pathogens, 2012. **8**(7): p. e1002813.

156. Apidianakis, Y. and L.G. Rahme, *Drosophila melanogaster as a model host for studying Pseudomonas aeruginosa infection.* Nature protocols, 2009. **4**(9): p. 1285.

157. Jander, G., L.G. Rahme, and F.M. Ausubel, *Positive correlation between virulence ofPseudomonas aeruginosa mutants in mice and insects.* Journal of bacteriology, 2000. **182**(13): p. 3843-3845.

158. Miyata, S., et al., *Use of the Galleria mellonella caterpillar as a model host to study the role of the type III secretion system in Pseudomonas aeruginosa pathogenesis.* Infection and immunity, 2003. **71**(5): p. 2404-2413.

159. Hoffmann, J.A., *The immune response of Drosophila.* Nature, 2003. **426**(6962): p. 33-38.

160. Ferrandon, D., et al., *The Drosophila systemic immune response: sensing and signalling during bacterial and fungal infections.* Nature reviews immunology, 2007. **7**(11): p. 862-874.

161. Clatworthy, A.E., et al., *Pseudomonas aeruginosa infection of zebrafish involves both host and pathogen determinants.* Infection and immunity, 2009. **77**(4): p. 1293-1303.

162. Hazlett, L.D., *Corneal response to Pseudomonas aeruginosa infection.* Progress in retinal and eye research, 2004. **23**(1): p. 1-30.

163. Cirioni, O., et al., *Protective effects of the combination of α-helical antimicrobial peptides and rifampicin in three rat models of Pseudomonas aeruginosa infection.* Journal of antimicrobial chemotherapy, 2008. **62**(6): p. 1332-1338.

164. Potvin, E., et al., *In vivo functional genomics of Pseudomonas aeruginosa for high-throughput screening of new virulence factors and antibacterial targets.* Environmental microbiology, 2003. **5**(12): p. 1294-1308.

165. Minardi, D., et al., *The antimicrobial peptide Tachyplesin III coated alone and in combination with intraperitoneal piperacillin-tazobactam prevents ureteral stent Pseudomonas infection in a rat subcutaneous pouch model.* Peptides, 2007. **28**(12): p. 2293-2298.

166. Takumida, M. and M. Anniko, *Protective effect of edaravone against the ototoxicity of Pseudomonas aeruginosa exotoxin A.* Acta oto-laryngologica, 2006. **126**(1): p. 15-19.

167. Hendricks, K.J., et al., *Synergy between Staphylococcus aureus and Pseudomonas aeruginosa in a rat model of complex orthopaedic wounds.* JBJS, 2001. **83**(6): p. 855-861.

168. Stoltz, D.A., et al., *Cystic fibrosis pigs develop lung disease and exhibit defective bacterial eradication at birth.* Science translational medicine, 2010. **2**(29): p. 29ra31-29ra31.

169. Shah, V.S., et al., *Airway acidification initiates host defense abnormalities in cystic fibrosis mice.* Science, 2016. **351**(6272): p. 503-507.

170. Rimmelé, T., et al., *Validation of a Pseudomonas aeruginosa porcine model of septic shock.* Journal of Infection, 2006. **53**(3): p. 199-205.

171. Chevaleyre, C., et al., *The pig: a relevant model for evaluating the neutrophil serine protease activities during acute Pseudomonas aeruginosa lung infection.* PloS one, 2016. **11**(12).

172. Brook, I., V. Hunter, and R.I. Walker, *Synergistic effect of Bacteroides, Clostridium, Fusobacterium, anaerobic cocci, and aerobic bacteria on mortality and induction of subcutaneous abscesses in mice.* Journal of Infectious Diseases, 1984. **149**(6): p. 924-928.

173. Berube, B.J., et al., *Impact of type III secretion effectors and of phenoxyacetamide inhibitors of type III secretion on abscess formation in a mouse model of Pseudomonas aeruginosa infection.* Antimicrobial agents and chemotherapy, 2017. **61**(11): p. e01202-17.

174. Haynes, A., et al., *Syndecan 1 shedding contributes to Pseudomonas aeruginosa sepsis.* Infection and immunity, 2005. **73**(12): p. 7914-7921.

175. Mukherjee, S., et al., *The RhlR quorum-sensing receptor controls Pseudomonas aeruginosa pathogenesis and biofilm development independently of its canonical homoserine lactone autoinducer.* PLoS pathogens, 2017. **13**(7): p. e1006504.

176. Zhang, Y., et al., *Glutathione activates Type III secretion system through Vfr in Pseudomonas aeruginosa.* Frontiers in cellular and infection microbiology, 2019. **9**: p. 164.

177. Huang, L.C., et al., *Cathelicidin-deficient (Cnlp−/−) mice show increased susceptibility to Pseudomonas aeruginosa keratitis.* Investigative ophthalmology & visual science, 2007. **48**(10): p. 4498-4508.

178. Warrener, P., et al., *A novel anti-PcrV antibody providing enhanced protection against Pseudomonas aeruginosa in multiple animal infection models.* Antimicrobial agents and chemotherapy, 2014. **58**(8): p. 4384-4391.

179. Cai, Y., et al., *Activity of colistin alone or in combination with rifampicin or meropenem in a carbapenem-resistant bioluminescent Pseudomonas aeruginosa intraperitoneal murine infection model.* Journal of Antimicrobial Chemotherapy, 2018. **73**(2): p. 456-461.

180. Christensen, L.D., et al., *Synergistic antibacterial efficacy of early combination treatment with tobramycin and quorum-sensing inhibitors against Pseudomonas aeruginosa in an intraperitoneal foreign-body infection mouse model.* Journal of antimicrobial chemotherapy, 2012. **67**(5): p. 1198-1206.

181. Christensen, L.D., et al., *Impact of Pseudomonas aeruginosa quorum sensing on biofilm persistence in an in vivo intraperitoneal foreign-body infection model.* Microbiology, 2007. **153**(7): p. 2312-2320.

182. Kadurugamuwa, J.L., et al., *Direct continuous method for monitoring biofilm infection in a mouse model.* Infection and immunity, 2003. **71**(2): p. 882-890.

183. Zhao, G., et al., *Delayed wound healing in diabetic (db/db) mice with Pseudomonas aeruginosa biofilm challenge: a model for the study of chronic wounds.* Wound Repair and Regeneration, 2010. **18**(5): p. 467-477.

184. Åstrand, A., et al., *Dapagliflozin-lowered blood glucose reduces respiratory Pseudomonas aeruginosa infection in diabetic mice.* British journal of pharmacology, 2017. **174**(9): p. 836-847.

185. Heeckeren, A.v., et al., *Excessive inflammatory response of cystic fibrosis mice to bronchopulmonary infection with Pseudomonas aeruginosa.* The Journal of clinical investigation, 1997. **100**(11): p. 2810-2815.

186. Huang, X., et al., *TLR4 is required for host resistance in Pseudomonas aeruginosa keratitis.* Investigative ophthalmology & visual science, 2006. **47**(11): p. 4910-4916.

187. De Simone, M., et al., *Host genetic background influences the response to the opportunistic Pseudomonas aeruginosa infection altering cell-mediated immunity and bacterial replication.* PloS one, 2014. **9**(9): p. e106873.

188. Sun, Y., et al., *TLR4 and TLR5 on corneal macrophages regulate Pseudomonas aeruginosa keratitis by signaling through MyD88-dependent and-independent pathways.* The Journal of Immunology, 2010. **185**(7): p. 4272-4283.

189. Skerrett, S.J., et al., *Cutting edge: myeloid differentiation factor 88 is essential for pulmonary host defense against Pseudomonas aeruginosa but not Staphylococcus aureus.* The Journal of Immunology, 2004. **172**(6): p. 3377-3381.

190. Emond, M.J., et al., *Exome sequencing of extreme phenotypes identifies DCTN4 as a modifier of chronic Pseudomonas aeruginosa infection in cystic fibrosis.* Nature genetics, 2012. **44**(8): p. 886-889.

191. Lorè, N.I., F.A. Iraqi, and A. Bragonzi, *Host genetic diversity influences the severity of Pseudomonas aeruginosa pneumonia in the Collaborative Cross mice.* BMC genetics, 2015. **16**(1): p. 106.

192. Miller, S.I., R.K. Ernst, and M.W. Bader, *LPS, TLR4 and infectious disease diversity.* Nature Reviews Microbiology, 2005. **3**(1): p. 36-46.

193. Hajjar, A.M., et al., *Human Toll-like receptor 4 recognizes host-specific LPS modifications.* Nature immunology, 2002. **3**(4): p. 354-359.

194. Chen, L., et al., *The murine excisional wound model: Contraction revisited.* Wound Repair and Regeneration, 2015. **23**(6): p. 874-877.

195. Wang, X., et al., *The mouse excisional wound splinting model, including applications for stem cell transplantation.* Nature protocols, 2013. **8**(2): p. 302.

196. Han, M.-L., et al., *Comparative Metabolomics and Transcriptomics Reveal Multiple Pathways Associated with Polymyxin Killing in Pseudomonas aeruginosa.* MSystems, 2019. **4**(1): p. e00149-18.

197. Jacob, H.J., *Functional genomics and rat models.* Genome research, 1999. **9**(11): p. 1013-1016.

198. Jacob, H.J., *The rat: a model used in biomedical research*, in *Rat genomics*. 2010, Springer. p. 1-11.

199. Cash, H., et al., *A rat model of chronic respiratory infection with Pseudomonas aeruginosa.* American Review of Respiratory Disease, 1979. **119**(3): p. 453-459.

200. Aigner, B., et al., *Transgenic pigs as models for translational biomedical research.* Journal of molecular medicine, 2010. **88**(7): p. 653-664.

201. Ridings, P.C., et al., *Protective role of synthetic sialylated oligosaccharide in sepsis-induced acute lung injury.* Journal of Applied Physiology, 1997. **82**(2): p. 644-651.

202. Bassi, G.L., et al., *A novel porcine model of ventilator-associated pneumonia caused by oropharyngeal challenge with Pseudomonas aeruginosa.* Anesthesiology: The Journal of the American Society of Anesthesiologists, 2014. **120**(5): p. 1205-1215.

203. Konrad, D., et al., *Effects of a topical silver sulfadiazine polyurethane dressing (Mikacure) on wound healing in experimentally infected wounds in the pig. A pilot study.* Journal of Experimental Animal Science, 2002. **42**(1): p. 31-43.

204. Steinstraesser, L., et al., *A novel titanium wound chamber for the study of wound infections in pigs.* Comparative medicine, 2006. **56**(4): p. 279-285.

205. Wilke, M., et al., *Mouse models of cystic fibrosis: phenotypic analysis and research applications.* Journal of Cystic Fibrosis, 2011. **10**: p. S152-S171.

206. Smirnova, G. and O. Oktyabrsky, *Glutathione in bacteria.* Biochemistry (Moscow), 2005. **70**(11): p. 1199-1211.

207. Lushchak, V.I., *Glutathione homeostasis and functions: potential targets for medical interventions.* Journal of amino acids, 2012. **2012**.

208. Reniere, M.L., et al., *Glutathione activates virulence gene expression of an intracellular pathogen.* Nature, 2015. **517**(7533): p. 170.

209. Ku, J.W. and Y.-H. Gan, *Modulation of bacterial virulence and fitness by host glutathione.* Current opinion in microbiology, 2019. **47**: p. 8-13.

210. Newton, G.L., et al., *Bacillithiol is an antioxidant thiol produced in Bacilli.* Nature chemical biology, 2009. **5**(9): p. 625.

211. Ung, K.S. and Y. Av-Gay, *Mycothiol-dependent mycobacterial response to oxidative stress.* FEBS letters, 2006. **580**(11): p. 2712-2716.

212. Fahey, R.C., *Glutathione analogs in prokaryotes.* Biochimica et Biophysica Acta (BBA)-General Subjects, 2013. **1830**(5): p. 3182-3198.

213. Meury, J. and A. Kepes, *Glutathione and the gated potassium channels of Escherichia coli.* The EMBO journal, 1982. **1**(3): p. 339-343.

214. Zhou, H., et al., *Modulation of Pseudomonas aeruginosa quorum sensing by glutathione.* Journal of bacteriology, 2019. **201**(9): p. e00685-18.

215. Van Laar, T.A., et al., *Pseudomonas aeruginosa gshA mutant is defective in biofilm formation, swarming, and pyocyanin production.* mSphere, 2018. **3**(2): p. e00155-18.

216. Zhang, Y. and K. Duan, *Glutathione exhibits antibacterial activity and increases tetracycline efficacy against Pseudomonas aeruginosa.* Science in China Series C: Life Sciences, 2009. **52**(6): p. 501-505.

217. Goswami, M. and N. Jawali, *N-Acetylcysteine-mediated modulation of bacterial antibiotic susceptibility.* Antimicrobial agents and chemotherapy, 2010. **54**(8): p. 3529-3530.

218. Song, M., et al., *Low-molecular-weight thiol-dependent antioxidant and antinitrosative defences in S almonella pathogenesis.* Molecular microbiology, 2013. **87**(3): p. 609-622.

219. Gamage, A.M., et al., *The proteobacterial species Burkholderia pseudomallei produces ergothioneine, which enhances virulence in mammalian infection.* The FASEB Journal, 2018. **32**(12): p. 6395-6409.

220. Fuchs, J.A. and H.R. Warner, *Isolation of an Escherichia coli mutant deficient in glutathione synthesis.* J Bacteriol, 1975. **124**(1): p. 140-8.

221. Murray, J.L., et al., *Intrinsic Antimicrobial Resistance Determinants in the Superbug Pseudomonas aeruginosa.* mBio, 2015. **6**(6): p. e01603-15.

222. Socransky, S., J. Dzink, and C. Smith, *Chemically defined medium for oral microorganisms.* Journal of clinical microbiology, 1985. **22**(2): p. 303-305.

223. Kuppusamy, P., et al., *Noninvasive imaging of tumor redox status and its modification by tissue glutathione levels.* Cancer research, 2002. **62**(1): p. 307-312.

224. Turnbull, A.L. and M.G. Surette, *Cysteine biosynthesis, oxidative stress and antibiotic resistance in Salmonella typhimurium.* Research in microbiology, 2010. **161**(8): p. 643-650.

225. Shukla, A., A.M. Rasik, and B.N. Dhawan, *Asiaticoside-induced elevation of antioxidant levels in healing wounds.* Phytotherapy Research: An International Journal Devoted to Pharmacological and Toxicological Evaluation of Natural Product Derivatives, 1999. **13**(1): p. 50-54.

226. Li, Y., G. Wei, and J. Chen, *Glutathione: a review on biotechnological production.* Applied microbiology and biotechnology, 2004. **66**(3): p. 233-242.

227. Kram, K.E. and S.E. Finkel, *Culture volume and vessel affect long-term survival, mutation frequency, and oxidative stress of Escherichia coli.* Appl. Environ. Microbiol., 2014. **80**(5): p. 1732-1738.

228. Babior, B.M., *Phagocytes and oxidative stress.* The American journal of medicine, 2000. **109**(1): p. 33-44.

229. Wang, G. and W.M. Nauseef, *Salt, chloride, bleach, and innate host defense.* Journal of leukocyte biology, 2015. **98**(2): p. 163-172.

230. Dwyer, D.J., et al., *Antibiotics induce redox-related physiological alterations as part of their lethality.* Proceedings of the National Academy of Sciences, 2014. **111**(20): p. E2100-E2109.

231. Tzeng, Y.-L., et al., *Cationic antimicrobial peptide resistance in Neisseria meningitidis.* Journal of bacteriology, 2005. **187**(15): p. 5387-5396.

232. Parra-Lopez, C., et al., *A Salmonella protein that is required for resistance to antimicrobial peptides and transport of potassium.* The EMBO journal, 1994. **13**(17): p. 3964-3972.

233. Bengoechea, J.A. and M. Skurnik, *Temperature-regulated efflux pump/potassium antiporter system mediates resistance to cationic antimicrobial peptides in Yersinia.* Molecular microbiology, 2000. **37**(1): p. 67-80.

234. Chen, Y.-C., et al., *A K+ uptake protein, TrkA, is required for serum, protamine, and polymyxin B resistance in Vibrio vulnificus.* Infection and immunity, 2004. **72**(2): p. 629-636.

235. Zhang, Y. and Y. Wei, *Impact of glutathione on the gene expression of exoY and exoS in Pseudomonas aeruginosa.* Wei sheng wu xue bao= Acta microbiologica Sinica, 2009. **49**(5): p. 603-608.

236. Solapure, S., et al., *In vitro and in vivo efficacy of β-lactams against replicating and slowly growing/nonreplicating Mycobacterium tuberculosis.* Antimicrobial agents and chemotherapy, 2013. **57**(6): p. 2506-2510.

237. Tuomanen, E., et al., *The rate of killing of Escherichia coli byβ-lactam antibiotics is strictly proportional to the rate of bacterial growth.* Microbiology, 1986. **132**(5): p. 1297-1304.

238. Dowd, S.E., et al., *Survey of bacterial diversity in chronic wounds using pyrosequencing, DGGE, and full ribosome shotgun sequencing.* BMC microbiology, 2008. **8**(1): p. 43.

239. Wolcott, R.D., et al., *Biofilm maturity studies indicate sharp debridement opens a time-dependent therapeutic window.* Journal of wound care, 2010. **19**(8): p. 320-328.

240. Holder, I.A., R.L. Brown, and D.G. Greenhalgh, *Mouse models to study wound closure and topical treatment of infected wounds in healing-impaired and normal healing hosts.* Wound Repair and Regeneration, 1997. **5**(2): p. 198-204.

241. Lewin, G.R., et al., *Large-scale identification of pathogen essential genes during coinfection with sympatric and allopatric microbes.* Proceedings of the National Academy of Sciences, 2019. **116**(39): p. 19685-19694.

242. Stacy, A., et al., *A commensal bacterium promotes virulence of an opportunistic pathogen via cross-respiration.* MBio, 2016. **7**(3): p. e00782-16.

243. Revelli, D.A., J.A. Boylan, and F.C. Gherardini, *A non-invasive intratracheal inoculation method for the study of pulmonary melioidosis.* Frontiers in cellular and infection microbiology, 2012. **2**: p. 164.

244. Priebe, G.P., et al., *Construction and characterization of a live, attenuated aroA deletion mutant of Pseudomonas aeruginosa as a candidate intranasal vaccine.* Infection and immunity, 2002. **70**(3): p. 1507-1517.

245. Cemek, M., et al., *Oxidative stress and enzymic–non-enzymic antioxidant responses in children with acute pneumonia.* Cell Biochemistry and Function:

Cellular biochemistry and its modulation by active agents or disease, 2006. **24**(3): p. 269-273.

246. Mustoe, T.A., K. O'Shaughnessy, and O. Kloeters, *Chronic wound pathogenesis and current treatment strategies: a unifying hypothesis.* Plastic and reconstructive surgery, 2006. **117**(7S): p. 35S-41S.

247. Chow, C.-W., et al., *Oxidative stress and acute lung injury.* American journal of respiratory cell and molecular biology, 2003. **29**(4): p. 427-431.

248. Mudge, B.P., et al., *Role of glutathione redox dysfunction in diabetic wounds.* Wound Repair and Regeneration, 2002. **10**(1): p. 52-58.

249. Aktunc, E., et al., *N-acetyl cysteine promotes angiogenesis and clearance of free oxygen radicals, thus improving wound healing in an alloxan-induced diabetic mouse model of incisional wound.* Clinical and Experimental Dermatology: Experimental dermatology, 2010. **35**(8): p. 902-909.

250. Al-Jawad, F., A. Sahib, and A. Al-Kaisy, *Role of antioxidants in the treatment of burn lesions.* Annals of burns and fire disasters, 2008. **21**(4): p. 186.

251. Ocal, K., et al., *The effect of N-acetylcysteine on oxidative stress in intestine and bacterial translocation after thermal injury.* Burns, 2004. **30**(8): p. 778-784.

252. Rahman, I. and W. MacNee, *Regulation of redox glutathione levels and gene transcription in lung inflammation: therapeutic approaches.* Free Radical Biology and Medicine, 2000. **28**(9): p. 1405-1420.

253. Lai, K., et al., *High-dose N-acetylcysteine therapy for novel H1N1 influenza pneumonia.* Annals of internal medicine, 2010. **152**(10): p. 687-688.

254. Zhang, Q., et al., *N-acetylcysteine improves oxidative stress and inflammatory response in patients with community acquired pneumonia: A randomized controlled trial.* Medicine, 2018. **97**(45).

255. Rietsch, A., et al., *ExsE, a secreted regulator of type III secretion genes in Pseudomonas aeruginosa.* Proceedings of the National Academy of Sciences, 2005. **102**(22): p. 8006-8011.

256. Gibson, D.G., et al., *Enzymatic assembly of DNA molecules up to several hundred kilobases.* Nature methods, 2009. **6**(5): p. 343.

257. Council, N.R., *Guide for the care and use of laboratory animals*. 2010: National Academies Press.

258. Dennis, P.P. and H. Bremer, *Macromolecular composition during steady-state growth of Escherichia coli B/r.* Journal of bacteriology, 1974. **119**(1): p. 270-281.

259. Wang, J.D. and P.A. Levin, *Metabolism, cell growth and the bacterial cell cycle.* Nature Reviews Microbiology, 2009. **7**(11): p. 822-827.

260. Hecker, M. and U. Völker, *General stress response of Bacillus subtilis and other bacteria.* 2001.

261. Neidhardt, F.C., *Effects of environment on the composition of bacterial cells.* Annual Reviews in Microbiology, 1963. **17**(1): p. 61-86.

262. Eudy, W. and S. Burrous, *Generation times of Proteus mirabilis and Escherichia coli in experimental infections.* Chemotherapy, 1973. **19**(3): p. 161-170.

263. Ombaka, E.A., R.M. Cozens, and M.R. Brown, *Influence of nutrient limitation of growth on stability and production of virulence factors of mucoid and nonmucoid strains of Pseudomonas aeruginosa.* Reviews of infectious diseases, 1983. **5**(Supplement_5): p. S880-S888.

264. McKenney, D. and D.G. Allison, *Effects of growth rate and nutrient limitation on virulence factor production in Burkholderia cepacia.* Journal of bacteriology, 1995. **177**(14): p. 4140-4143.

265. Lu, C., M.J. Brauer, and D. Botstein, *Slow growth induces heat-shock resistance in normal and respiratory-deficient yeast.* Molecular biology of the cell, 2009. **20**(3): p. 891-903.

266. Notley, L. and T. Ferenci, *Induction of RpoS-dependent functions in glucose-limited continuous culture: what level of nutrient limitation induces the stationary phase of Escherichia coli?* Journal of bacteriology, 1996. **178**(5): p. 1465-1468.

267. Ihssen, J. and T. Egli, *Specific growth rate and not cell density controls the general stress response in Escherichia coli.* Microbiology, 2004. **150**(6): p. 1637-1648.

268. Cozens, R., et al., *Evaluation of the bactericidal activity of beta-lactam antibiotics on slowly growing bacteria cultured in the chemostat.* Antimicrobial Agents and Chemotherapy, 1986. **29**(5): p. 797-802.

269. Newton, D.F., S. Macfarlane, and G.T. Macfarlane, *Effects of antibiotics on bacterial species composition and metabolic activities in chemostats containing defined populations of human gut microorganisms.* Antimicrobial agents and chemotherapy, 2013. **57**(5): p. 2016-2025.

270. Brown, M., P.J. Collier, and P. Gilbert, *Influence of growth rate on susceptibility to antimicrobial agents: modification of the cell envelope and batch and continuous culture studies.* Antimicrobial agents and chemotherapy, 1990. **34**(9): p. 1623.

271. Maw, J. and G. Meynell, *The true division and death rates of Salmonella typhimurium in the mouse spleen determined with superinfecting phage P22.* British journal of experimental pathology, 1968. **49**(6): p. 597.

272. Yang, L., et al., *In situ growth rates and biofilm development of Pseudomonas aeruginosa populations in chronic lung infections.* Journal of bacteriology, 2008. **190**(8): p. 2767-2776.

273. Poulsen, L.K., et al., *Physiological state of Escherichia coli BJ4 growing in the large intestines of streptomycin-treated mice.* Journal of Bacteriology, 1995. **177**(20): p. 5840-5845.

274. Kragh, K.N., et al., *Polymorphonuclear leukocytes restrict growth of Pseudomonas aeruginosa in the lungs of cystic fibrosis patients.* Infection and immunity, 2014. **82**(11): p. 4477-4486.

275. Gasch, A.P., et al., *Genomic expression programs in the response of yeast cells to environmental changes.* Molecular biology of the cell, 2000. **11**(12): p. 4241-4257.

276. Brauer, M.J., et al., *Coordination of growth rate, cell cycle, stress response, and metabolic activity in yeast.* Molecular biology of the cell, 2008. **19**(1): p. 352-367.

277. Michie, K.L., et al., *The Role of Pseudomonas aeruginosa Glutathione Biosynthesis in Lung and Soft Tissue Infection.* Infection and Immunity, 2020.

278. Ratkowsky, D.A., et al., *Relationship between temperature and growth rate of bacterial cultures.* Journal of bacteriology, 1982. **149**(1): p. 1-5.

279. Pietikäinen, J., M. Pettersson, and E. Bååth, *Comparison of temperature effects on soil respiration and bacterial and fungal growth rates.* FEMS microbiology ecology, 2005. **52**(1): p. 49-58.

280. ROLINSON, G.N., *Effect of β-lactam antibiotics on bacterial cell growth rate.* Microbiology, 1980. **120**(2): p. 317-323.

281. Vorob'eva, L., *Stressors, stress reactions, and survival of bacteria: a review.* Applied biochemistry and microbiology, 2004. **40**(3): p. 217-224.

282. Whiteley, M., E. Brown, and R.J. McLean, *An inexpensive chemostat apparatus for the study of microbial biofilms.* Journal of microbiological methods, 1997. **30**(2): p. 125-132.

283. Novick, A. and L. Szilard, *Description of the chemostat.* Science, 1950. **112**(2920): p. 715-716.

284. Gresham, D. and J. Hong, *The functional basis of adaptive evolution in chemostats.* FEMS microbiology reviews, 2015. **39**(1): p. 2-16.

285. Ferenci, T., *Bacterial physiology, regulation and mutational adaptation in a chemostat environment.* Advances in microbial physiology, 2007. **53**: p. 169-315.

286. Cornforth, D.M., et al., *Pseudomonas aeruginosa transcriptome during human infection.* Proceedings of the National Academy of Sciences, 2018. **115**(22): p. E5125-E5134.

287. Ibberson, C.B. and M. Whiteley, *The Staphylococcus aureus Transcriptome during Cystic Fibrosis Lung Infection.* mBio, 2019. **10**(6).

288. Subashchandrabose, S., et al., *Host-specific induction of Escherichia coli fitness genes during human urinary tract infection.* Proceedings of the National Academy of Sciences, 2014. **111**(51): p. 18327-18332.

289. Rokbi, B., et al., *Assessment of Helicobacter pylori gene expression within mouse and human gastric mucosae by real-time reverse transcriptase PCR.* Infection and immunity, 2001. **69**(8): p. 4759-4766.

290. Bina, J., et al., *ToxR regulon of Vibrio cholerae and its expression in vibrios shed by cholera patients.* Proceedings of the National Academy of Sciences, 2003. **100**(5): p. 2801-2806.

291. Houser, J.R., et al., *Controlled measurement and comparative analysis of cellular components in E. coli reveals broad regulatory changes in response to glucose starvation.* PLoS computational biology, 2015. **11**(8).

292. Kwon, T., et al., *Protein-to-mRNA ratios are conserved between Pseudomonas aeruginosa strains.* Journal of proteome research, 2014. **13**(5): p. 2370-2380.

293. Vogel, C., et al., *Sequence signatures and mRNA concentration can explain two-thirds of protein abundance variation in a human cell line.* Molecular systems biology, 2010. **6**(1).

294. de Sousa Abreu, R., et al., *Global signatures of protein and mRNA expression levels.* Molecular BioSystems, 2009. **5**(12): p. 1512-1526.

295. Hua, Q., et al., *Analysis of gene expression in Escherichia coli in response to changes of growth-limiting nutrient in chemostat cultures.* Appl. Environ. Microbiol., 2004. **70**(4): p. 2354-2366.

296. Palmer, K.L., et al., *Cystic fibrosis sputum supports growth and cues key aspects of Pseudomonas aeruginosa physiology.* Journal of bacteriology, 2005. **187**(15): p. 5267-5277.

297. Jorth, P., et al., *Metatranscriptomics of the human oral microbiome during health and disease.* MBio, 2014. **5**(2): p. e01012-14.

298. Mertins, P., et al., *Reproducible workflow for multiplexed deep-scale proteome and phosphoproteome analysis of tumor tissues by liquid chromatography–mass spectrometry.* Nature protocols, 2018. **13**(7): p. 1632-1661.

299. Yang, F., et al., *High-pH reversed-phase chromatography with fraction concatenation for 2D proteomic analysis.* Expert review of proteomics, 2012. **9**(2): p. 129-134.

300. Rinker, T.E., et al., *Microparticle-mediated sequestration of cell-secreted proteins to modulate chondrocytic differentiation.* Acta biomaterialia, 2018. **68**: p. 125-136.

301. Martin, M., *Cutadapt removes adapter sequences from high-throughput sequencing reads.* EMBnet. journal, 2011. **17**(1): p. 10-12.

302. Langmead, B. and S.L. Salzberg, *Fast gapped-read alignment with Bowtie 2.* Nature methods, 2012. **9**(4): p. 357.

303. Liao, Y., G.K. Smyth, and W. Shi, *The Subread aligner: fast, accurate and scalable read mapping by seed-and-vote.* Nucleic acids research, 2013. **41**(10): p. e108-e108.

304. Winsor, G.L., et al., *Enhanced annotations and features for comparing thousands of Pseudomonas genomes in the Pseudomonas genome database.* Nucleic acids research, 2016. **44**(D1): p. D646-D653.

305. Team, R.C., *R: A language and environment for statistical computing.* 2013.

306. Gatto, L. and K.S. Lilley, *MSnbase-an R/Bioconductor package for isobaric tagged mass spectrometry data visualization, processing and quantitation.* Bioinformatics, 2012. **28**(2): p. 288-289.

307. Smyth, G.K., *Limma: linear models for microarray data*, in *Bioinformatics and computational biology solutions using R and Bioconductor*. 2005, Springer. p. 397-420.

308. Benjamini, Y. and Y. Hochberg, *Controlling the false discovery rate: a practical and powerful approach to multiple testing.* Journal of the Royal statistical society: series B (Methodological), 1995. **57**(1): p. 289-300.

309. Riccillo, P.M., et al., *Glutathione is involved in environmental stress responses in Rhizobium tropici, including acid tolerance.* Journal of Bacteriology, 2000. **182**(6): p. 1748-1753.

310. Boyer, M.J. and D.W. Hedley, *Measurement of intracellular pH*, in *Methods in cell biology*. 1994, Elsevier. p. 135-148.

311. Mitchell, A., et al., *Glutathionylation of Yersinia pestis LcrV and its effects on plague pathogenesis.* MBio, 2017. **8**(3): p. e00646-17.

312. Deslouches, B., et al., *De novo-derived cationic antimicrobial peptide activity in a murine model of Pseudomonas aeruginosa bacteraemia.* Journal of antimicrobial chemotherapy, 2007. **60**(3): p. 669-672.

313. Lewis, A.J., C.W. Seymour, and M.R. Rosengart, *Current murine models of sepsis.* Surgical infections, 2016. **17**(4): p. 385-393.

314. Giamarellou, H., et al., *Evaluation of ciprofloxacin in the treatment of Pseudomonas aeruginosa infections*, in *Ciprofloxacin*. 1986, Springer. p. 103-106.

315. Hodson, M., et al., *Oral ciprofloxacin compared with conventional intravenous treatment for Pseudomonas aeruginosa infection in adults with cystic fibrosis.* The Lancet, 1987. **329**(8527): p. 235-237.

316. Estrela, J.M., et al., *Elimination of Ehrlich tumours by ATP-induced growth inhibition, glutathione depletion and X-rays.* Nature medicine, 1995. **1**(1): p. 84-88.

317. Kato, T., et al., *Cisplatin and radiation sensitivity in human head and neck squamous carcinomas are independently modulated by glutathione and transcription factor NF-κB.* Head & Neck: Journal for the Sciences and Specialties of the Head and Neck, 2000. **22**(8): p. 748-759.

318. Srinivasan, B., et al., *TEER measurement techniques for in vitro barrier model systems.* Journal of laboratory automation, 2015. **20**(2): p. 107-126.

319. Bédos, J.-P., et al., *Pharmacodynamic activities of ciprofloxacin and sparfloxacin in a murine pneumococcal pneumonia model: relevance for drug efficacy.* Journal of pharmacology and experimental therapeutics, 1998. **286**(1): p. 29-35.

320. Hayashi, K., et al., *Efficacy of quinolones against secondary pneumococcal pneumonia after influenza virus infection in mice.* Antimicrobial agents and chemotherapy, 2006. **50**(2): p. 748-751.

321. Martignoni, M., G.M. Groothuis, and R. de Kanter, *Species differences between mouse, rat, dog, monkey and human CYP-mediated drug metabolism, inhibition and induction.* Expert opinion on drug metabolism & toxicology, 2006. **2**(6): p. 875-894.

322. Cantin, A., et al., *Normal alveolar epithelial lining fluid contains high levels of glutathione.* Journal of applied physiology, 1987. **63**(1): p. 152-157.

323. Şener, G., et al., *Melatonin improves oxidative organ damage in a rat model of thermal injury.* Burns, 2002. **28**(5): p. 419-425.

324. Elkins, J.G., et al., *Protective role of catalase in Pseudomonas aeruginosa biofilm resistance to hydrogen peroxide.* Appl. Environ. Microbiol., 1999. **65**(10): p. 4594-4600.

325. Wilson, R., et al., *Measurement of Pseudomonas aeruginosa phenazine pigments in sputum and assessment of their contribution to sputum sol toxicity for respiratory epithelium.* Infection and immunity, 1988. **56**(9): p. 2515-2517.

326. Zollinger, E., et al., *Collection of exhaled breath and exhaled breath condensate in veterinary medicine. A review.* Veterinary quarterly, 2006. **28**(3): p. 105-117.

327. Weicker, S., et al., *Noninvasive measurement of exhaled nitric oxide in a spontaneously breathing mouse.* American journal of respiratory and critical care medicine, 2001. **163**(5): p. 1113-1116.

328. Karna, S.R., et al., *T3SS and alginate biosynthesis of Pseudomonas aeruginosa impair healing of infected rabbit wounds.* Microbial Pathogenesis, 2020: p. 104254.

329. Tirouvanziam, R., et al., *High-dose oral N-acetylcysteine, a glutathione prodrug, modulates inflammation in cystic fibrosis.* Proceedings of the National Academy of Sciences, 2006. **103**(12): p. 4628-4633.

330. Griese, M., et al., *Inhalation treatment with glutathione in patients with cystic fibrosis. A randomized clinical trial.* American journal of respiratory and critical care medicine, 2013. **188**(1): p. 83-89.

331. Jelsbak, L., et al., *Molecular epidemiology and dynamics of Pseudomonas aeruginosa populations in lungs of cystic fibrosis patients.* Infection and immunity, 2007. **75**(5): p. 2214-2224.

332. Fine, D.H., et al., *How we got attached to Actinobacillus actinomycetemcomitans: a model for infectious diseases.* Periodontology 2000, 2006. **42**(1): p. 114-157.

333. Fine, D.H., et al., *Aggregatibacter actinomycetemcomitans and its relationship to initiation of localized aggressive periodontitis: longitudinal cohort study of initially healthy adolescents.* Journal of clinical microbiology, 2007. **45**(12): p. 3859-3869.

334. Lee, M.-R., et al., *Mycobacterium abscessus complex infections in humans.* Emerging infectious diseases, 2015. **21**(9): p. 1638.

335. Esther Jr, C.R., et al., *Chronic Mycobacterium abscessus infection and lung function decline in cystic fibrosis.* Journal of Cystic Fibrosis, 2010. **9**(2): p. 117-123.

336. Orth, J.D., I. Thiele, and B.Ø. Palsson, *What is flux balance analysis?* Nature biotechnology, 2010. **28**(3): p. 245-248.

337. Mashburn, L.M., et al., *Staphylococcus aureus serves as an iron source for Pseudomonas aeruginosa during in vivo coculture.* Journal of bacteriology, 2005. **187**(2): p. 554-566.

338. Wessel, A.K., et al., *Oxygen limitation within a bacterial aggregate.* MBio, 2014. **5**(2): p. e00992-14.

339. Airoldi, E.M., et al., *Predicting cellular growth from gene expression signatures.* PLoS computational biology, 2009. **5**(1).

340. Tibshirani, R., *Regression shrinkage and selection via the lasso.* Journal of the Royal Statistical Society: Series B (Methodological), 1996. **58**(1): p. 267-288.